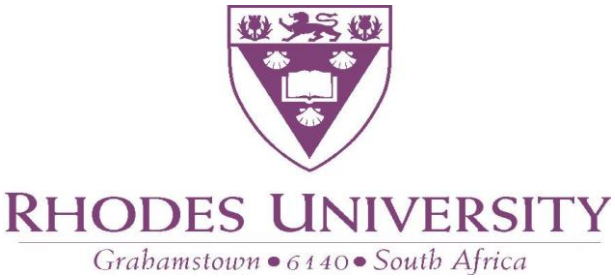

Exploration for sediment-hosted copper mineralization in Kaponda Prospect, Central African Copperbelt, Democratic Republic of Congo

By

Ghislain Mwape Kabunda

A dissertation submitted in partial fulfillment of the requirements for the degree of
MASTER OF SCIENCE
(Exploration Geology)

MSc Exploration Geology Program
Geology Department
Rhodes University
P.O. Box 94
Grahamstown 6140
South Africa

January 2014

DECLARATION

I, GHISLAIN MWAPE KABUNDA, declare this dissertation to be my own work. It is submitted in fulfillment of the Degree of Master of Science at the University of Rhodes. It has not been submitted before for any degree or examination in any other University or tertiary institution.

Signature of the candidate: …….

Date: ……

ABSTRACT

The Kaponda Prospect represents a surface of 915.8 km^2 located at about 10 km south of the town of Lubumbashi and 33km NW of Kasumbalesa in the Democratic Republic of Congo (DRC). It lies within Neoproterozoic sedimentary rocks of the Katangan Supergroup in the Central African Copperbelt (CACB). In this province, copper mineralization occurs at different stratigraphic level with different associated alteration. Mineralization is of multistage origin from synsedimentary, diagenetic to post orogenic.

Since the discovery of the CACB in the early 20's century, several exploration techniques have been used to delineate Cu deposits. A review and application of these methods including remote sensing, geological mapping, geochemical and geophysical surveys, and drilling, gives an insight of their effectiveness and limitation before analyzing their results from the Kaponda Prospect.

The geology and structure of the Prospect is represented by a series of two NW trending disharmonic tight anticlines, locally domal, with cores occupied by either Roan Group or "Grand Conglomerat" Formation. These anticlines are separated by an open syncline made of Kundelungu rocks. Two mains direction of faults are recognized, the NW and NE trending structures. The latter direction are normal transfer faults which can serve as conduit for mineralization. They are related to the late orogenic extension of the Lufilian belt. However NE trending faults are believed to be associated to the climax of Lufilian folding or represents synsedimentary intergrowth faults.

Exploration approach for sediment-hosted Cu within Kaponda Prospect, take into account the integration of all information derived from different techniques. Remote sensing is used as aid to geology. Landsat and Google earth images show lineaments that corresponds to lithostratigraphy boundary and domal anticline. Geological mapping identified reduced horizons which can potentially host mineralization, whereas analysis of structure measurements reveals the geometry of fold and direction of its axial plane and hinge. Statistical methods such as the main + 2 standard deviation, the frequency histogram and probability plot, together with experiential method are used to constrain and define Cu and Co thresholds values in soil samples. It appears that in this region, log-probability plot and histogram methods combined

with spatial representation and the experience of the region, are the best practice to constrain and separate geochemical background from anomaly data.

Ground and airborne magnetic, and radiometric images show specific signatures which map alteration and particularly lithostratigraphy such as “Roan” Group, “Grand Conglomerat” unit, “Nguba” cap carbonates and “Kundelungu” siliciclastic units. Analysis of faults interpreted from geophysical maps identified three major directions: E-W, NE-SW and NW-SE. The E-W faults are also interpreted as normal transfer faults such NE-SW structures, consistent with regional geological map.

Although pole-dipole array of induced polarization (IP) survey was directly targeting disseminated Cu sulphide, its results suffer in responding to graphitic rocks and barren pyrite. Only relative small chargeable bodies need to be tested in drilling follow-up. A total of 15 targets have been generated through re-interpretation and integration of both geological mapping and remote sensing, geochemical and geophysical data, as well as existing drilling. Specific recommendations of follow-up works are advised for each type of target.

***Keywords**: Copperbelt, synsedimentary, early diagenetic, post orogenic, remote sensing, disharmonic tight anticline, lineaments, threshold, landscape geochemistry, pole-dipole array, induced polarization, target*

This Dissertation is dedicated to My Wife Carine Muteb and sons, Rozen and Reinis Kabunda, for their enduring love, support and sacrifice when I was away for study.

ACKNOWLEDGEMENTS

I would like to thank First Quantum Minerals Management for funding this MSc study, particularly Doug Jack, the Southern Africa Exploration Manager, for granting me the opportunity to pursue my study at Rhodes University.

Prof Yong Yao is specially thank for his supervision and guidance of this dissertation.

It is a pleasure to acknowledge and thank Ms Ashley Goddard, the Exploration Geology Secretary, for her unconditional administrative and logistic supports during the period of study in Grahamstown.

I am grateful to all First Quantum Minerals geologists with whom I worked in exploring the North Pedicle of the D.R. Congo and generated together some of the data used in this dissertation. Special gratitude to Mike Parker, the former DRC North pedicle Exploration Manager, for his support.

Finally I wish to thank my Parents for their huge initial contribution to my education without whose I will never have reached and accomplished this MSc study.

TABLE OF CONTENTS

LIST OF FIGURES

LIST OF TABLES

Chapter 1 INTRODUCTION

1.1. BACK GROUND

The Central African Copperbelt (CACB) is well known for its world class stratiform and stratabound Cu-Co deposits. These deposits are located in the Democratic Republic of Congo (DRC) and Zambia. They are hosted within Neoproterozoic sedimentary rocks of the Katangan Supergroup, deposited in a series of intracontinental rift basins. During Pan African Lufilian orogeny, the Katangan rocks underwent a long tectonic history producing over 500 km EW arcuate fold-and-thrust belt known as the Lufilian or Katangan belt (Fig.1). A less deformed plateau molasses were syn-tectonically deposited in the Northern Katangan foreland basin, it consists of the upper most member of the Katangan Supergroup (Kundelungu Group; Batumike et al., 2007; Master et al., 2005).

Since the discovery of the Central African Copperbelt in early 1900's several exploration techniques including remote sensing, geological mapping, trenching, geochemical and geophysical surveys, and drilling has been used to delineate deposits. Combined production and reserve of over 200Mt Cu has been identified through deposits in DRC and Zambia. These deposits display different style, texture and associated alteration, and occur within different lithology (conglomerate, schists, arenites, shale, carbonates, diamictite) at several stratigraphic levels (Hitzman et al., 2010). The mineralization is either or both fine grained dissemination or vein-hosted coarse grained sulphides. Therefore, supergene enrichment forming oxidized or mixed ore (sulphide + oxides) is very common in the DRC.

In the Congolese Copperbelt (CCB), the bulk of deposits, from Kimpe to Kolwezi (Fig.1), are hosted within carbonate rocks of Mines Subgroup and were discover in the first three quarters of the twentieth century. Most of these deposits were outcropping forming prominent hills. They were easily delineated by aerial photograph or satellite image, followed by trenching and pitting in order to determine their structural setting and surface extension. Afterward drilling was carried aiming to delineate the ore body at depth and define the ore resource.

Several exploration techniques including soil geochemistry, aerial photography, and electrical self-potential were used in Zambia (Mendelsohn, 1961) to detect mineralization and subsequently ore bodies. The Zambian Copperbelt deposits are located in the Southeastern part

of the Lufilian belt, and they represent a cluster of deposits (e.g. Konkola, Nchanga, Chambeshi, Nkana, Mufulira, Lwansha…) including some deposits in the DRC such as Musoshi, Kinsenda, Lubembe, Frontier and Lonshi. The majority of the deposits show mineralization within 200 m interval of siliciclastic rocks (argillite or arenite) of the Ore Member at the base of the Katanga Supergroup, unconformably underlain by a granitic basement (Selley et al., 2005).

The most recent discoveries (Frontier and Kamoa Cu deposits) in the Central African Copperbelt and other existing deposits (e.g. Kinsanfu and Chibuluma) were define primarily through soil geochemistry survey (Broughton and Rogers, 2010; Hitzman et al., 2012; Fleischer, 1984), although additional exploration methods may have been also used afterwards.

The last decade has seen a higher demand of commodities, boosting metal price (e.g. Copper price hits its all-time records of over US $ 9,000 per metric tons in 2008). Nowadays exploration activity has been carried by different private companies with an aim of discovering new deposits though there are huge competition to acquire exploration lease and challenge from social, environmental and politic issues in developing countries. In the CACB, only concealed Cu deposits are likely to remain hidden underground. Exploration geologists should use collectively different techniques, such as remote sensing, geological mapping, geochemical and geophysical method, and drilling to delineate such mineralization.

1.2. LOCATION OF STUDY AREA

The Kaponda Prospect represents 915.8 square km located at about 10 km South of the City of Lubumbashi, 2.5 km SE of the town of Kipushi and 35 km NW of Kasumbalesa, in the Katanga province of the Democratic Republic of Congo (Fig.1). On its southwestern boundary, Kaponda Prospect lies along the international border of the DRC and Zambia.

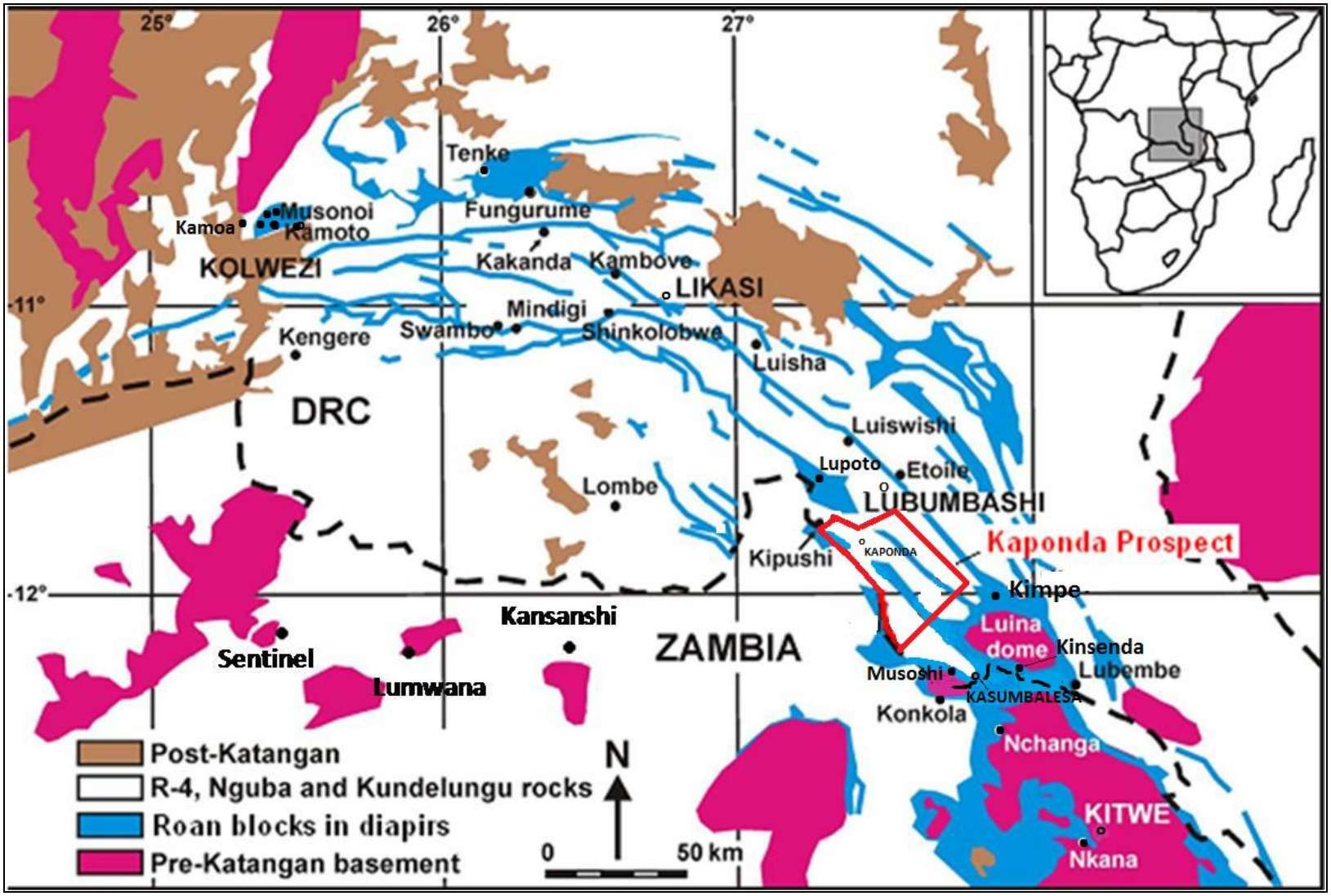

Fig.1. Geological map of the Central African Copperbelt showing location of study area in red box (Kaponda Prospect) and major copper deposits in black dots (modified from El Desouky et al., 2010)

Access to the study area is mainly via the main national road N1, which links the Katanga province to the Copperbelt province in Zambia, from Lubumbashi to Kasumbalesa border post. Additional tributary gravel roads pass through the Prospect.

The Prospect name derives from the local municipality of the same name ("Secteur de Kaponda"), and one of its main village name (Fig.1). However First Quantum Minerals (FQM), a Canadian based mining company, which did significant exploration works in this region, renamed some of the localities as "Kipushi East", "Village" and "Village South" which will be referred in this dissertation by their local names as Nakarimba, Baya and Lumata respectively.

1.3. EXPLORATION HISTORY

From 1906 to 1966, mining and Exploration permits in the Congolese Copperbelt belong exclusively to "Comité Spécial du Katanga" (CSK) and "Union Minière du Haut-Katanga" (UMHK), a company formed by a merger of a Belgium holding company named "Société Générale de Belgique", and British Company Tanganyika Concessions Ltd (Büttgenbach, 1906.). In those early days, exploration was focused on mapping, trenching and pitting of outcropping copper mineralization, from which the first deposits were discovered by UMHK. Etoile and Rwashi Cu-Co deposits, located approximately 15 km N of the study area (Fig.1) were discovered respectively in 1911 and 1919; while Kipushi Zn-Cu-Pb deposit was discovered and mined since 1922 (Kampunzu et al, 2009).

Franz Edward Studt, Jules Cornet and Henri Buttgenbach did the first regional geological mapping of the Katanga province at a scale of 1:500,000 in the early 1900's (Studt et al. 1908; Studt 1908, 1913). Later in 1930 to 1960's more detailed geological map was produced based on exploration activities of pitting, leading to the discovery of several other near surface Cu deposits. The geological map of Congo (former Zaire) at 1/2,000,000 scale, was published by Lepersonne et al. (1974) under the Mines Department of Congolese state services.

In 1966, Gécamines ("Générale des Carrières et des Mines") a Congolese state owned company took over UMHK through nationalization process. The Congolese company was mostly focused on the development of existing high grade copper deposits (e.g. Kolwezi, Kakanda, Kambove and Kipushi deposits) without any significant regional exploration operation.

In the Kaponda Prospect, only large scale-space small pits of 1m of diameter and 5 to 10 m deep, were dug in order to identify bed rocks, generally covered by regolith aiming to produce regional geological map on 1/500,000 to 1/100,000 scale. Any systematic exploration was conducted until 2003 when COMISA ("Compagnie Minière de Sakania") a 100% First Quantum Minerals (FQM) subsidiary, acquired a number of permits including the Kaponda Prospect.

From 2004, exploration activities were carried out including soil geochemical survey, geological mapping, airborne and ground geophysics, reverse circulation and diamond drilling. In September 2010, FQM was forced to withdraw all mining and exploration activities in D.R. Congo, resulting in termination of prospecting work within Kaponda. Being part of FQM team of geologists who worked in the area from scratch to the end, most the data and interpretation presented in this dissertation are from my own work opinion and experience except where referenced otherwise.

1.4. AIM OF THE STUDY

The purpose of this dissertation is to provide a guide line for exploration of sediment-hosted copper mineralization in the tropical environment of the Central African Copperbelt from a green to brown field stages. Exploration techniques, such as remote sensing, geological mapping, soil geochemistry, geophysics, and drilling, are considerably discussed, in order to give their effectiveness and their limitation in this specific metallogenic province of the central African Copperbelt.

Exploration data from a real grass root exploration case study are analyzed and discussed. The interpretation and integration of all geological information derived from different exploration methods will help to generate targets for further drilling follow-up and subsequently identify zone of less interest (e.g. area to neglect). Hence a review of exploration methods which can directly or indirectly delineate sediments-hosted Cu mineralization, is presented in the next chapter.

Chapter 2 REVIEW OF EXPLORATION METHODS

2.1. REMOTE SENSING

Aerial photography has been used by geologist for interpretation of the landscape. In early 1970's the introduction of satellite imagery (Landsat1) has contributed to the improvement of interpretation of terrains. Since then the technology has improved in term of resolution of the images, even in terms of GIS software that processes the primary data to produce the thematic maps. The range of satellite imagery varies from the most available to the public and free satellite images such Landsat and Google earth, to more specific images like Aster; and commercial and very high resolution images (e.g. Spot, Aster, Ikonos, Quickbird) which can be purchased from respective manufactured companies (Whateley, 2009).

Application in mineral Exploration of Remote sensing using the above imageries aims to provide a basic geological map by identifying lithological pattern, rocks boundaries; to detect hydrothermal alteration and to map the structure or any type of lineament. The latter is represented by a line structurally controlled by fracture, joint, fault and vein. These features can be associated to ore mineral system (e.g. NE trend transfer fault is associated to Kipushi Zn-Cu-Pb deposit; Kampunzu et al., 2009).

The geological interpretation of remote sensed image uses two approaches: the spectral and photogeological approaches. Firstly, the spectral approach directly detects surface material based on spectral reflectance. Hunt and Salisbury (1970, 1971a, 1971b) determine the spectra for common rock forming minerals such as silicate, oxide, carbonate and sulfate. While spectra of hydrothermal alteration such as potassic, argillic, phyllitic and propyllitic, have been also determined by Hunt and Ashley (1979). Secondly, the photogeological approach is based on topographical expression to imply geological structure (fault, fold and fracture), lineaments or rock outcrops and boundaries. The key features to evaluate for interpretation are the relief, the textural and tonal variations, the drainages pattern and texture and the vegetation (Lillesand et al., 2004). Due to the thick vegetation cover in the CACB, it is worth to mention that remote sensing is generally used for structure analysis than rock and alteration identification. Lithology and alteration can be directly identified by geological mapping. However satellite images and aerial photographs have been used in the Congolese Copperbelt to identify Mines Series

megabreccia which are associated to classic Cu-Co deposits of this region. These tectonic megabreccia outcrop on hill crest devoid of vegetation due to the high metal content in soil.

2.2. GEOLOGICAL MAPPING

The geological mapping is usually one of the first field works that exploration geologists undergo aiming to delineate outcrop lithology on a fact map and taking structure measurement to understand strain and geometry of the region. Subsequently mapping will identified any structure and lithological unit associated to sought mineralization. The purposes of the mapping (e.g. regional, prospect or pit mapping) will determine the scale on which to map. Hence the amount of details on a map will depend on its scale. For instance regional mapping will be done on small scale (e.g.1:25,000); and pit mapping on a bigger scale (1:500). Exploration mapping mostly starts with small scale map in order to cover a large area thereafter once the area of interest is identified, a more detailed mapping (from 1:10,000 to 1:5,000) will be limited to designated sites.

There are different mapping techniques in exploration: grid mapping, remote sensed image and topographic map base methods, mapping with GPS or DGPS, as well as mapping with tape measure and compass (Marjoribanks, 2010). The first three techniques are the most used in Exploration, the last one is mostly applied for pit and underground mapping on big scale where more details are needed even few meters away from each other. The grid mapping consists of a set of profiles constantly spaced on which geologists will follow as guide to look for outcrops. This technique can be used in established prospect on big scale (1:500 to 1:2,500) on which the same grid controls (pegs) are used for all other exploration method (e.g. soil geochemistry, geophysics).

On the other hand, satellite images of the area to map (worldview, lidar, Google earth…) can be used as a base, with a transparency paper on top, where outcrops and structure measurements are plotted. The advantage of this method is the fact that outcrops and structure measurements are plotted accurately combined with landscape features, associated to large structure that could not be seen from the ground. Interpretation of remote sensed image should be

done before, during and after mapping field work. Geophysical and geochemical data can be used as aid to geological mapping especially in places without outcrops.

2.3. GEOCHEMICAL TECHNIQUES

The mains objectives for geochemical exploration are (1) to identify target for further follow-up using other exploration techniques (e.g. ground geophysics, drilling) in order to delineate mineralization at depth; (2) to be able to identify subsequently area of no interest to negate, and (3) to possibly map lithostratigraphy by using geochemical multielement signatures if available.

To meet these three objectives, a geochemical survey need to be carried out. There are many methods applied in geochemical exploration, including soil sampling, stream sediment, termite sampling, heavy mineral concentrate sampling. The selection of the best technique is normally obtained after doing an orientation survey which will test the effectiveness of different sampling methods on a prospect of similar geological, topographical and climate settings. Aspects to be considered in an orientation survey are well documented by Closs and Nicol (1989). They suggest to take in consideration some of the following features: knowledge of target deposit type, nature of the mineralization dispersion, surficial processes, sample type, sample collection procedures, sample size for analysis, sample spacing, grid orientation and density, sample preparation requirement, analytical method and element to analyze.

Executing an orientation survey can be cost effective and time consuming, but it worth doing it rather than spending much money on a non-effective sampling method. Otherwise a literature reviews for the region, a comparison from the previous historical exploration in the region and consultation of experts, might be convenient to assess the sampling method to use in geochemical survey. In both orientation survey and past experience consultation, the sampling method to choose is the one enhancing the contrast of sought element.

Regardless of the sampling method used, any exploration geochemical survey is subdivided in three parts: sampling, analysis and interpretation. Failure to execute one component correctly will negatively impact the overall exploration outcome. The sample collection and preparation are the most costly stages of geochemical survey. Most of the errors

(contamination, mislabeled, sampling of the wrong horizon…) are also associated to these two processes apart from those related to the chemical analysis (laboratory). A regular and consistent sampling procedure and systematic sampling density and analysis should be applied across the property.

Sample preparation involves three processes including drying, defragmentation and sieving in order to obtain the adequate fraction size for analysis. All these steps are carried out in the field. As suggested by Fletcher (1986a), the choice of the fraction size should be identified from the orientation survey result. It will indicate which fraction is reliable at giving a good contrast of the background and anomaly threshold. Alternatively the fraction size can be also obtained from previous successful exploration work.

Analytical method and results are less of a geochemical concern than sample collection and preparation. Assuming that the sampling is correctly executed, it is a responsibility of the analyzer to ensure the quality of the results. Fletcher (1986b) suggests four main analytical methods: (1) colorimetry, (2) Atomic Absorption Spectrometry (AAS); (3) X-ray fluorescence (XRF) and Inductively Coupled Plasma Spectrometry. The differences between these methods are the detection limit of analysis, speed of analysis and the need to take ion mater into solution. Nowadays, with the advance of technology XRF portable machine are available. They are easy to manipulate, provides faster results that can guide the near term exploration targeting. Analysis results have to be precise and reproducible. To monitor the quality of analysis, exploration geologists and laboratory's chemists should insert into batch of samples, reference materials such standards, duplicates and blanks, in order to check the accuracy, precision and contamination respectively (Thompson, 1983).

The selection of target will be based on the assessment of geochemical data and definition of threshold after analyzing and interpreting the results. The combination of statistical and experiential techniques are used to define background and threshold values. A good geochemical interpretation should consider both negative and positive anomalies. The latter is assumed to be the result of element abundance caused by weathering of ore deposit. However negative anomaly may also express depletion in some elements during rock alteration accompanying ore formation (McQueen, 2008). The absence of positive anomalies does not absolutely prove that a property have no economic potential, maybe the sampling technique was

not adequate for the terrain. For instance a soil survey over area of deep transported overburden will give a typically flat response without any significant contrast (Thomson, 1986). Moreover a concealed ore body completely covered by thick young regolith or barren rock formation which does not allow metal dispersion, will not display geochemical anomalies at the surface. In this case, only appropriate geophysical method can favorably react to a concealed mineralized body.

2.4. GEOPHYSICAL TECHNIQUES

Detailed description of geophysical techniques is beyond the scope of this dissertation. A brief summary of the application of the most commonly used geophysical surveys for base metal exploration is given. Geophysical methods measure physical properties of rocks such as magnetic susceptibility, density (gravity), electromagnetic reflectance, radioactivity; electrical conductivity or resistivity. Unlike ground and down hole geophysics, airborne geophysics are the most cost effective quickest way of obtaining geological information of a large area (Milsom, 2009). In an area of pour outcrop cover like the Central African Copperbelt, geophysics is used to interpret concealed geology.

Therefore geophysical survey are two main objectives in mineral exploration: (1) mapping the physical characteristics of rocks and (2) locate ore minerals (Marjoribanks, 2010). The geophysical method to choose should be able to show contrast between the physical features of the rock hosting the ore body and the surrounding rocks. Depending on the physical variable to measure, exploration geophysics use different methods including magnetic, gravity, radiometric, electromagnetic, electrical surveys.

2.4.1. MAGNETIC SURVEY

It is the most used geophysical method and the cheapest. This survey measures the total magnetic field which includes contribution from the crust and earth's core. A TMI map (Total Magnetic Intensity) will be produced after correction and processing of the primary data. Generally both airborne and ground magnetic maps define domains of similar magnetic background, structures, linear discordant features such as faults, trend lines within different domains. However assigning rock type to different magnetic patterns is very ambiguous as the

ranges of magnetic susceptibility of different rocks are wide and overlapping. Mafic rocks have generally the highest susceptibilities and sedimentary rocks the lowest (Thomas et al., 2000). The magnetic response is mostly function of the amount of magnetite in the rocks or other less magnetic minerals such as pyrrhotite, maghemite and hematite.

A batch of derivatives of the residual total magnetic field is very useful for geological interpretation of the geophysical data. They include the First Vertical Derivative (1VD), the second vertical derivative (2VD), the Analytic Signal (AS), the Total Horizontal Derivative (THD) and Tilt derivative (TDR). On map of these products anomalies are better resolved, the deep (longer wavelength) anomalies are significantly reduced for the 1VD and AS, while low and high amplitude anomalies are normalize in TDR maps. The 1VD is most used for faults analysis, as the anomalies are still dipolar and better resolved because the fall-off rate is more rapid. However the AS anomalies are symmetric and non-dipolar with the pick lying directly on top of the causative body. THD maps the anomaly inflection which lie close to the contacts, therefore AS and THD are good for contact mapping; while TDR with its improved continuity is used for fabric mapping (Corner, 2012). Another transformation of TMI is the reduction to the pole (RTP) to remove the dipolar effect and see anomalies as if they were at the magnetic pole. RTP maps center the anomalies above the causative body; they are used for identifying structures.

To sum up, magnetic data are generally used to map structures and geological features. High resolution magnetic survey can be used directly for the search of iron ore in BIF (Banded Iron Formation), IOCG mineralization style (e.g. Olympic Dam, Reeve et al., 1990; Prominent hill, Belperio et al., 2007), magnetite skarns, pyrrhotite-bearing massive sulphides (e.g. Broken Hill, Walter et al., 2002) and oxidized porphyry copper intrusive.

2.4.2. GRAVITY SURVEY

This survey measures the gravity field which is, to the very minor extent, a function of the density of underlying rocks. To isolate variation related to crustal causes, primary gravity measurements are corrected from effects of earth tides and elevation factors. Two corrections are made to eliminate the elevation factor: (1) compensation of distance variation between the point of measurement and the earth's center of mass (the free-air correction), and (2) to correct the

gravity effect of rock mass between the observation point and the datum, usually sea level (the Bouguer correction, Ford et al., 2006). The gravity maps are commonly displayed in Bouguer gravity anomaly which is the difference between the corrected gravity and the theoretical value of gravity on the reference ellipsoid at the point of measurement.

Ground gravity survey is more accurate and of high resolution than the airborne survey although the former has a slow rate of covering large area. For these reasons, ground gravity survey is mostly used in exploration for base metal, to follow-up anomalies detected by other methods such as magnetic, electrical, electromagnetic or geochemical surveys. The use of gravity to identify a conductive anomaly related to either low-density graphite and carbonaceous shale, or a higher-density sulphide mineralization (Ford et al., 2006).

The method is also used to target directly excess masses or massive sulphides mineral bodies. For example gravity survey played a key role in the discoveries of Neves Corvo massive sulphides deposits in Portugal (Leca, 1990); the high-grade Hishikari epithermal gold deposit of Japan (Izawa et al., 1990); and Olympic Dam and Prominent Hill IOCG deposits in Australia where it was associated to magnetic data (Rutter and Esdale, 1985; Belperio et al., 2007). The interpretation of gravity data has to incorporate the understanding of the local geology as well as the use of data from other exploration techniques.

2.4.3. RADIOMETRIC SURVEY

This survey measures the natural radiation emitted by rocks at the surface. Radiometric images represent the surface materials and have not any depth penetration. K, U and Th are the most significant radioactive elements in rocks and soils (Telford et al., 1990). Of the three elements, the K is the most abundant in the crust. It is mainly incorporated into crystal structure of orthoclase of primary origin such as granite, or from secondary alteration associated to mineralized fluid. Th is found in monazite which is generally an accessory mineral of some granite and pegmatite; whereas U is rarely concentrated and constitutes sought elements for explorers. It can be seen at low concentration in highly fractioned granite or black shale (Marjoribanks, 2010).

Ground and airborne radiometric surveys are used to directly target uranium deposits. Total count and K radiometric data are used to discriminate: (1) alkali igneous rock, (2)

sediments such as arkose deriving from these rocks and (3) potassic alteration (e.g. K feldspar) which might be associated to some base metal mineralization. Radiometric ratios such as U/Th, K/U maps or composite ternary image (K-Th-U) can be used to discriminate different rock types.

2.4.4. ELECTRICAL SURVEYS

These methods are all ground based surveys. A generator supply high voltage electrical current directly into the ground through current electrodes, while an array of receivers measures the electrical conductivity of underlying rocks and minerals. Receiver's configuration will varies from dipole-dipole, pole-dipole, pole-pole, schlumberger, Wenner and gradient arrays. Wenner, pole-pole and gradient are used to investigate the lateral variation of resistivity and chargeability. Schlumberger, pole-dipole and dipole-dipole arrays are used to map the variability of resistivity and chargeability at depth levels by changing the distance between electrodes. However the resolution decreases with the increment of investigated depth (Milsom, 2009). Of the electrical techniques, resistivity and induce polarization (IP) are the most applied in mineral exploration.

Electrical Resistivity survey measures apparent resistivity of the subsurface at different depth depending on receiver's electrodes configuration. Then the apparent resistivity will be computed to generate pseudo cross-section of the true resistivity. The method is used firstly for direct targeting of ore bodies (e.g. Mississipi Valley type); secondly to investigate interfaces such as water tables and horizontal bed rock surfaces and therefore to map the overburden thickness (Ford et al., 2006).

Induced Polarization (IP) survey measures chargeability of the ground in either time-domain or frequency-domain. The chargeability of the ground is how well rock tend to retain electrical charges. After switching off the primary current, the decay of the secondary voltage created on the boundary of the sulphide grains will be measured as well as the size and position of the chargeable body. IP surveys is widely used in mineral exploration because it depend on the surface area of conductive mineral grains rather than their connectivity. As a result IP serves particularly to directly detect concealed disseminated sulfide and massive conductive ore bodies. It led to the discoveries of the San Nicolas VMS deposit in Mexico (Johnson et al., 2000); and the sediment-hosted Pb-Zb Gortdrurn deposit in Ireland (Hitzman and Large, 1986).

Interpretation of electrical survey is sometime ambiguous, as many zones within a rock (with saline underground water) or other rock type (e.g. graphite, carbonaceous shale, barren pyrite-rich rock), have higher chargeability and low resistivity just like disseminated sulphide and massive body (Marjoribanks, 2010). Only a good knowledge of the local geology will allow giving a relevant interpretation of the geophysical anomalies.

2.4.5. ELECTROMAGNETIC SURVEY (EM)

EM survey measures the conductivity of rocks using either natural electromagnetic primary field in the crust or transmitting an external magnetic field. These primary fields induce current flow in conductive rocks which generate a secondary field measured by a receiver. EM survey uses two methodology: the frequency domain (FDEM) where an alternating current generated by transmitter varies sinusoidal; and the time domain (TDEM) where current is pulsed on and off in a duty cycle.

Both ground and airborne EM surveys are among the most commonly used in mineral exploration. It is directly used for delineation of conductive base metal deposits set into resistive country rock and thin regolith cover. However other conductive sources such as swamps, shear and fracture zones, water-filled faults, and graphitic shale, magnetite-rich zone and barren metallic conductors, create a major source of ambiguity in the interpretation of EM anomalies (Ford et al., 2006). Deep weathering and salty groundwater can make EM either unworkable or difficult to interpret. In contrast, the method is most successful in the regions where fresh rock outcrops. EM methods was very decisive in the discovery of massive sulphide deposits of Kidd Creek in Canada and Crandon in the United States (Marjoribanks, 2010 and here within cited).

The Magnetotelluric (MT) method is another electromagnetic survey which measures the natural electrical and magnetic field by recording higher frequencies deeper and long period soundings. Investigated depth can vary from 300 to 10,000m. The MT resistivity combined with Direct Current (DC) Resistivity and IP chargeability form the Titan 24 method developed by Quantec Geosciences, for deep penetration images. Titan 24 utilizes multiple array and measures IP up to depth of 750m and beyond 1500m for MT measurements. The technique can highlight features through thick overburden and cultural noise, it applied to several commodity and

deposits styles such as porphyry Cu, gold, massive sulphide, uranium, magmatic nickel and diamond deposits (Legault et al., 2002; McMonnies and Gerrie, 2007).

2.4.6. BOREHOLE GEOPHYSICAL SURVEY

Several geophysical methods can be adapted in borehole surveys. With the development of the technology in last two decades, the application of downhole survey has become very common in minerals exploration. The technique consists of lowering down hole a probe (a tool that has sensors: transmitter and receiver) which will take measurements and send them simultaneously at the surface through a logging cable. A desktop or laptop is recording data.

There are different type of measurements to be measured by probes as summarized by Killeen (1997): physical property such as magnetic susceptibility and radioactivity; acoustic velocity and density; seismic velocity and resistivity. Also borehole walls can be studied using the acoustic, optical and electrical televiewers.

Information generated from different borehole logs can be used to build 2D or 3D models such as the tomographic image of physical property of the formation between boreholes. The interpretation of borehole geophysical data follows same rules as for the equivalent ground or airborne survey.

2.5. DRILLING

Drilling is one of the most expensive phases of exploration aiming to evaluate mineral resources. Target should be generated accordingly, generally after integration of all available geological, geochemical and geophysical data. There are several types of drilling: auger, rotary air blast (RAB), air core, reverse circulation (RC) and diamond drillings. The application, advantages and disadvantages of each drilling type are given in table 1.

The choice of the drilling method will be function of the purpose of the exploration program. For instance, hand and power auger drilling is used for geochemical sampling in swamp areas where the top soil is deeply developed. RC and diamond drillings are the most used in mineral exploration. Due to its low cost RC will mostly be used for testing geochemical

anomalies if they are related to the underneath bedrock; while diamond drilling is imperatively recommended for resource estimation and provides as well geotechnical and structural data.

Table 1. Comparison of exploration drilling methods (Marjoribanks, 2010)

Drill type	Indications	Advantages	Disadvantages
Hand auger	Geochemical sampling in upper few meters of unconsolidated material	Hand portable and operable. Uncontaminated sample. Cheap	Poor penetration
Power auger (post-hole digger)	Geochemical sampling in upper few metres of unconsolidated material	Small lightweight machine – vehicle mounted or hand operated. Quick, cheap	Poor penetration (better than hand auger). Sample contamination
Rotary air blast (RAB)	Geochemical sampling to base of regolith Ideal regolith sampling tool	Large sample volume. No site preparation needed. Quick and relatively cheap. Some rock chip geological data	Poor penetration of hard rocks. Sample contamination. Limited depth. No structural data
Air core	Geochemical sampling where good characterisation of bedrock required	Small rock core return. Minimal contamination. Relatively quick and cheap. Can penetrate heavy clay/mud	Small sample size
Reverse circulation (RC)	Geochemical sampling hard and soft rocks to 200 m + Ore body proving above water table	Uncontaminated large volume sample. Rock chip geological data. Relatively quick and cheap cf. diamond	Large heavy rig may need access preparation. Limited structural data. Poor orientation control
Diamond	Ore targeting and proving to 1,000 m + High quality sample. Geological/structural understanding	Maximises geological information. Uncontaminated, undisturbed high-recovery sample. Accurate hole positioning/control	Some site preparation required. Water supply required. Relatively small sample size. Slow. Expensive

Chapter 3 REGIONAL GEOLOGY OF THE KATANGA SUPERGROUP

3.1. TECTONIC SETTING AND BASIN EVOLUTION

The folded Lufilian belt is located between the Congo and the Kalahari cratons (Fig.2, a). It is among the Pan-African orogenic belts that led to the assembly of the west and east Gondwana during Neoproterozoic to early Paleozoic age (Wilson et al., 1993; Porada & Behorst, 2000). In the southern Africa, Pan-African belts, including Damara, Zambezi, and Lufilian, show the Neoproterozoic extension followed by basin development and finally prolonged tectonic quiescence for a period of about 200 Ma (Porada, 1989).

The Archean basement rocks of the Kalahari and the Congo cratons are separated from the Neoproterozoic Lufilian formation by Mesoproterozoic Irumide and Kibaran belts, respectively (Fig.2, b).

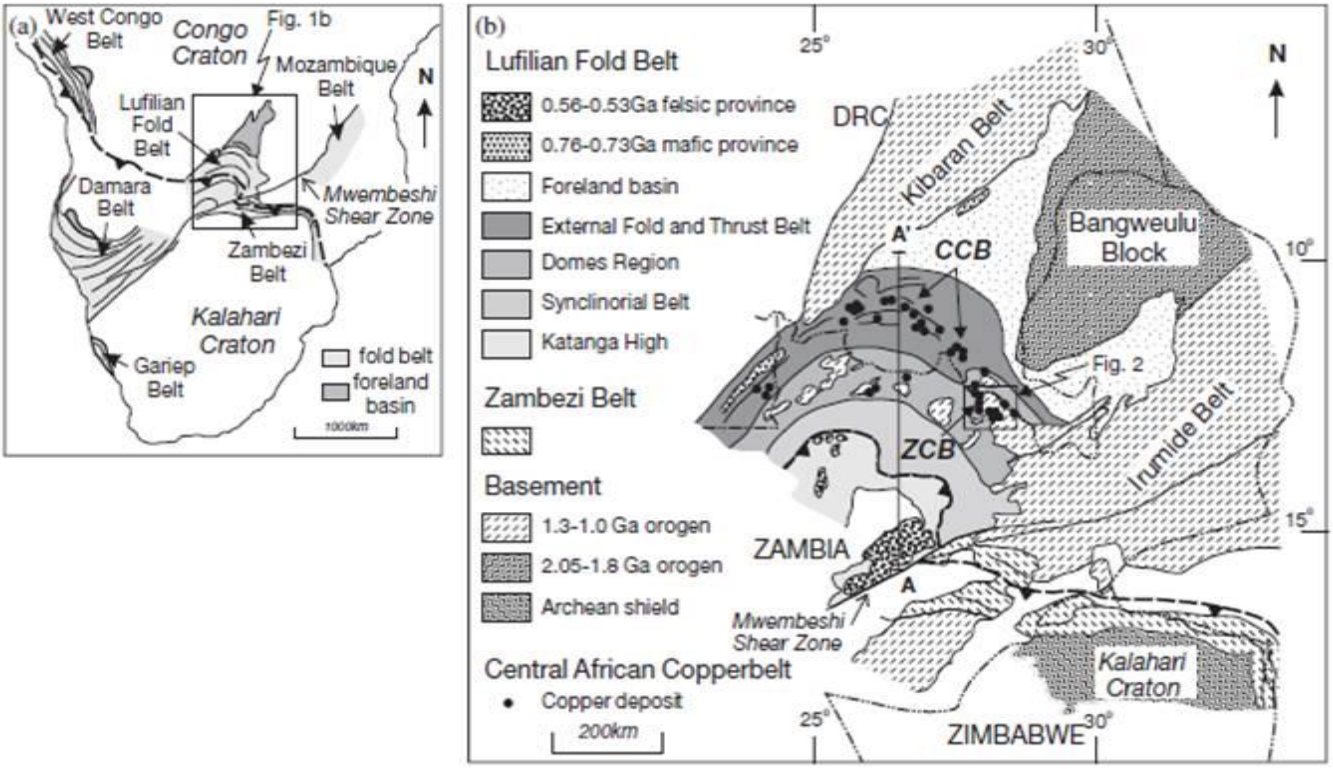

Fig.2. Tectonic setting and structural domains of the Lufilian belt. (a) Pan-African system of central and southern Africa. (b) Tectonic domains of the Lufilian belt with copper deposits location (Selley et al., 2005).

The Katangan basin was formed as result of the fragmentation of Rodinia, a surpercontinent to Gondwana, forming eastward younging basins from Namibia to Mozambique between 1100 and 850 Ma (Unrug, 1997). The Katanga sequence was then deposited in intracontinental rifting system, or accumulated in bifurcating rifts (Unrug, 1988; Porada, 1989). The continental rifting leading to the formation of the passive continental margin, was accompanied by magmatism such as Kafue rhyolite (879Ma), Nchanga granite (877Ma) and Lusaka granite (865Ma) (Porada & Berhorst, 2000).

The Katanga Supergroup consists of approximately 10 km thick sediments (Batumike et al., 2007) deposited between 883-573Ma (Armstrong et al., 2005; Master et al., 2005). Initially the Katanga basin was respectively filled by coarse and medium grained terrigenous siliciclastic basal units, represented by fluvial conglomerate and sandstone devoid of volcanic activity. They are overlain by finer grained carbonate and evaporitic sequence that record a transition to marine or lacustre environment within relatively restricted fault controlled intracontinental basin (Selley et al., 2005).

A second extension period occurs within the Katangan belt between 765-735 Ma (Key et al., 2001). It is reflected by gabbroic to dioritic sill bodies in the western Zambia, and pyroclastic or extrusive units in the northern part of the Lufilian arc of the DRC (Kampunzu et al., 2000). The Basin inversion marked the beginning of the Lufilian orogeny which span a period of over 100 Ma with the main orogenic phase occurring between 560 to 530Ma (Hanson et al., 1993). The switch from the extension to compression regime results in the opening of Kundelungu foreland basin situated between the Kibaran belt and the Bangwelu block (Fig.2,b); and therefore the deposition of glacial tillite ("Petit Conglomerat"), cap carbonate and overlying terrigenous siliciclastic tabular and undeformed formation (Batumike et al, 2007; Master et al., 2005).

Mendelsohn (1989), Binda (1994) and Jackson et al. (2003) argued against the full-scale rifting environment for the deposition of the Katanga sequence, favoring a passive style of basin development, without significant rifting, where the influence of eustasy outweighed that of slow subsidence rates. For the above authors, the lower Katangan (Roan group) being a low-energy lithostratigraphy unit, with the lateral extension and continuity of the mineralization along the Lufilian belt in Zambia and Congo favored an epicontinental marine embayment with minor

fault. The absence of early volcanism until late Roan (Cailteux et al, 1994), dikes swarms and magnetic anomalies does not approve a rift setting (Jackson et al., 2003)

3.2. LITHOSTRATIGRAPHY

The stratigraphic subdivision of the Neoproterozoic Katanga Supergroup in the DRC has changed through time (François 1974, 1987, 1995; Cailteux et al 1994; Wendorff, 2003; Cailteux, 2003; Batumike et al., 2007) and has been also subject of controversy (Wendorff 2000, 2003, 2005; Kampunzu et al., 2003, 2005; Cailteux et al., 2005a). Traditionally the Katanga Supergroup was subdivided into the Roan, Lower and Upper Kundelungu (Francois, 1995; Cailteux et al., 1994). Nowadays most researchers are using lithostratigraphy subdivision of Cailteux (2003), Cailteux et al. (2005a) and Batumike et al. (2007); consisting of Roan, Nguba (formerly Lower Kundelungu) and Kundelungu (ex-Upper Kundelungu; Table 2).

On one hand, Wendorff (2003, 2005) suggests a Katangan stratigraphy subdivision of five Groups: Roan, Nguba, Kundelungu, Fungurume and Plateau, assuming that the Congo-type lower Roan formations (RAT, Mines and Dipeta Subgroups) were tectonically deposited in the Katangan foreland basin during Lufilian orogeny. He considers the mentioned formations as partly coeval with the Biano (Plateau) Subgroup, the uppermost member of the Katangan sequence. On the other hand, lithological and geochemical data from Kampunzu et al. (2005) Batumike et al. (2006, 2007), combined with previous structural and geochronological studies (Demesmaeker et al., 1963; Kampunzu and Cailteux,1999) do not support Wendorff (2003, 2005) stratigraphy succession. In this dissertation, we adopt the lithostratigraphy scheme and terminology of Cailteux (2003) and Cailteux et al. (2005a) with some amendment from Batumike et al. (2007); the Katangan Supergroup divided into three Groups: Roan, Nguba and Kundelungu.

Table 2. Lithostratigraphy of the Katangan Supergroup in DRC (Batumike et al., 2007)

Supergroup	Group	Subgroup	Formation	Former nomenclature (François, 1987)	Members and lithologies
±500 Ma	Kundelungu Ku (formerly Upper Kundelungu)	Biano Ku 3		Ks 3	Arkoses, conglomerates, argillaceous sandstones
		Ngule Ku 2	Sampwe — Ku 2.3	Ks 2.2	Dolomitic pelites, argillaceous to sandy siltstones
			Kiubo — Ku 2.2	Ks 2.1	Dolomitic sandstones, siltstones and pelites
			Mongwe — Ku 2.1	Ks 1.3	Dolomitic pelites, siltstones and sandstones
		Gombela Ku 1 (formerly Likasi)	Lubudi — Ku 1.4	Ks 1.2.4	Alternating pink oolitic limestone ("Calcaire de Lubudi") and sandy carbonate beds
			Kanianga — Ku 1.3	Ks 1.2.2 and 1.2.3	Carbonate siltstones and shales
			Lusele — Ku 1.2	Ks 1.2.1	Pink to grey micritic dolomite ("Calcaire Rose")
(±620 Ma)			Kyandamu — Ku 1.1	Ks 1.1	Petit Conglomérat tillite/diamictite
	Nguba Ng (formerly Lower Kundelungu)	Bunkeya Ng 2	Monwezi — Ng 2.2	Ki 2	Dolomitic sandstones, siltstones and pelites
			Katete — Ng 2.1	Ki 1.3	Dolomitic sandstones or siltstones in northern facies; alternating shale and dolomite beds ("Série Récurrente") in southern facies
		Muombe Ng 1	Kipushi — Ng 1.4	Ki 1.2.2	Dolomite with dolomitic shale beds
			Kakontwe — Ng 1.3		Carbonates
			Kaponda — Ng 1.2	Ki 1.2.1	Carbonate shales and siltstones; "Dolomie Tigrée" at the base
±750 Ma			Mwale — Ng 1.1	Ki 1.1	Grand Conglomérat tillite/diamictite
	Roan R	Mwashya (formerly Upper Mwashya) R 4	Kanzadi — R 4.3	Upper Mwashya R 4.2	Sandstones or alternating siltstones and shales
			Kafubu — R 4.2		Carbonaceous shales
Katangan			Kamoya — R 4.1		Dolomitic shales, siltstones, sandstones, including conglomeratic beds and cherts in variable position
		Dipeta R 3	Kansuki — R 3.4	Lower Mwashya R 4.1	Dolomites including volcaniclastic beds
			Mofya — R 3.3		Dolomites, arenitic dolomites, dolomitic siltstones
			R 3.2		Argillaceous to dolomitic siltstones with interbedded feldspathic sandstones or white dolomites; intrusive gabbros
			R.G.S. — R 3.1		Argillaceous dolomitic siltstones ("Roches Gréso-Schisteuses")
		Mines R 2	Kambove — R 2.3		Stromatolitic, laminated, shaly or talcose dolomites; locally sandstones at base; beds of siltstones at top
			Shales Dolomitiques — R 2.2		Dolomitic shales including three carbonaceous horizons; occasional dolomites
			Kamoto — R 2.1		Stromatolitic dolomite (R.S.C.), silicified/arenitic dolomites (R.S.F./D.Strat.), grey argillaceous dolomitic siltstone at the base (Grey R.A.T.)
		R.A.T. R 1			Red argillaceous dolomitic siltstones and sandstones ("Roches Argilo-Talqueuses")
	Base of the R.A.T. sequence unknown				
<900 Ma					Basal conglomerate

3.2.1. ROAN GROUP

Within the thrust-and-fold belt in the DRC, the Roan Group is subdivided from bottom to top in four: RAT ("Roches Argilo-Talqueuses" or R 1), Mines (R 2), Dipeta (R 3) and Mwashya (R4) Subgroups (Table 2). The Roan succession contains several transgressive and regressive sequences (Lefebvre, 1978) characterized by two major cycles of continental to sub-continental deposition followed by carbonate platform-sediments (Cailteux, 1994). Although its basal part is unknown, RAT formations are believed to be deposited transgressively over pre-Katangan basement with siliciclastic coarse grained rock (sandstone) within its lower part and dolomitic sequence (dolomitic siltstone) in its upper part (Cailteux et al., 2005a). Oxidized red massive to interbedded terrigenous dolomitic siltstone of RAT are believed to be continental and supratidal (Katekesha, 1975).

The Mines Subgroup (R2) overlies RAT. The former is believed to be the carbonate platform of the first Roan deposition cycle. Unlike RAT Subgroup deposited in oxidized conditions, R2 sedimentation occurs in a reduced, intertidal, lagoonal and algal environment. It hosts the bulk of copper-cobalt deposits in the DR Congo (Cailteux, 1994). The Mines Subgroup is subdivided into three Formations (Cailteux, 1994, 2003): (1) Kamoto (R 2.1) which marks a major lithological change and a marine transgression; (2) "Shale Dolomitiques" (SD or R 2.2) and (3) Kambove or CMN (Calcaire à Minerai Noir or R 2.3) (Table 01).

After the deposition of Mines Subgroup, a regression occurs during Dipeta (R3) sedimentation period, depositing siliciclastic rocks comprising oxidized hematitic, dolomitic siltstone and sandstone similar to the RAT facies (Cailteux, 1994; Hitzman et al., 2012). The upper part of R3 comprises evaporitic lagoonal deposits of carbonates, dolomitic shale and siltstone.

The Mwashya (R4), is the uppermost member of the Roan Group and represents a transgressive cycle evolving from reef barrier facies in its lower parts to a lagoonal or marine in the upper formation (Lefebvre, 1978). It comprises dolomitic shale, siltstones, carbonaceous shale and feldspathic sandstone; and also contains pyroclastic units with magnetite-hematite banded iron formation both considered as markers for the Lower Mwashya (Lefebvre, 1973,

1975; Cailteux, 1994). Mwashya rocks are overlain by a regional diamictite forming the base of the Nguba Group (Francois, 1974; Cailteux, 2003; Batumike et al., 2007).

Wendorff (2003) and Master et al. (2005) consider Mwashya Subgroup to be the lowermost part of the Nguba Group. According to these authors, the Mwashya rests unconformably on the upper Roan (Dipeta) and passes conformably into Grand Conglomerat in some localities (Cahen, 1978).

3.2.2. NGUBA GROUP

Formerly named Lower Kundelungu (Francois, 1973; Cailteux 1994), the Nguba Group is the second member of the Katangan Supergroup, overlaying the Roan Group. It is divided into two major units, namely the Muombe and Bunkeya Subgroups (Table 01). The base of the Nguba is represented by a regional diamictite marker, the "Grand Conglomerat" also called Mwale Formation (Batumike et al., 2007).This is the most continuous formation within the entire Katangan basin. It is a diamictite deposited between 765-735 Ma during worldwide sturtian glaciations (Master and Wendorff, 2011). Its thickness decreases southward with a maximum of 1300m in Nzilo area. The Grand Conglomerat is fine to medium grained matrix-supported conglomerate with pebble and cobbles of different origin (Francois, 1987). There is evidence of glacial origin for this diamictite based on its polymictic texture, striated clasts, poorly sorted and fined grained matrix supported diamictite, and dropstone (Francois, 1973; Binda et Van Eden, 1972; Master et al., 2005; Batumike et al, 2007, Master and Wendorff, 2011).

Throughout the Katanga basin, the Grand Conglomerat varies in facies from continental, to shallow marine and deep marine. This change of facies is controlled by sedimentation environment, ongoing tectonic and variation of climate and ice dynamic (Master and Wendorff, 2011).The Grand Conglomerat has a cup carbonate like its equivalent tillites from other regions of the world. The overlaying units consist of dolomitic shale and dolomites belonging to Kaponda, Kakontwe and Kipushi Formations of the Muombe Subgroup (Table 01). There is also a facies change in these formations, with more siliciclastic rocks in the North of the Katangan basin, and more carbonates in South (e.g. Kipushi area) (Batumike et al, 2007). The upper part of

Nguba Group, the Bunkeya Subgroup consists of siliciclastic units made of sandstone and pelite (Batumike et al., 2006).

3.2.3. KUNDELUNGU GROUP

A second glaciogenetic diamictite, the "Petit Conglomerat" marks regionally the base of Kundelungu (Cahen 1954; Francois, 1987). The Petit Conglomerat overlies the Nguba Group with a probable erosional unconformity (Wendorff 2003). Its thickness increases northward with 80 m in Kalule area (Vanden Brande, 1936) and 24m in Kipushi area (Master et al., 2005). However the Petit Conglomerat also thins toward the northwestern margin of the Katanga basin with 25m in Makonga region next to the Kibaran belt (Dumond and Cahen, 1977). The North-South facies change from sandy to pelitic matrix, and bedding suggests glacio-marine deposition in the South (e.g. in Kipushi and Luiswishi areas; Batumike et al., 2007).

Although the Petit Conglomerat is overlying by a cup carbonate ("Calcaire rose"), the remaining upper members of the Kundelungu are made up of siliciclastic rocks, except from the oolitic limestone of the Lubudi Formation (Table 2). The upper most member of Kundelungu, the Biano Subgroup and the Sampwe formation, represent undeformed and tabular sediments deposited in the Katangan foreland basin after the Lufilian orogeny (Master et al, 2005; Batumike et al., 2007).

Wendorff (2000) interpreted RAT formation (the lower Roan, Table 2) as syn-orogenic sediments of the Katangan foreland basin, younger than Kundelungu where it deposited on angular unconformity. However Cailteux et al (2005a), demonstrate the sedimentation continuity between RAT and the overlaying Kamoto Formation. Moreover geochemical data of Kampunzu et al. (2005) shows continuity between RAT and overlaying Mines Subgroup, both deposited within a same rift basin of euxinic and evaporitic environment.

Furthermore, geochronological data constrains RAT rocks to be older than Kundelungu. Uranium veins crosscutting RAT in Shinkolobwe and Luiswishi deposits date respectively >690 Ma and 625Ma, relatively older than the base of Kundelungu and much older than it upper part (Loris et al., 1997; Kampunzu and Cailteux, 1999). The "Petit Conglomerat" at the base of Kundelungu is correlated to the world wide Marinoan glacial deposits (+/-620 Ma), or

specifically correlated to Ghaub diamictite of the Damara belt dated at 635.5+/-1.2 Ma (Hoffmann et al., 2004; Master et al., 2005). The Biano Group (Masters et al., 2005) at top of Kundelungu sequence indicates a younger detrital muscovite age of 573+/-5Ma to be maximum age for sedimentation of Kundelungu Group.

3.3. STRUCTURE

The compression regime initiated the convergence of the Congo and the Kalahari craton, resulting in the detachment of the Katangan sedimentary rock succession from the basement, causing a north-directed folding and thrusting that led to the formation of the Lufilian belt (Unrug, 1987). The Lufilian fold belt consists of four tectonic units, north convex and arcuate structural domains namely from north to south, the external fold-and-thrust belt (the outer Lufilian), the domes region (Middle Lufilian), the synclinorium belt (the Inner Lufilian), and the Katanga High (Fig.2, b & Fig.3).

In the Congolese Copperbelt, copper deposits occur within the External fold-and-thrust belt. This tectonic domain preserves the thickest Katanga unit where basement rock is not observed. The absence of basement is generally considered to reflect widespread decoupling along evaporitic strata at depth, such that lower strata of the Katangan Supergroup were thrust emplaced toward the top of the tectonic pile (Kampunzu and Cailteux, 1999; Porada and Berhorst, 2000; Jackson et al., 2003). Evaporites likely facilitated fluid over pressuring beneath thrust sheets and halokinesis (François, 1973; De Magnée and François, 1988; Cailteux and Kampunzu, 1995; Jackson et al., 2003).This Outer Lufilian belt consists of thin skinned thrust-dominated geometry, with complex, macro scale fragmentation (Fig.3).

Further south of the external fold-and-thrust belt is the Dome Region (Fig. 2, b). The latter appears mainly in Zambia where basement inliers form tectonic stacked thrust sheets (Fig.3) of Katanga metasediments (Coward and Daly, 1984; Cosi et al., 1992) with upright to recumbent high amplitude folds (Selley et al., 2005). Exposed basement units are believed to represent culminations above thrust ramps (Daly et al., 1984). The synclinorium belt occurring entirely in Zambia (Fig.2, b), is poorly exposed and characterized by large scale open folding (Fig.3) at a low metamorphic grade (Loughlin, 1979). It reflects a change from a marginal shelf

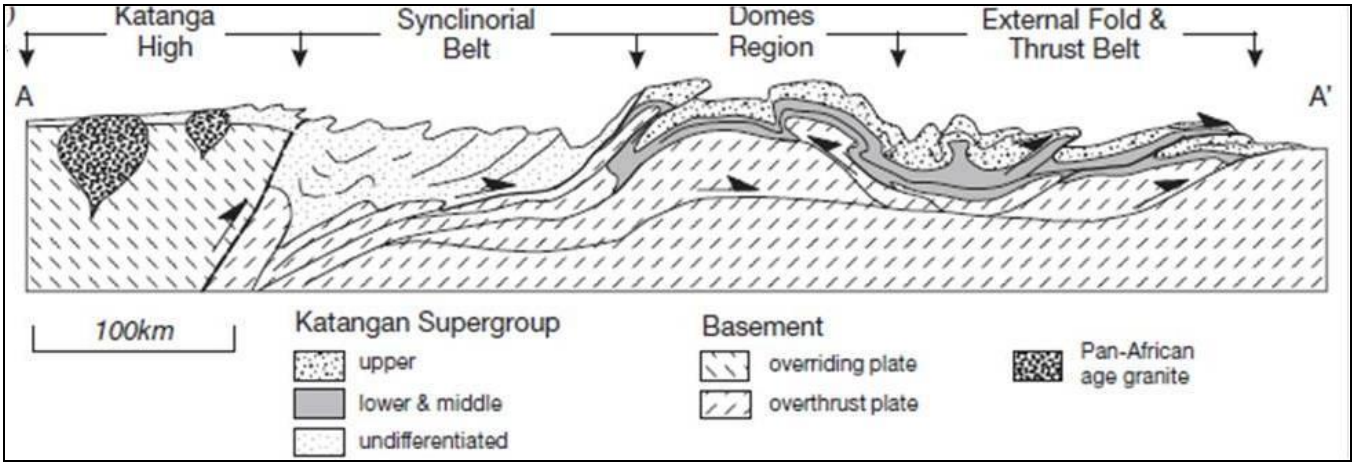

Fig.3. Cross section AA' (located on Fig.2, b) showing structure within different tectonic domains of the Lufilian belt (Selley et al., 2005).

in the north, to a deeper basin (Cosi et al, 1992).

Finally the Katanga high in the southern end of the Lufilian belt is poorly known with only higher parts of the Katanga Supergroup outcropping along with Neoproterozoic to early Paleozoic granitic body (Hanson et al., 1993). The southern margin of the Katanga high is represented by sinistral, east-northeast–trending Mwembeshi shear zone (Fig.2, b). Kinematic indicates northwest- to northeast-directed thrusting during Neoproterozoic to Cambrian convergence of the Kalahari and Congo cratons (Daly, 1986).

3.4. MAGMATISM

Unlike in the pan African Zambezi belt where bimodal volcanic rocks occur at its base (Hanson et al, 1994), the Katangan Supergroup did not record any syn-rift volcanism in it lowermost part suggesting an initial basin evolution during a time of relatively subdued crustal heat flow and attenuation (Selley et al., 2005). Mafic to intermediate igneous bodies and basaltic lava occur in the Northwestern zone of the Lufilian belt (Key at al., 2001) in the middle part of the Katangan Supergroup (Mwashya period) dated around ~765 to 763. A NE trending basaltic lava occurs from the NW of Zambia into the DRC up to Kibambale area (Unrug, 1987; Kabengele et al, 1987; Kampunzu et al 1993). Pyroclastic units are also observed within Lower

Mwashya in the Congolese Copperbelt (Lefebvre, 1973; Cailteux, 1994). These mafics are interpreted to be a result of extension associated with significant stage of intracontinental rifting.

The Katanga high in the southern part of the Lufilian belt (Fig.2, b) is intruded by Paleoproterozoic granitoids dated at 570-530 Ma (Hanson et al., 1993). Young intrusions of nepheline-syenite from Mukumi area North of the Mwombezhi Dome has been reported in the North western province of Zambia (Cozi et al., 1992), interpreted as continuation of post – orogenic uplift and slow cooling of the Lufilian Orogeny (Rainaud et al., 2005).

3.5. METAMORPHISM

In the Lufilian belt and it foreland basin, the degree of metamorphism varies from one tectonic zone to another. The Katanga foreland basin in the North comprises undeformed to tabular rocks deposited after the Lufilian orogeny, therefore it did not undergo any metamorphism (Batumike et al, 2007). On the other hand, in the outer Lufilian belts or the fold-and-thrust belt (Fig.2b), rocks undergo several phases of deformation during basin inversion and subsequent orogeny. Surprisingly the degree of metamorphism remains generally law grade (Belliere, 1969). However it increases from north to South from prehnite-pumpellyite to lower green schist facies (Drysdall et al., 1972; Selley et al., 2005); with chlorite, sericite and locally biotite occurring in the South East (Cluzel, 1986).

In the dome, the degree of metamorphism decreases eastward from amphibolite to upper green schist facies (Selley et al., 2005). Biotite and phlogopite appear in the Zambian Copperbelt province (Ramsay and Ridgeway, 1977). The Northwestern province of Zambia records the highest metamorphism of the Lufilian belt where Garnet-kyanite assemblage are common with local development of talc-kyanite white schist (Cosi et al., 1992; Broughton et al., 2002) or kyanite-phlogopite. No evidence of eclogite facies has been observed in the region (Outhwaite et al., 2010, unpubl.).

The metamorphism within the Synclinorium belt is of law grade reflecting a change from marginal shelf in the north to a deeper basin (Cosi et al., 1992; Porada and Berhorst, 2000). In short, the variation of Katangan metamorphism is attributed to crustal exhumation and thrust stacking of the basement rocks and Katangan rocks associated to closure of the southern ocean

basin (Porada and Berhorst, 1998; John et al., 2004).

3.6. MINERALIZATION

The Central African Copperbelt is the word largest sedimentary copper district with over 200Mt contained copper in both the Congolese and Zambian Copperbelts, including the North western province of Zambia. Deposits are hosted in several lithologies (Fig.04) at different stratigraphy level (Hitzman et al., 2012; Selley et al., 2005). Different size of Cu deposits (Fig.05) occur in the CACB, from giant of more than 10Mt Cu (e.g. Konkola, Lwanshya, Nchanga, Mufulira, Nkana, Kamoa, Tenke-Fungurume and Kolwezi district) to big and medium-size deposits (e.g. Lumwana, Sentinel, Kipushi, Kansanshi, Chambeshi, Frontier) and many other smaller deposits. These deposits are mostly associated with other base metals such as Cobalt, Lead, Zinc, Nickel, Uranium; or precious metal (Au, Ag, PGE) (Cailteux et al., 2005b).

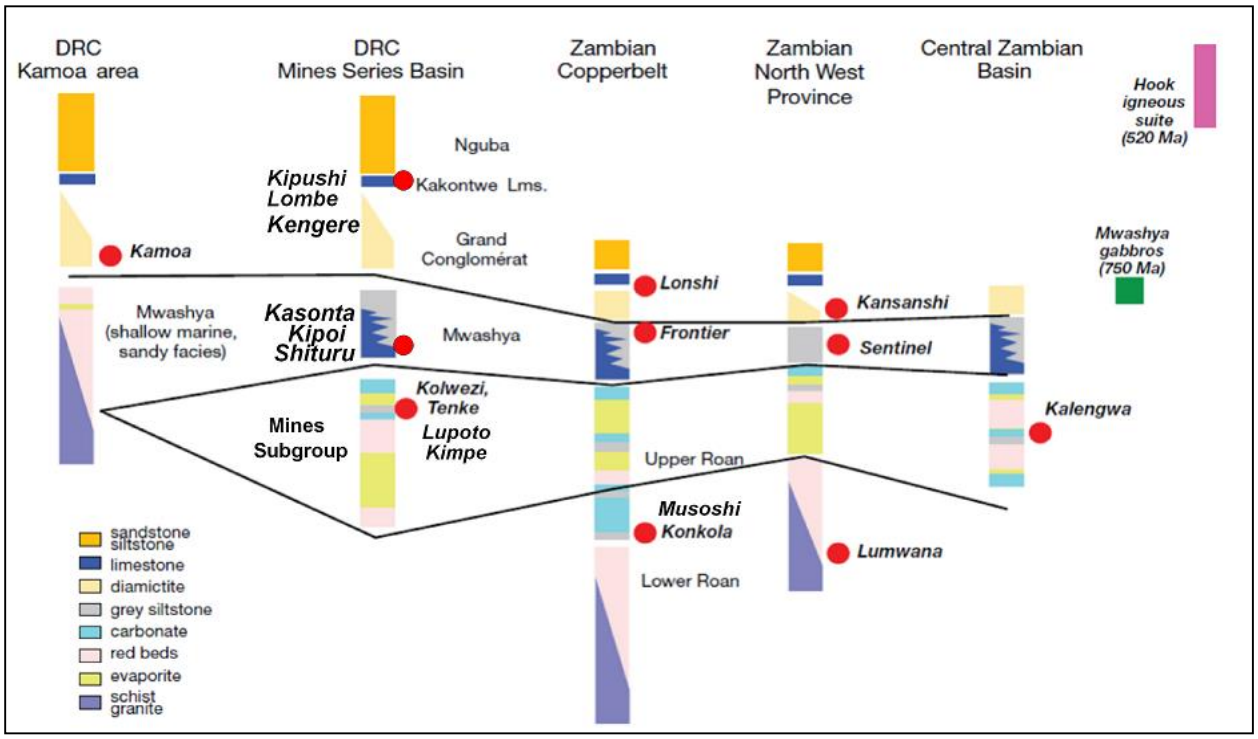

Fig.4. Generalized stratigraphic columns correlation between Congolese, Zambian Copperbelts and the Northwestern Province area showing stratigraphic location of selected deposits (modified from Hitzman et al., 2012).

There are three regional metal zonation within the Congolese fold-and-thrust belt (Fig.5) containing in total approximately half of copper of the CACB (Hitzman et al, 2012). Firstly an association Cu-Co mineralization appears in the northern outer part of the fold-and-thrust belt (e.g. Kimpe, Etoile, Luisha, and Kambove, Fungurume, and Kolwezi deposits). Copper is generally associated to cobalt at average ratio of Co: Cu =1:13 (Cailteux et al., 2005b). Secondly an inner part of the belt rich in U-Cu-Ni mineralization (e.g. Shinkolobwe, Menda, Midingi deposits). Finally the southern part of the Congolese Copperbelt comprises the association Zn-Cu-Pb (e.g. Kipushi, Lombe and Kengere deposits).

Traditionally Cu-Co deposits occurs within dolomitic rocks of the Kamoto Formation and Dolomitic Shale (SD Formation), respectively the lower and upper ore bodies of the Mine Subgroup (Cailteux et al., 2005b). These deposits appear as allochthonous scrambled Mines Subgroup blocks ("écailles") of 10 to 1000's meters in length and down dip, folded and faulted within diapiric megabreccia (Schuh et al., 2012; Hitzman et al, 2012).

Megabreccia are interpreted to derive from fragmentation along evaporitic horizons associated to 150km of syn-orogenic northward mobilization of Roan thrust sheets during Lufilian inversion (Francois, 1973,1974; Kampunzu et Cailteux, 1999; Porada and Berhorst 2000). Jackson et al., 2003 suggest, for the origin of the megabreccia, a salt tectonic model that started during basin extension and continue in the inversion period. Even though primary sulphide mineralization is represented by dissemination, blebs and fracture filling (veins) of chalcopyrite, carrollite and bornite (El Desoulky et al., 2010); the bulk of this Congolese type of mineralization is supergene enriched sulphides (e.g. chalcocite) and oxide ore (malachite, azurite, chrysocolla, heterogenite) grading on average from 4 to 6% Cu (Hitzman et al, 2012) .

Epigenetic Zn-Pb-Cu massive sulphide deposits are hosted within carbonate rocks of the Lower Nguba Group (Francois, 1974) and consist of Kipushi, Kengere and Lombe (Fig.5). In the central province of Zambia, similar Zn-Pb-Cu mineralization occurs in Kabwe (Kampunzu et al, 2009).

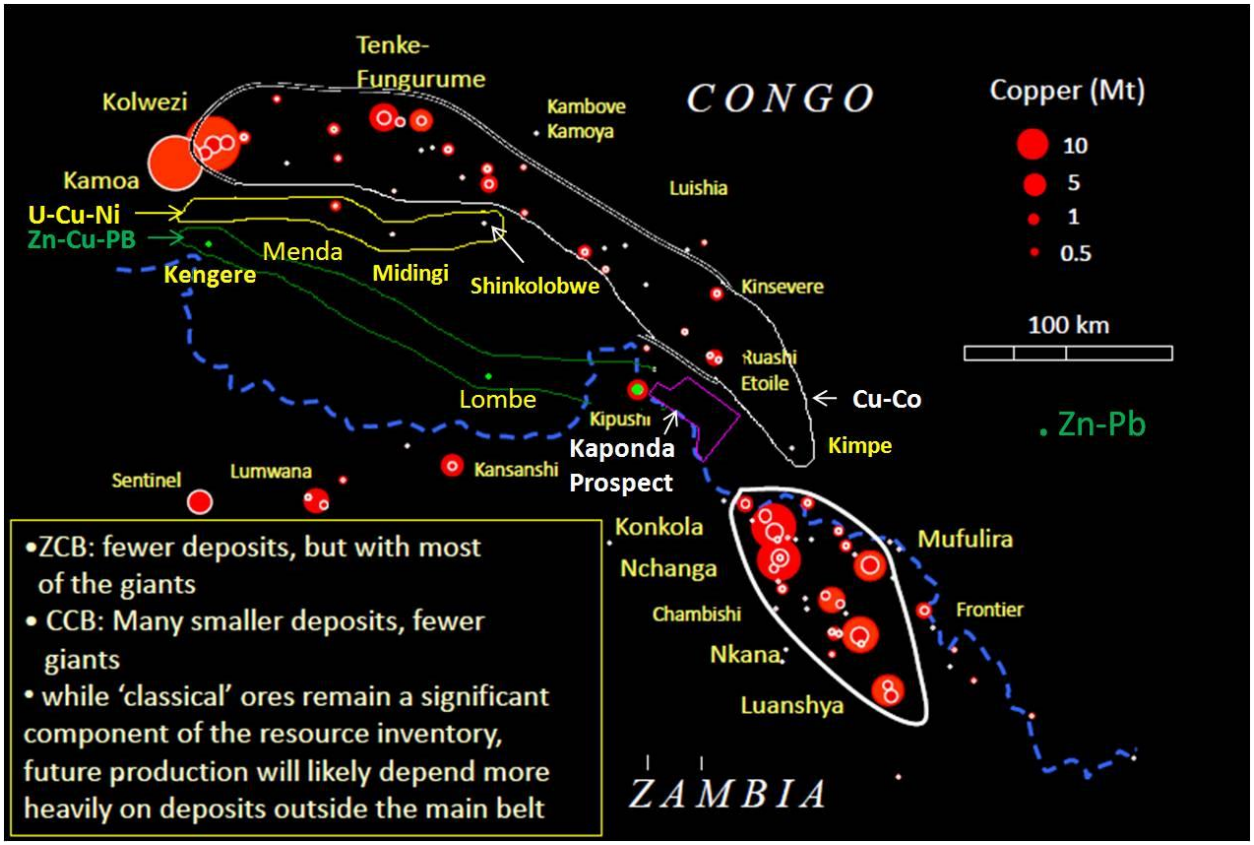

Fig.5. Distribution of copper deposit in the Central African Copperbelt and metal zonation (modified from Selley, 2012).

As far as this dissertation is concerned, Kipushi Zn-Cu-Pb deposit is very important for two reasons: (1) its size and mineralization style, and (2) its location comparing to the Kaponda Prospect, our study area. Firstly, the deposit is one the biggest multielement deposit with over 6.6Mt Zn and 4Mt Cu mined from ore grading 11 wt% Zn and 6.8 wt% Cu. The remaining ore resource down to the 1500 m level is estimated at >5 Mt Zn, >500,000 tons Cu, and 100,000 tons Pb from ores averaging 21.4 wt % Zn, 2.1 wt. % Cu and 0.88 wt. % Pb with additional trace metals of Cd (763 ppm), Co (100 ppm), Ge (68 ppm), Ag (28 ppm) and Re (3 ppm) (Cailteux, 1992; Kampunzu et al., 2009). Secondly, the deposit is located in the northern limb of a NW–SE trending anticline that continues to the SW into Kaponda Prospect.

Kipushi deposit is associated to NE trend transfer fault, it is also characterized by a faulted axial breccia filled with a megabreccia known as axial breccia. The latter consists of silicified, talc-rich dolomites with chloritic and silty matrix. This extruded breccia contains fragment deriving from the Dipeta Subgroup (De Magnée and François, 1988). Primary Zn-Cu-

Pb sulphide mineralization (sphalerite, chalcopyrite, bornite, and galena) forms larger discordant and minor sub-concordant ore bodies within respectively carbonates of Kakontwe formation and dolostones of Kipushi-Katete Formations. Additional discordant ore body is within a second generation of collapsed breccia that postdates and crosscuts the axial breccia (Intiomale and Oosterbosch, 1974). This second generation of breccia may be related to salt tectonic that affected the Lufilian belt (De Magnée and Francois, 1988).

Other examples of different lithostratigraphy hosting stratiform and stratabound Cu deposits hosted in Mwashya, Grand Conglomerat and Kundelungu. There are few know deposits such as Shituru, Kipoi, Kansota in Likasi and Lwishya districts, occurring in lower Mwashya Subgroup (Fig.4) above the traditional Mines Subgroup (Cailteux et al, 2005b). For instance, in Shituru (Likasi district), supergene copper mineralization (up to 10% Cu and 2% Co), is hosted within dolomitic shale in a southern limb of a faulted anticline along its fold axial plane (Lefebvre, 1974). Frontier Cu deposits in the SE of the Congo near Mufulira, is hosted in shale of the Upper Mwashya (Hitzman et al., 2012).

Interestingly, recent discoveries have revealed Cu deposits (Kamoa, Dikulushi, Lukufwe deposits) in the western and northern Lufilian Foreland basins. The Kamoa giant copper deposit occurs adjacent to a large N-NE–trending structure defining the boundary between deformed salt-associated rocks of the Kolwezi district to the east and the flat-lying sedimentary sequence of the Western foreland to the west (Key et al., 2001).The giant Cu deposit has a resource estimated at 810Mt ore at 2.69% Cu (Schmandt et al., 2013). It is hosted within Grand Conglomerat (Fig.4) of the Nguba Group at the lowest stratigraphy redox boundary where sulphide mineralization occurs as fine-grained disseminations in the matrix of the diamictite and as coarse-grained rims around clasts. The hanging hall is a pyritic siltstone (Broughton and Rogers, 2010).

Dikulushi Cu-Ag deposit located 20 km west of Lake Moero, and Lukafwe Cu-deposit situated are among the other deposits occurring in Northern Kundelungu foreland basin. Mineralization at Dikulushi is veins-types with a contain reserve of over167,000 t Cu and 517 t Ag (Lemmon et al., 2003) or 1.94Mt at an average grade of 8.5% Cu and 226g/t Ag (Tassel, 2003).

Another major copper districts of the Central Africa Copperbelt are the Copperbelt and the Northwestern provinces of Zambian. The classic Zambian Cu deposits-type are located within the dome region of the Copperbelt Province in Zambia. They occur within siliciclastic rocks (ore shale, siltstone or arenite) in fault-controlled sub-basin architecture setting (Selley et al., 2005). These deposits are located in the SE part of the Lufilian belt (Fig.05) where sulphides represent the most significant mineral phase which appear in two main styles: fine grained dissemination and vein-hosted.

Three main alteration are widely associated to host-rocks indicating the large scale passage of basinal brine. A calcic-magnesian alteration assemblage of anhydrite, dolomite, calcite and phlogopite characterize early diagenetic to early lithification. Potassic alteration is represented by K-feldspar and sericite-muscovite. Then a late stage sodic alteration (albite and scapolite) associated to veins (Selley et al., 2005; Hitzman et al., 2005).

The Northwestern province in Zambia is another prospective Cu district, containing three majors deposits (Fig.5) namely Kansanshi, Lumwana and Sentinel. Kansanshi Cu-Ag deposit is a vein-hosted type occurring in the Nguba Group (Broughton et al, 2002). Sentinel, the recent Cu developed deposit, is hosted in carbonaceous phyllite which is believed to be Mwashya (Hitzman et al., 2012). At last Lumwana is pre-Katangan basement schist hosted Cu-Co deposit (Bernau, 2007, unpubl.).

3.7. GENESETIC MODEL FOR COPPER MINERALIZATION

The source of metal in the Central African Copperbelt is still a debate. To account for the large copper province, the metal would probably derive from different origin or a combination of the following sources:

1. Leaching of red beds underlying the ore bodies (Selley et al., 2005)
2. Convection of basinal fluid into basement along major crustal fault and remobilization of metal from the granite, and metal leaching from local strata above and below the ore body (Hitzman et al., 2010)
3. Erosion of metalliferous Pre-Katangan highland rock (Cailteux et al., 2005b)
4. Katangan igneous rocks and related hydrothermal processes

Fluid pathways are mainly structures such as normal faults, shear zone, and wide spread regional alteration. Since the discovery of the Central African Copperbelt in the early 1990, the Genetic model of copper deposit is also a debate among geoscientists. Genetic model ranges from syngenetic, diagenetic and orogenic, to multistage origin.

3.7.1. SYNGENETIC ORIGIN

The syngenetic model or synsedimentary rises since the early days in 1930's. This model is based on the mineralization style and texture of sulphide disseminated along sedimentary strata, or associated to sedimentological structures such as paleocurrent direction and stratigraphy architecture (Schneiderhohn, 1931; Garlic, 1961; Garlic and Fleischer, 1972; Binda, 1975; Fleischer et al, 1976). The syngenetic model authors suggest erosion of metal from highland surrounding the Katanga basin as a source. The metal would have been precipitated from seawater during transgression and regression cycles, within an euxinic and reduced environment controlled by bacteria and decomposition of organic matter. This model attributes post-depositional features such as metasomatism, deformation, vein-associated mineralization to post ore remobilization (Sweeney et al, 1991).

However this model could not explain the wide spread potassic alteration associated to mineralization in the Zambian Copperbelt (Darnley, 1960). The lack of systematic correlation between the sulphide mineralization and the transgression-regression cycles; plus the discontinuity of mineralization within the same stratigraphic formation, saw an alternative model of syngenetic to early digenetic proposed by Annels (1974); Sweeney and Binda (1994), and Cailteux et al. (2005b).

The first sulphide to precipitate is believed to be a framboidal pyrite at temperature between 20 and 60^{o}C and at about neutral pH due to bacteriogenic process (Bartholomé, 1974; Okitaudji, 2001). This syngenetic to early diagenetic model suggested the same source of metal being the metalliferous highland of the Paleoproterozoic Bangwelo block with it low grades porphyry copper deposits and the Zimbabwe craton containing multiple Cu-Co-Ni occurrences (Cailteux et al., 2005b).

3.7.2. DIAGENETIC ORIGIN

The diagenetic model was proposed since 1970's (Bartholomé et al, 1973; Bartholomé, 1974; Unrug, 1988; Cailteux et al., 2005b). After forming the early diagenetic framboidal pyrite, Cu-Co brines circulated resulting in the formation of the main mineralization during sediment burial. This model is supported by: (1) the mineral paragenesis where sulphides (carrolite, bornite and carrolite) are associated to diagenetic mineral such as dolomite; (2) a broadly transgressive nature of ore zones relative to the lithology and (3) the clear relationship of metal and redox front and the replacement texture observed in the sulfide mineral paragenetic sequence.

Alternatively, Annels (1989) suggest a model involving upward migration of mineralizing fluid along faults from the basement and a lateral fluid flow in impermeable arenites and below impermeable horizons. A late diagenetic to early orogenic mineralization is recorded in the Zambian Copperbelt, by prefolding bedding-parallel sulphide veinlets (Selley et al., 2005); and evidence of sulphide precipitation after interaction of ore fluid with mobile hydrocarbon (Annels, 1979; Selley et al., 2005). Fracture filling and veinlet mineralization crosscutting stratiform mineralized lithology, has been also reported in DRC to be of late diagenesis to orogenic mineralization (Bartholomé et al., 1973; Levebvre, 1976).

3.7.3. MULTISTAGE ORIGIN

Recent works have suggested a combination of several mineralizing events from early diagenetic to syn-orogenic and supergene enrichment to post-orogenic; with the bulk of primary mineralization formed during burial diagenesis (Selley et al, 2005; Dewaele et al., 2006; Schuh, 2008; Schuh et al., 2012; El Desouky et al, 2010; Hitzman et al, 2012). It has been widely demonstrated that the mineralization processes in the central African Copperbelt was spin along a period over 100 Ma (Hitzman et al., 2012). The classic DRC Cu-Co deposit-type of the Mines Subgroup is proved to be formed before the deformation event. Conversely, post-orogenic mineralization has been identified by fluid inclusion studies in Lukafwe (El Desouky et al., 2008), and dated at 451Ma in Kipushi (Schneider et al., 2007). Moreover biotite and muscovite

intergrowing sulphide in Samba (Hitzman et al, 2012) was dated respectively at 490Ma and 463Ma.

Chapter 4 GEOLOGY OF THE KAPONDA PROSPECT

4.1. LITHOSTRATIGRAPHY

This section will give the petrographic description of some of the rocks outcropping within specific stratigraphic units of the Kaponda Prospect (Fig.6). The description will be limited to available data from field mapping (outcrops) and drill core samples. Due to the high rainfall that characterized wet tropical regions, regolith and overburden (soil, laterite, saprolite…) are very developed, consistent with the very high weathering profile in our study area. Therefore, outcrops are limited to less than 10% of the landscape within the Kaponda Prospect. Also the geological mapping which will be described in the last chapter did not cover the whole Prospect. The hardest rocks such as siliciclastic (e.g. sandstone, conglomerate, shale) are the most cropping, whereas carbonate are naturally altered into red soil or other related regolith.

4.1.1. DIAMECTITE –The Grand Conglomerat Formation

This unit is the most continuous formation within the entire Katangan basin. In Kaponda Prospect, the Grand Conglomerat is represented by a shaly to silty matrix supported pebbles, cobbles and boulders (Fig.7, a).When outcropping, it forms prominent small hill due to its higher content of hard cobbles and boulders made of quartzite and granite. Its facies varies depending on the sedimentation environment which is correlated to the type of its underlying rock. In general the fined grained, shaly and carbonaceous Grand Conglomerat lies directly on Mwashya graphitic Shale like the one occurring in Kipushi surrounding. Conversely its matrix becomes silty to sandy, when directly overlying an arkosic sandstone of the upper Mwashya (e.g. in the area close to Lubumbashi). Master and Wendorff (2011) attribute the facies change to the variation of the sedimentation condition (regression, transgression), ongoing tectonic and variation of climate and ice dynamic.

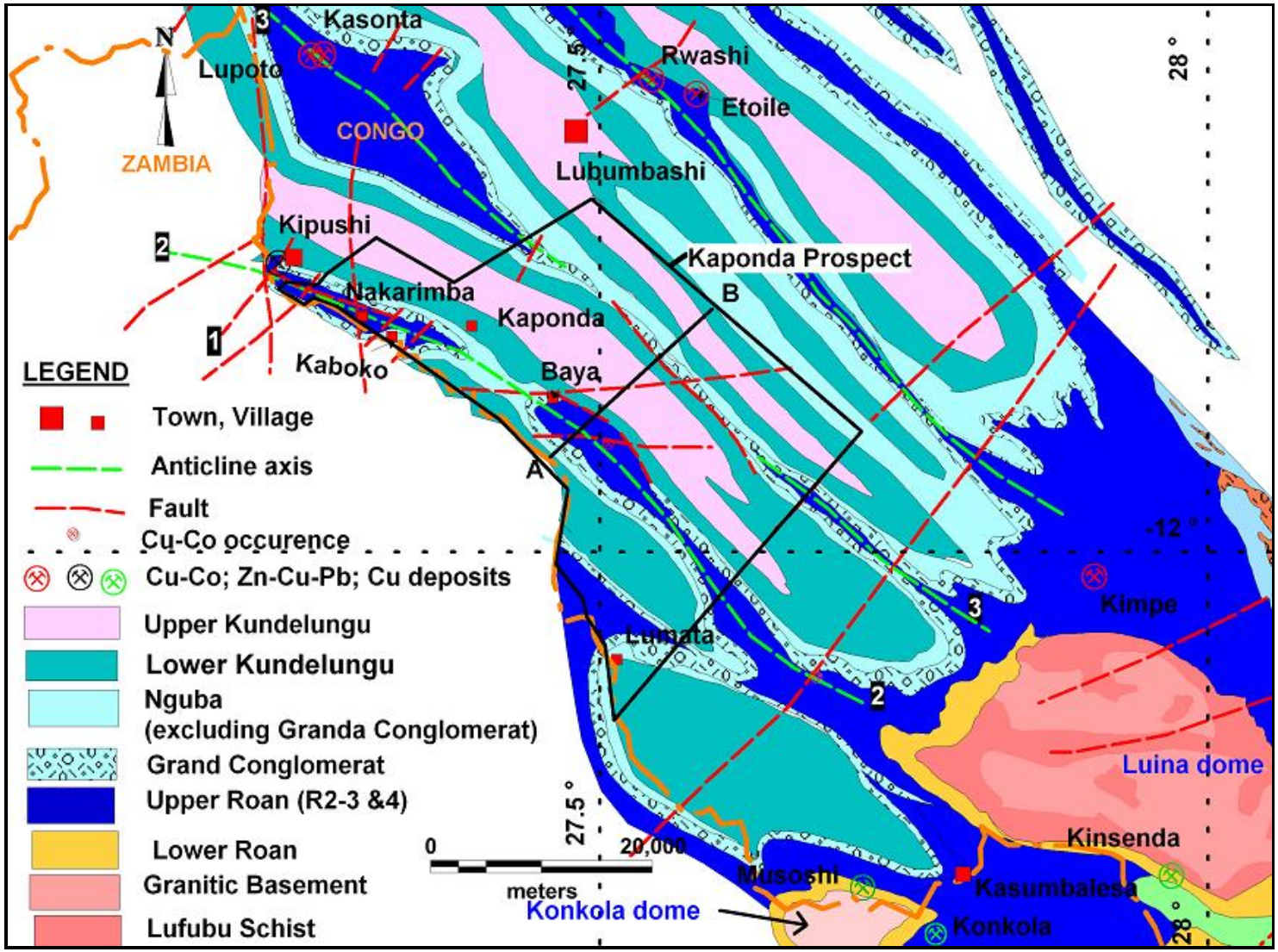

Fig.6. Geological setting of the Kaponda Prospect area showing the local lithostratigraphy, fold axis and major faults (modified from Jigsaw, 2009, unpubl, and Lepersonne et al., 1974). Note 1= Kipushi fault, 2=Kipushi anticline axis, 3 =Lupoto anticline axis; and AB black line is the location of geological section (of Fig.15).

The diamictite is made of a wide range of poorly sorted, lithified terrigenous sediments with different size and shape; rounded to subangular faceted clasts. The largest clasts are observed toward its bottom contact with the Mwashya Group. In Nakarimba area, they are made of 20 to 30cm rounded cobbles and boulders of quartzite and granite (Fig.7, b). Other smaller size pebbles varying from millimeters to few centimeters, consist of siltstone, shale, sandstone, carbonaceous shale and dolomitic shale. The Grand Conglomerat is generally massive, foliated to law strain when occupying the fold hinge or closure developing weak crenulation cleavage. Its maximum thickness within the study area varies from 300 to 500 m.

Different style and type of sulphide occurs mostly in the carbonaceous facies of the diamictite. Pyrrhotite is the most common mineral; it consists of dissemination and blebs within the rock matrix. Pyrite and chalcopyrite are minor mineral phase generally infill foliation and joints, or associated to later stage crosscut quartz-carbonate veins.

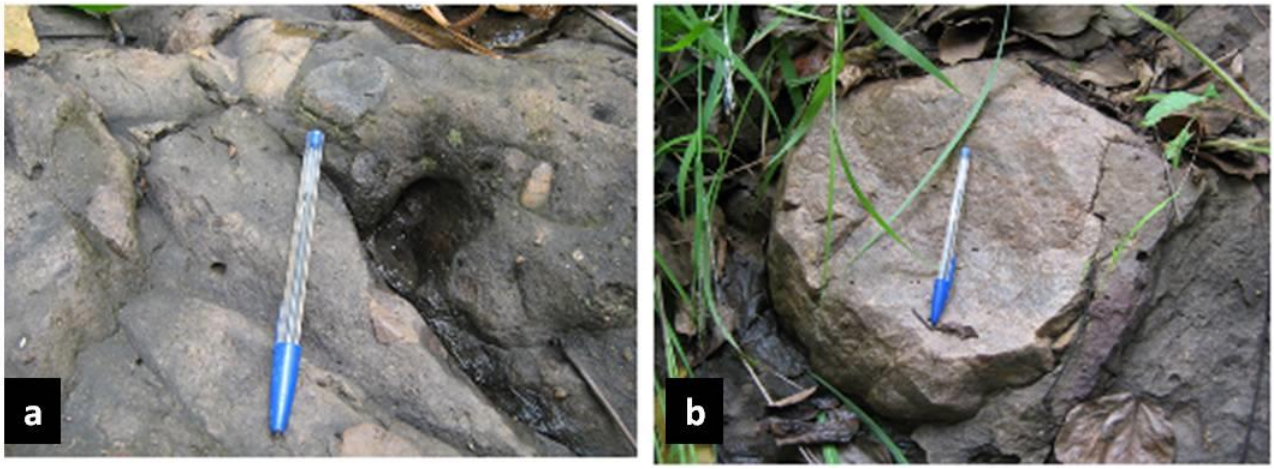

Fig.7. Silty matrix supported diamictite (Grand Conglomerat) outcrop. (a) Pebbles and cobbles; (b) quartzite boulder.

4.1.2. CAP CARBONATE–Nguba Group

The Grand Conglomerat being a tillite developed during worldwide sturtian glaciation is overlain by cap carbonates. Available field data for this dissertation including drilling and mapping does not cover the cap carbonated units overlying the Grand Conglomerat. Therefore

they are documented by Intiomale (1982), Batumike et al. (2007) and Kampunzu et al. (2009) for the Kipushi area. These carbonates comprise three Formations: Kaponda, Kakontwe and Kipushi (Table 2). The cap carbonate Formations are a series of carbonaceous dolomitic shale, cherty dolomite, massive dolomite, and black carbonaceous dolomite with chert and oolite. They likely weathered into regolith (red soil) near the surface.

4.1.3. CARBONACEOUS SHALE OR BLACK SHALE - Upper Mwashya

This unit consists of fined grained carbonaceous to graphitic shale, commonly called "Black Shale", due to its dark grey and black color (Fig.8). This is the most reduced formation of the entire sequence. It contains mainly fine-grained fragment of detrital quartz, silt, muscovite with a high content of carbon. The black shale has centimeter-size parallel bedding. Sometime shaly layers alternates with centimeter-size carbonated sandy siltstone. Locally it lacks bedding and appears as carbonaceous mudstone or argillite.

Abundant pyrite can be seen as dissemination along bedding and into the rock matrix, or either associated to lenticular bedding-parallel calcite veinlets and crosscutting quartz-calcite veins. The average amount of pyrite in this rock may vary from 1 to 3%, with local concentration of more than 5 volume %. Locally seldom chalcopyrite can be associated to crosscut carbonate veins.

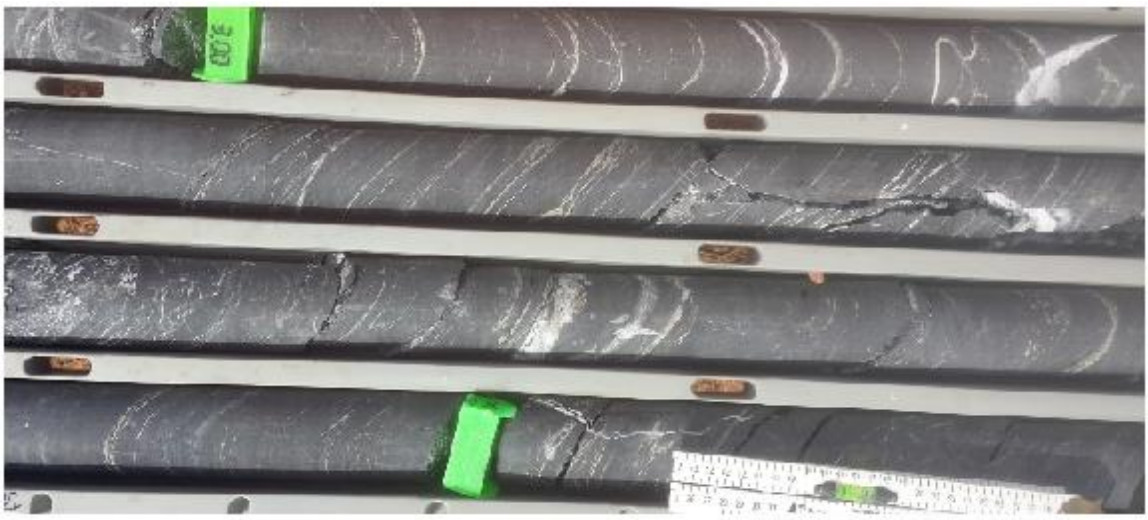

Fig.8. Carbonaceous shale of Mwashya core sample, showing dissemination pyrite, bedding-parallel veinlet and crosscut vein of quartz-carbonate associated to pyrite.

In Nakarimba area, drilling intersect 250 m thick graphitic shale. Despite the facies variation in terms of carbonate and silt content, the Black Shale remain a regional lithostratigraphy marker for the Upper Mwashya in DRC (Cailteux et al, 2007). It is also one of the most continuous lithostratigraphy of the Katangan Supergroup beyond the Grand Conglomerat (Francois, 1973; Mendelsohn, 1961).

4.1.4. LIMONITIC BANDED SHALE – Upper Mwashya

The banded shale is a fined grained silty matrix with centimeter-size regular bedding. In the NW corner of the Kaponda Prospect where this formation outcrops, it is steeply to upright dipping to the NE. It consists of alternating colored layers, from light grey, yellow to purple bands (Fig.9, a, b, c, & d). The purple strata are rich in hematite while yellow layers are rich in limonite. A process of replacement can be seen where limonite is overgrowing around hematite making the latter to be early mineral (Fig.9, a.). In addition limonite is also overgrowing along crosscut fracture and joints (Fig.9, b, d). With this established mineral relationship, it is clear that a generation of limonite is formed after hematite. However there is a strata parallel limonite layers which might be of biogenic origin and synsedimentary (Fig.9, c).

The limonitic banded shale has already been identified in the Kipushi area, where it is considered as a local stratigraphic maker for the lowermost part of the Upper Mwashya (De Magnee and François, 1988). Although the Limonitic banded Shale is generally separated with the overlying black shale by a dolostone (Buffard and Muhangaze, 1981), it appears be a redox boundary between oxidized limonitic and hematitic banded Shale and the more reduced carbonaceous Shale, suggesting a different sedimentation conditions for the deposition of the two horizons.

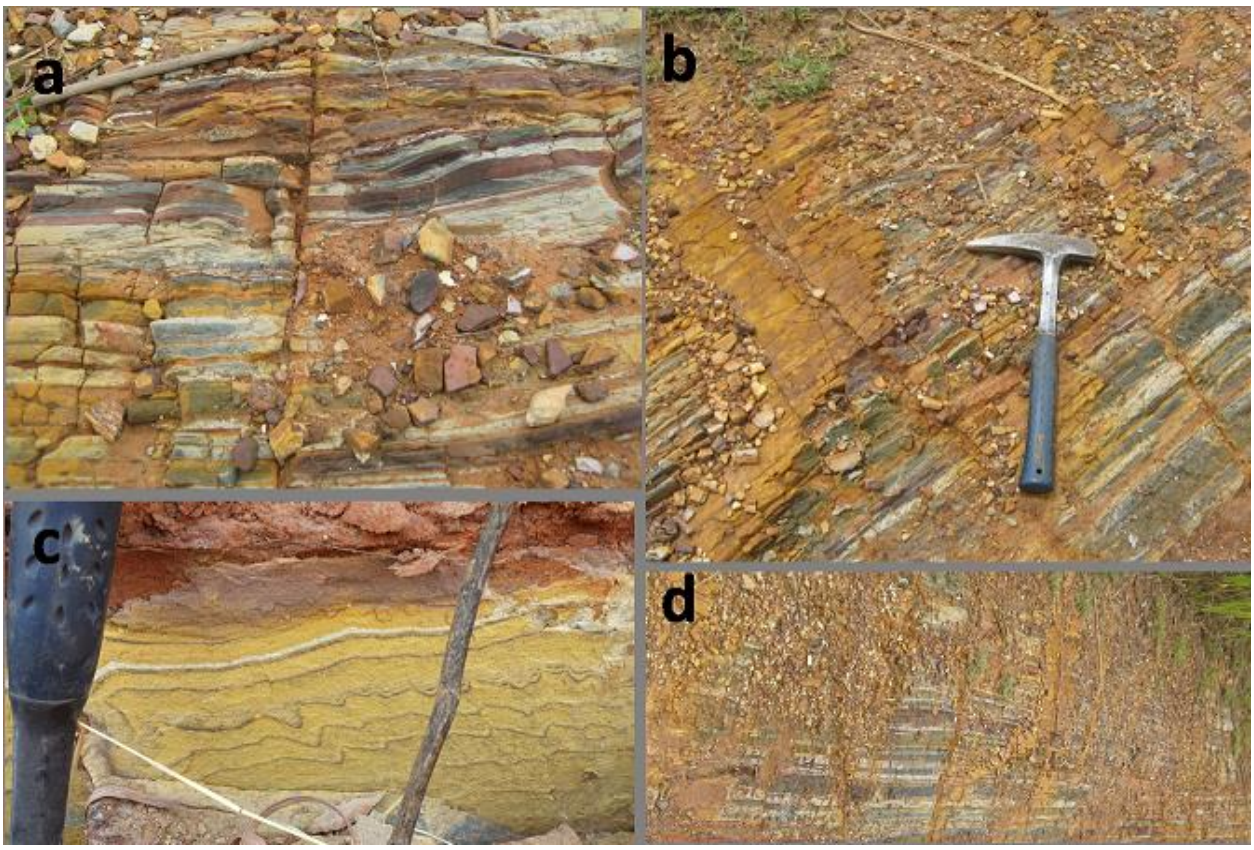

Fig.9. Limonitic banded shale, showing: (a) replacement of hematite (red) by limonite (yellow); (b) & (d) crosscutting limonite overgrowing along fractures; (c) stratified limonite of biogenic origin probably.

4.1.5. DOLOMITIC SHALE- Lower Mwashya

Drill hole in NW part of Kaponda Prospect (Nakarimba area, Fig.6) intersected dolomitic shale in contact with tectonic axial breccia. The dolomitic shale is a fined grained rock, containing alternation of dark grey argillic bands and talc-dolomitic bands. This unit is generally bedded but can be also locally brecciated (Fig.10, a). Some rounded silica and dolomite nodules are developed along bedding; some of them are even rimed by pyrite (Fig.10.b). Stratigraphically the nodule-content rock might be the equivalent of the Kamoya Formation of Batumike et al. (2007) (Table 01) and Cailteux et al. (2007). The latter described an oxidized and weathered facies in Kamoya open pit of Kambove, as ferruginous conglomeratic matrix supported round nodules clasts. Thereafter he refers this horizon as the conglomerate of Mwashya.

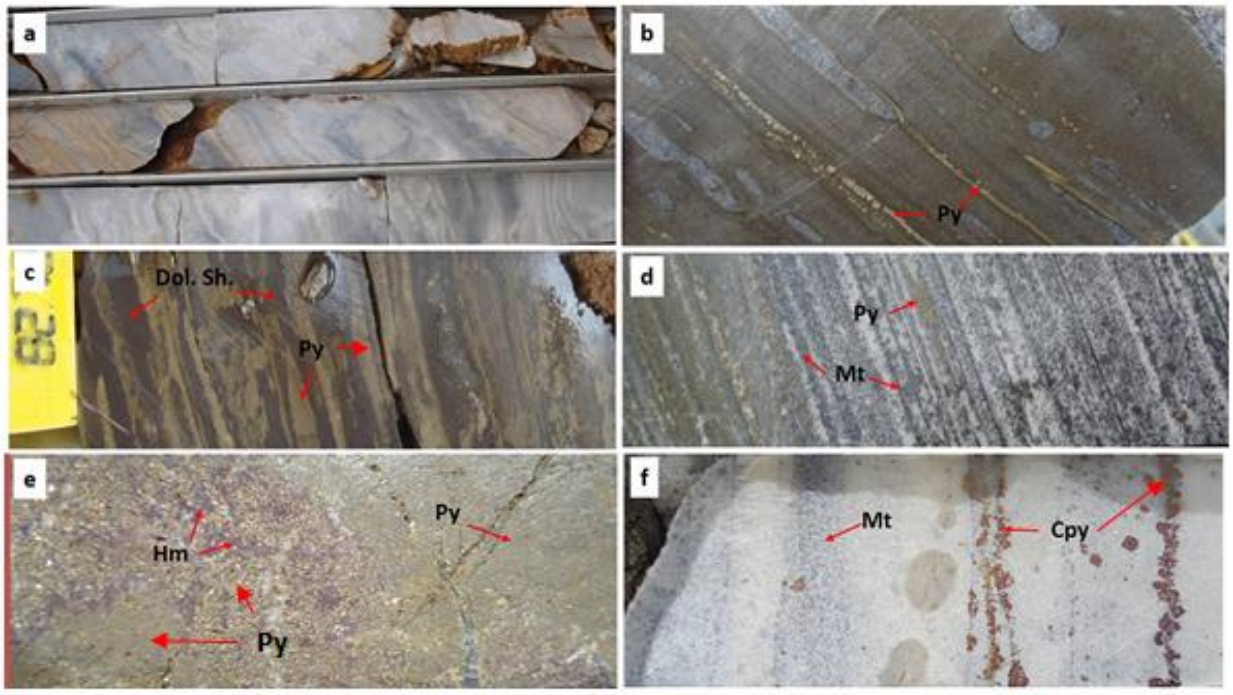

Fig.10. Drill core samples of dolomitic shale from Nakarimba area: (a) brecciated dolomitic shale with white talc-dolomitic bands; (b) dolomitic nodule formed sub-parallel to bed; (c) pyrite replacing host rock; (d) pyrite replacing bed-parallel blebs of magnetite; (e) pyrite replacing hematite (f) chalcopyrite replacement of magnetite sub-parallel to bedding (picture modified from Jigsaw, 2009; unpubl.). Note Py=pyrite, Cpy=chalcopyrite, Mt=magnetite, Hm=hematite, Dol.Sh.=dolomitic shale

Within the interval of 10 to 25m toward the contact between the dolomitic shale and the underlying breccia, drill holes reveal a zone of high massive pyrite. Pyrite is completely replacing both host rock and occupies up to 50 vol. % of the rock (Fig.10, c), bed-parallel blebs of magnetite (Fig.10, d) and hematite (Fig.10, e)

This dolomitic shale is also mineralized in chalcopyrite. Mineralization is represented by bleb of chalcopyrite occurs in or closer to the high Pyrite-Magnetite zone, as layers parallel replacing magnetite (Fig.10, f) or in carbonate veins associated to pyrite and crosscutting the bedding at a higher angle (Fig.11). From this minerals relationship, the paragenesis sequence in order of appearance is: dolomite-magnetite-hematite-pyrite-chalcopyrite+calcite.

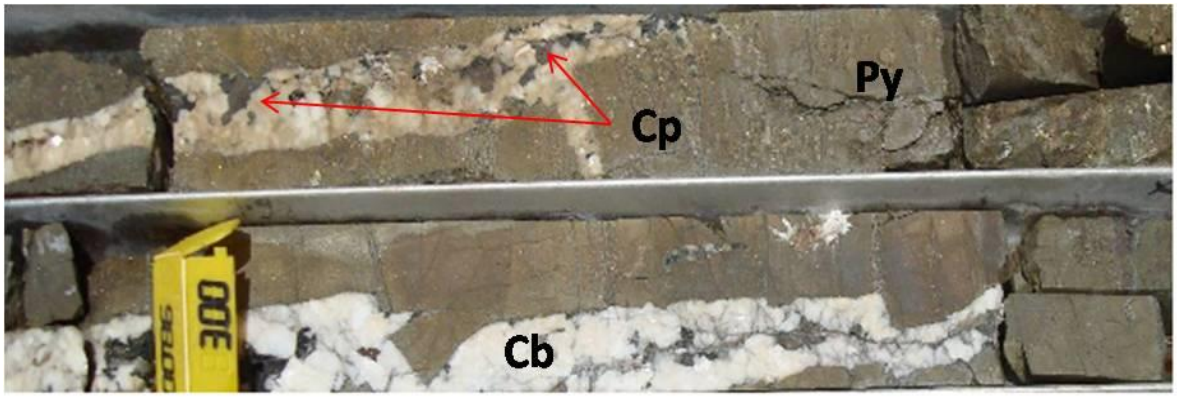

Fig.11. Massive pyrite crosscut by carbonate veins associated to chalcopyrite, with smaller veinlet parallel to bedding (picture modified from Jigsaw, 2009, unpubl.). Py=pyrite, Cp=chalcopyrite, Cb=carbonate vein.

4.1.6. IRON FORMATION - Lower Mwashya

A fine to medium grained, highly ferruginous and silty rock observed on outcrop lying from nearly 3km SW of Kipushi to Nakarimba area (Fig.6), where artisanal small scale mining workers are excavating subsurface iron ore with picks and shovels (Fig.12, a). On surface, this iron formation has an average width of 4m. It is generally bedded into centimeter-size bands (Fig.12, b) which composed various layering including combinations of bands of massive hematite-magnetite, ferruginous quartz-silicate and ferruginous silty rocks. In places, brecciated iron formation is enriched in iron minerals up to above 50% hematite (Fig.12, c), suggesting remobilization and concentration of iron ore through hydrothermal processes.

The main iron minerals are generally hematite, magnetite, goethite and limonite (Fig.12, d). Hematite is the most abundant and can be seen replacing magnetite. Goethite and limonite are a later phase resulting from hydration of hematite or magnetite. They appear as replacement to hematite or within fractures. Silica or chert content of this lithological unit is relatively low to locally absent.

Stratigraphically the iron formation might be the oxidized equivalent of the high pyrite zone of dolomitic shale described at depth in drill core samples from the previous section where primary magnetite and hematite was replaced by pyrite.

Fig.12. Iron formation outcrops: (a) local diggers pitting along iron formation; (b) NE dipping banded iron formation; (c) brecciated and enriched iron formation associated to whitish carbonate veinlets; (d) layering composition of the iron formation showing magnetite (metallic), hematite reddish metallic, goethite and limonite (yellow). Note Gt=Goethite, Hm=hematite, Lm=limonite, Mt=magnetite;

However more observations and analyze of both drill core samples and outcrops, together with their spatial location should be taken into consideration to well constrain stratigraphy. This Iron formation along with the pyroclastic unit are regional stratigraphic markers that François (1987) used to identify the Lower Mwashya.

4.1.7. AXIAL BRECCIA

This unit consists of chlorite rich silty matrix supporting angular clasts or rocks fragments of different types. Unsorted clasts range from siltstone, dolostones and sandstone. The most abundant clasts are siltstones and white talcose dolomite. Size of clasts and rock fragment varies from few millimeters to decimeters (Fig.13).This polymictic breccia occupied the core of a tight anticline and have more fragments which are believed to be originated from Dipeta Group such as greenish chloritic siltstone.

Fig.13. Polymictic axial breccia showing angular clasts of siltstone, dolostones, shale and sandstone (picture from Jigsaw, 2009, unpubl.)

On outcrop, only silicified portion of the breccia resists to the weathering forming a ferruginous silicified medium grained matrix (Fig.14). Most clasts are angular and consist of quartz, hematitic and siltstone. Strong silica and hematite alteration overprint the composition of the breccia described above as chloritic. Some clasts are even replaced completely by hematite (Fig.14).

This breccia is believed to be originated from the regional tectonic responsible for the thrusting and folding of the Congolese Copperbelt. It has been identified in the vicinity of Kipushi Zn-Cu-Pb deposit (Intiomale, 1982; Kampunzu et al, 2009), along the NW trending anticline axis, and referred as axial breccia. Similar structural setting with equivalent axial breccia occurs at Shituru Cu-Co deposit in Likasi where the axial breccia is reported to be tectonic.

Fig.14. Ferruginous matrix of polymictic axial breccia, outcropping in Nakarimba area

4.2. STRUCTURE

The prominent structures of Kaponda Prospect are represented by NW trending folds, and NE and NW directed faults (Fig.6). In fact, the Prospect lies within a series of NW-SE trending disharmonic tight anticlines namely Kipushi and Lupoto (Fig.15) as interpreted from map of Fig.6. They are separated by an open syncline made of Kundelungu Group. These folds result from compressional regime that affected the central African Copperbelt during the basin inversion of the Lufilian orogeny. The core of anticlines are mainly occupied by Roan or Nguba Groups overlain by their respective younger stratigraphy units which appear in fold limbs. After analyzing thickness variation of lithostratigraphy units within the two limbs of a same fold, it is clear to see the most continuous unit of the Katangan basin, the Grand Conglomerat, thickening in the northeastern and southwestern limbs of Lupoto and Kipushi anticlines respectively. This is interpreted as a result of synsedimentary intergrowth faults, also observed in the surrounding of Kasonta and Lupoto Cu-Co deposits (Hitzman, 2010)

As previously mentioned, there are two mains directions of faults (Fig.6). Firstly the NE trending faults are normal transfer faults. They are believed to be related to the late orogenic extension of the Lufilian belt inducing mineral remobilization, such as Shituru Cu-Co deposit (Kipata et al., 2013) and Kipushi Zn-Cu-Pb deposit associated to the NE trending Kipushi fault (Kampunzu et al., 2009).

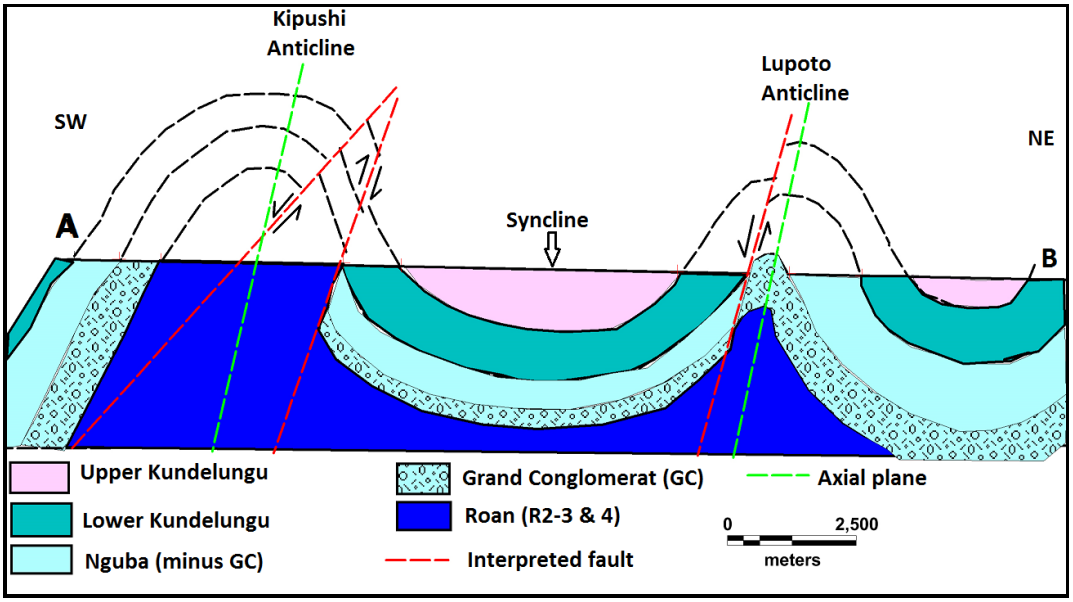

Fig.15. Generalized interpreted geological section showing fold geometry, reverse and normal faults (red dash line). The location of the section is shown on Fig.6 as AB black line.

Secondly the NW-SE structure represents either synsedimentary intergrowth faults or fault related to the folding event during Lufilian orogeny. These faults are parallel to axial plans. The intersection of NW with NE transfer faults may play an important role at trapping or redistributing mineralization.

4.3. MAGMATISM AND METAMORPHISM

No significant magmatism has been encountered within the Prospect. As anywhere else in the Congolese Copperbelt, only small diorite dykes intersected in drill holes are seen intruding Mwashya formations in Nakarimba area. These mafic units are associated to the regional basic magmatic event occurred within the second intracontinental rifting within the Katangan basin (Kampunzu et al., 2000). Further 25 km SE of the Kaponda outcrops the Luina dome (Fig.6) where granite bodies intruding Lufubu schist, represent the basement of the Katangan sediment sequence.

The degree of metamorphism within Kaponda Prospect is of very low grade. The presence of chlorite, sericite, seldom muscovite and biotite correspond to the lower green schist facies which is consistent with the observed law strain rocks. To illustrate the law strain rocks, the following features have been observed in the NW part of the study area: spherical nodule within dolomitic shale are not considerably flattened (Fig.10, b); wide-space and non-penetrative crenulation and weak axial planar cleavage within upright fold (Jigsaw, 2009, unpubl.).

4.4. MINERALIZATION OCCURRENCE

The only known near surface or outcropping Cu mineralization occur in Baya area (Fig.6), within pits of artisanal diggers and small scale mining activities. This mineralization represents a leaching zone of copper and cobalt minerals, mainly malachite, chrysocolla, azurite and heterogenite; associated to iron oxides. At the surface, mineralization occurs within brecciated siltstone and residual argillic to silicified units which are interpreted to be RAT breccia and Mines Subgroup. In addition, drilling intersects pyrite and chalcopyrite sulphide minerals within carbonaceous shale which are believed to be Mwashya.

Elsewhere, near Lumata and Nakarimaba areas, drilling intersects Cu mineralization at depth, even though its continuity and extension have not been well defined. In Nakarimba for instance, mineralization is represented by chalcopyrite replacing magnetite (Fig.10, f), crosscut carbonate veins associated to blebs of chalcopyrite (Fig.11) and residual oxidized mineralization made of malachite, chrysocolla and native copper.

Chapter 5 EXPLORATION CASE STUDY IN THE KAPONDA PROSPECT

5.1. REMOTE SENSING

In the Congolese Copperbelt, since the first half of the 21st century, aerial photograph has been used effectively to delineate Mines Subgroup blocks ("écailles") associated Cu-Co mineralization. These "écailles" occur as higher topography lineaments. In fact the RSC ("Roche Siliceuse Cellulaire") an upper member of the Kamoto Formation in the Mines Subgroup, is a completely silicified dolomite that resists to weathering. It remains on hill crests with underlain and overlain Mine Subgroup sequence on both sideways. Hence Mines Subgroup occupies high topography devoid of vegetation which is easily mappable by remote sensing images supported by the good knowledge of the regional geology. The natural vegetation clearing is due to the excess of copper and other byproduct metals, in soil developed above ore bodies.

For this type of setting, a follow up of geological mapping, pitting or trenching is enough to confirm the presence of outcropping and near surface Mines Subgroup associated to mineralization. This is the case for the majority of the Congolese Co-Cu deposits that occur in the Mines Subgroup including the deposit cluster of Kolwezi and Fungurume districts.

In Kipushi-Lubumbashi area and Kaponda Prospect, Landsat image and Google earth images show lineaments corresponding to lithostratigraphic units and rock boundaries. There is a positive correlation between remote sensing lineament and geological map of Kaponda Prospect, like elsewhere in the Congolese Copperbelt. On satellite images, lineaments comprising existing copper deposits (e.g. Lupoto, Rwashi, and Etoile) can also be mapped and followed southeastward into the Kaponda Prospect (Fig. 16 & 17).

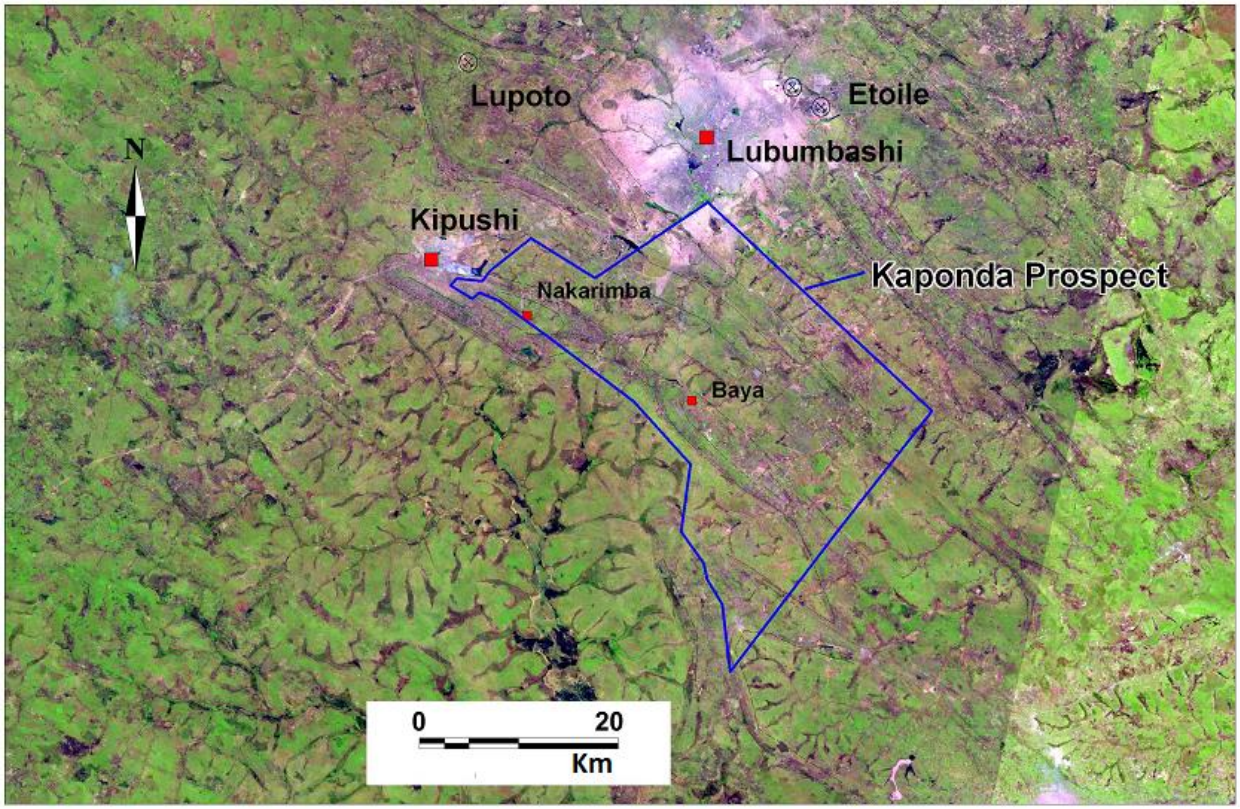

Fig.16. Landsat image of the Kaponda Prospect area showing major NW trending lineaments.

Assuming that Cu mineralization is stratiform or stratabound, highlighting such lineament associated to known deposits, indicates potential prospective zones within the study area.

It is also clear that transfer faults crosscutting lithology are not well constrained on Landsat and Google earth images due to their law spectral resolution. Alternatively Spot image for instance, by its high resolution visible (HRV) imaging system (Moon et al., 2009) with its 10 to 20 m ground resolution will be able to pick up all the regional and local structures. Even better will be the use of highest resolution images such as Quickbird and Ikinos in order to detect structures. However the economic aspect should still be considered for these high resolution images as they are expensive.

Despite identifying high topography Mines Subgroup outcrop, the major challenge of the remote sensing in the Central African Copperbelt remains the difficulty to directly determine lithological and alteration types. Unlike in desert or arid regions where the lithology and alteration can be easily enhanced and identified by analyzing spectral reflectance of satellite image, the thick vegetation cover coupled to a very cloudy sky especially in rainy season,

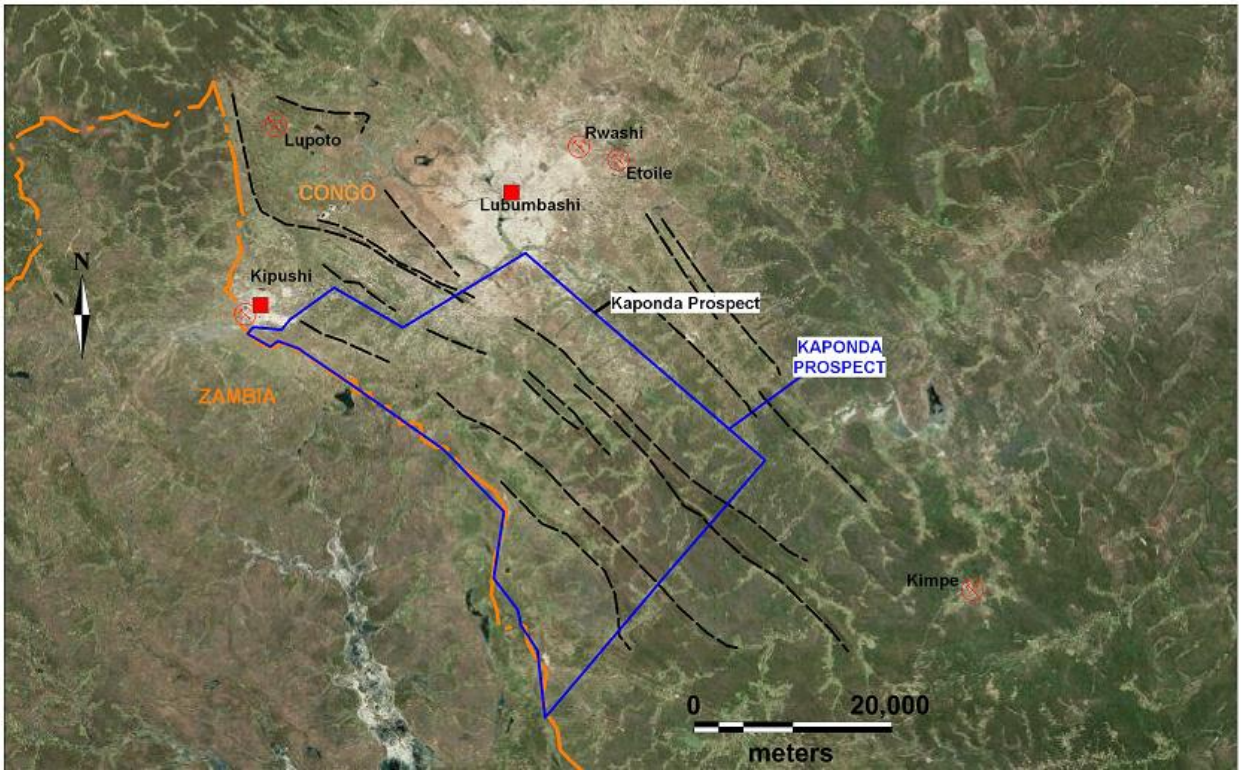

Fig.17.Google earth image of Kaponda Prospect showing lineaments (black dash line) interpreted to be lithostratigraphy boundaries.

and the scarcity of outcrops make remote sensing image tougher to work out in CACB.

To compensate the limitation of satellite imagery, a use of aerial photograph if available can be important as in a region of only 5% outcrop there is an higher amount of information that photogeology can provide in terms of relief, tone of the ground surface, the drainage pattern and texture, erosion form and vegetation (Moon et al., 2009). These features are associated to geological characteristic. For instance the high topography implies hard rock's hence a change of topography will mean a change in rock type. Erosion will be associated to zone of weakness such as fracture, joints or faults. However most of these interpretation remain subjective, they can change from one region to another. A part from structure analysis, the other major application of remote sensing in the Congolese Copperbelt is the utilization of rivers drainage network in order to plan stream sediment sampling or to interpret soil geochemistry data.

Since all the data and interpretation of remote sensing are done without any physical contact with the area, it is imperative to go on the field and verify geological facts. Geological mapping is in many cases the next step in reconnaissance exploration after desk study that

includes remote sensing. Nevertheless remote sensing images must be analyzed before, during and after mapping to optimize its interpretation.

5.2. GEOLOGICAL MAPPING

Systematic mapping campaign of Kaponda was conducted during 2009 to 2010, after soil geochemical and airborne geophysical surveys, and drilling. The latter was conducted between 2005 and 2008, as a result drilled holes directions was only based on old regional geological map. Unlike in Kaponda, geological mapping has to be traditionally executed before other exploration field works such as drilling. Mapping defines the geometry of the area in order to avoid drilling of geological units and mineralization along dip, especially when the sought mineralization is stratiform or stratabound.

In Kaponda, mapping data covers less than 50 % of the study area, focusing on the prospective zones (Fig.18, a), identified during previous exploration works. The aims of the geological mapping was (1) to provide a fact map based on outcrops; (2) to understand the geometry of the area and (3) to identify any lithostratigraphy or structure controls of mineralization.

Maps on 1:10,000 scales were produced using grid and GPS mapping methods. A grid of 400 m spaced traverse lines, SW-NE directed (40^{o}) and perpendicular to lithology strike were set as reference lines (Fig.18, a). Geologists walked along these traverses, recording position of outcrop and their structure measurements, as well as float location. Recorded geological and structure data were plotted at on plan map for interpretation. The advantage of this mapping method is the systematic coverage of surface where small and medium size outcrops might be hidden by thick vegetation and not shown on satellite image. However the grid mapping has two disadvantages: (1) it is time consuming as geologists have to walk on prefixed grid whether or not outcrops occur; (2) regional structures such as those provided by remote sensing image are only incorporated in the interpretation phase after mapping.

The outcome of the mapping campaign shows that the diamictite (Grand Conglomerat) is the most outcropping unit, appearing from area near Kipushi (Fig.7) to the SE of Baya. The Grand

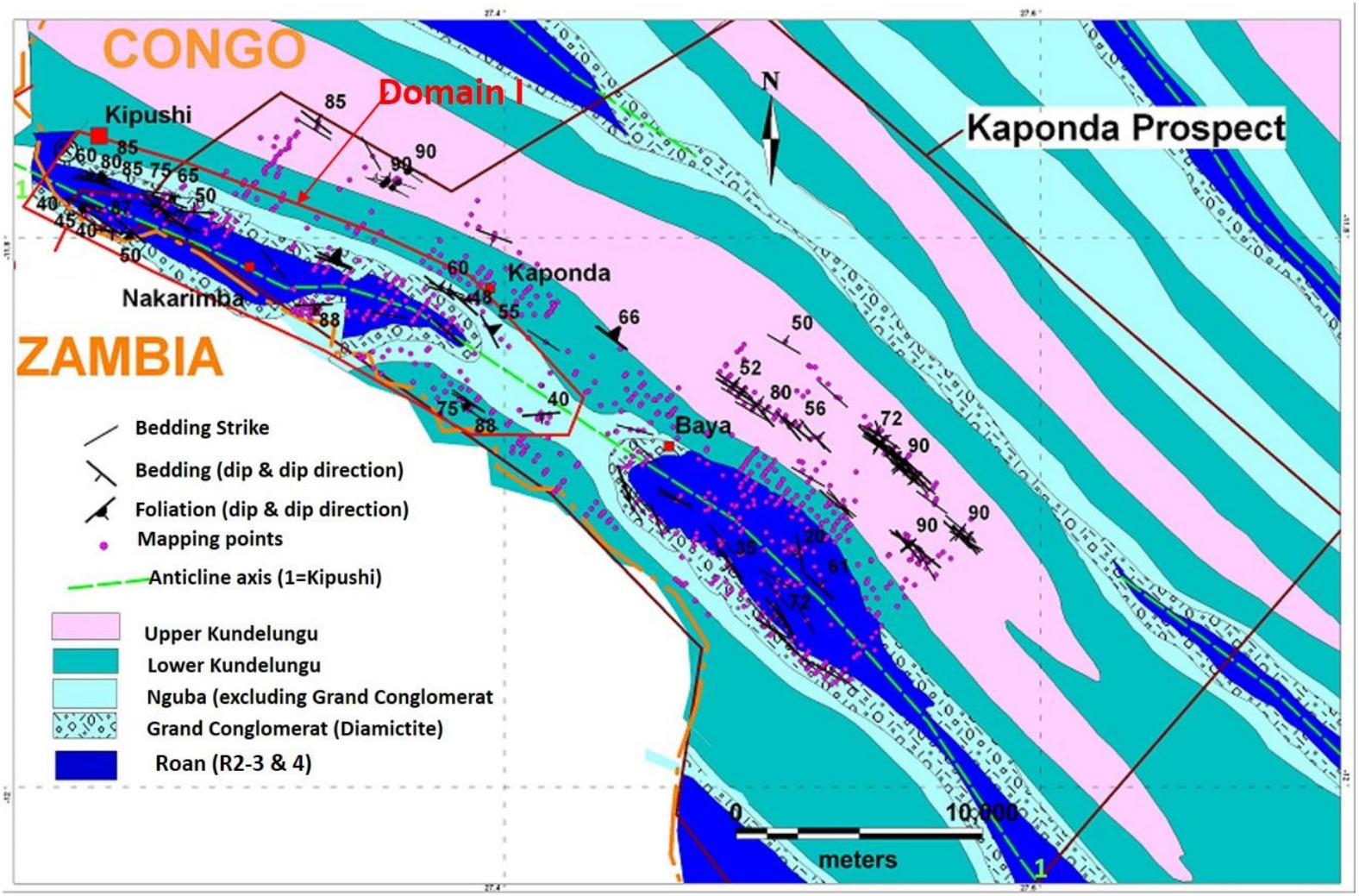

Fig.18, a. Mapping structure measurements plotted on modified geological map modified from Jigsaw (2009, unpubl.). Note the mapping points (purple dots) representing outcrops and floats, they are aligned along 400m spaced grid traverse lines. Zoom in of Domain I area (in red polygon) is shown in Fig.18, b.

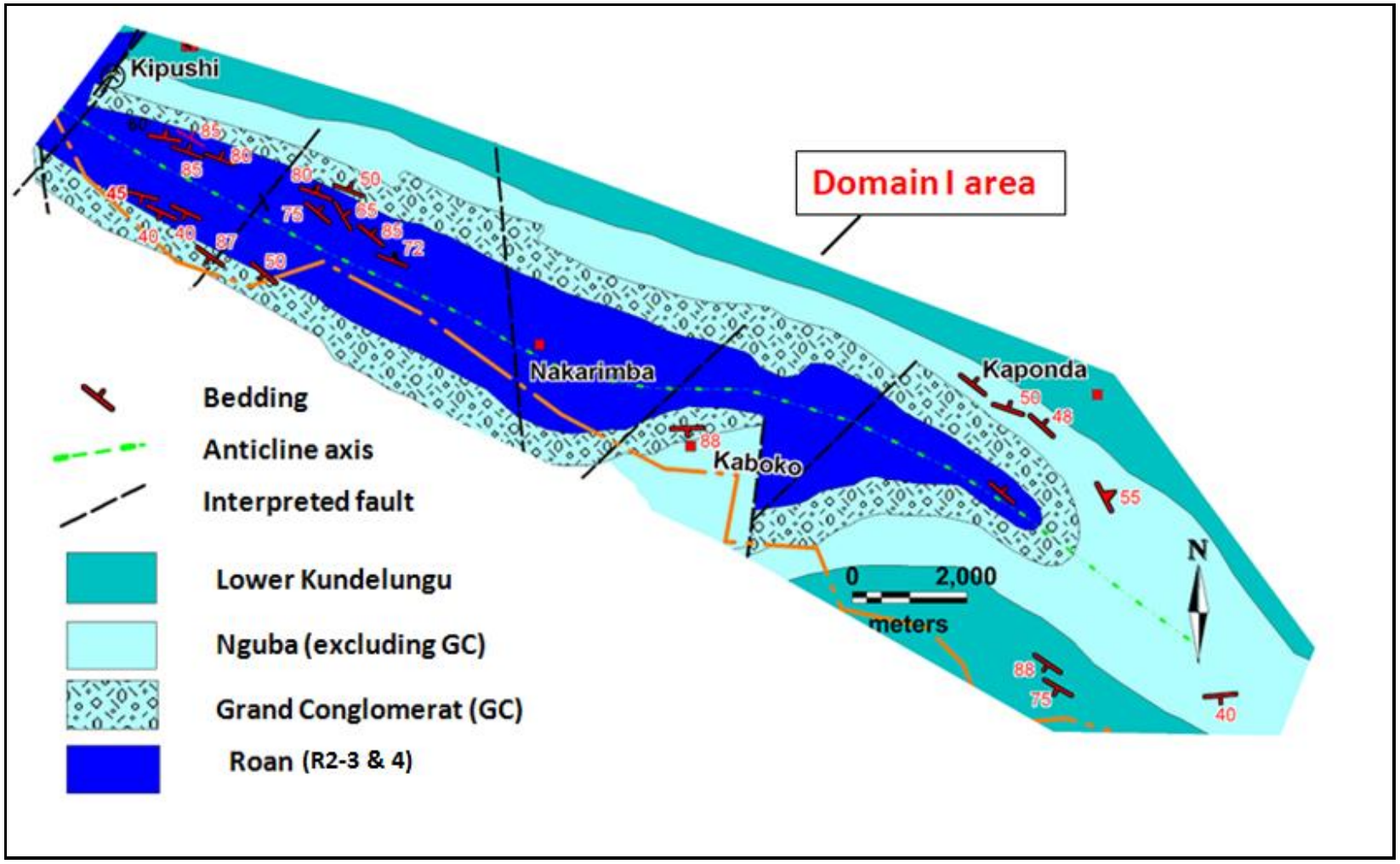

Fig.18.b. Zoom in of Domain I area as located in Fig.18, a., showing only bedding structure measurements in dip and dip-direction format. Note the dipping of bedding confirming the folding. Note the fold closure toward the SE with Roan pinch-out and Grand Conglomerat sitting in the fold nose.

Conglomerat occupies crest of small hills. Boulders and cobbles of quartzite and granites are abundant in the lower part of the diamictite, making the later resistant to weathering. The overlying cap carbonates units are not exposed on surface, but transformed into reddish residual soil. Siliciclastic rocks of Kundelungu represented by pinkish siltstone, outcrop mainly East and Southeast of Baya. Localized upright limonitic shale of Upper Mwashya (Fig.9) occurs near Kipushi, while continuous outcrop of iron formation outcrops along 7km in NW corner of the study area (Fig. 12). Limited axial breccia are exposed as massive chloritized and ferruginous coarse grained polymictic rock, in the core of domal Kipushi anticline (Fig.14). Another breccia is also present in Baya area where it is believed to belong to RAT Subgroup.

Despite the general weak strain of rocks in Kaponda Prospect, very little information about strain were recorded during mapping campaign apart from observation from drill core previously mentioned. Only localized ductile domain represented by weak foliation in Grand Conglomerat were observed near the fold closure in the surrounding of Kaboko. Neither significant brittle deformation (e.g. faults) nor were kinematic indicators recorded during the mapping campaign.

A total of 957 point data were recorded within Kaponda including positions and description of lithological units for both floats and outcrops (Fig.18, a). 132 structure measurements of beddings are in dip and strike format, with respect to true north. In this dissertation structure, data are reprocessed and plotted on map using MapInfo 12.0.1. and Discover 2013 software package (Fig.18,a & b), while GEOrient. Ver 9.5.0 is used to perform structural analysis (Fig.19). However the inconsistency during collection of structure data by using both left and right hand rules when taking dip and strike measurements, and the absence of an indication of the dipping quadrant within the data set, does not allow the conversion of all structural data into dip and dipping direction format. As a result, only 73 measurements are converted into dip and dip-direction format. Only strike measurements will consider for the remaining data prior to spatial representation and structural plots.

Since 45 % of structure measurements does only have strike without dip values, the rose diagram is firstly used to analyze the entire data set of 132 bedding measurements. The analysis indicates an average strike direction of 129-309^{o} (Fig.19, a), a SE-NW direction consistent with the general trend of lithostratigraphic units of the interpreted regional geological map (Fig.18, a).

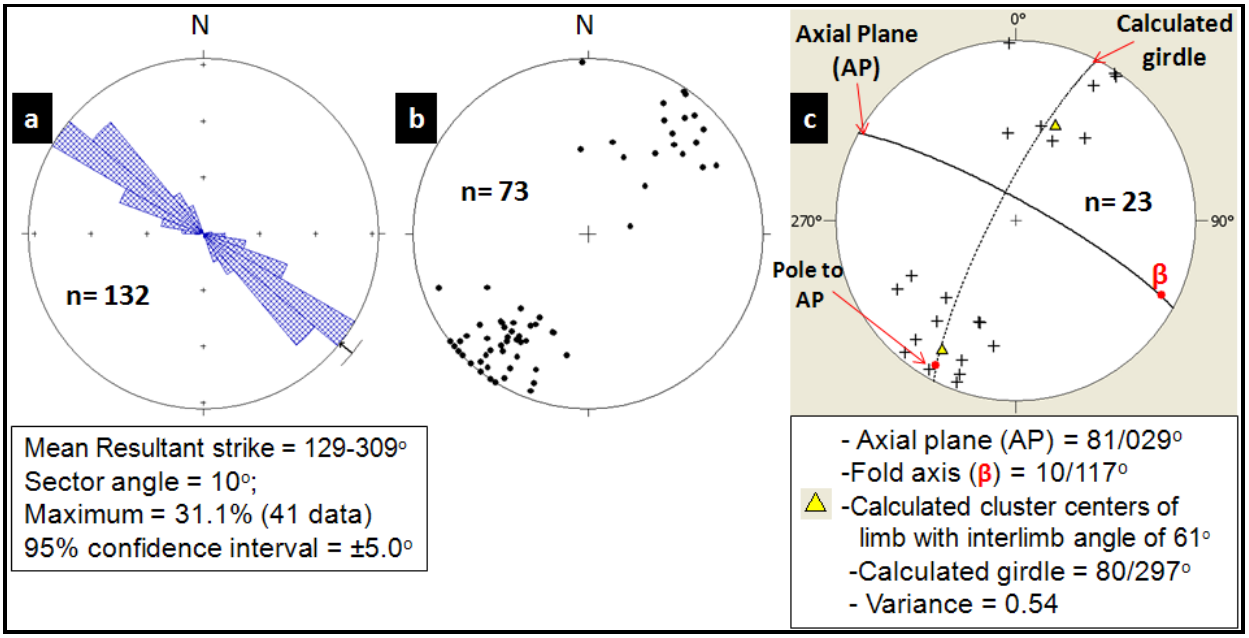

Fig.19. Plots for bedding structure measurements from geological mapping in Kaponda Prospect. (a) Rose diagram of bedding strike with arrow showing the average orientation; (b) equal area stereoplot of bedding showing two clusters of points representing two limbs of fold, dipping either to the NE or SW; (c) equal area stereoplot of isolated bedding from Domain I area (Fig.18).Note the geometry of the axial plane and fold axis.

Secondly bedding measurements with dip and dip-direction values are analyzed in stereoplot (Fig.19, b). It shows two clusters of points interpreted as two NW-SE oriented limbs of folds, dipping toward two opposite directions. They are either steeply to upright dipping to the NE or SW. This is consistent with the regional map pattern (Fig.6 & 18, a) showing SE directed succession and repetition of old and young lithostratigraphic units, from Roan to Kundelungu and vice versa; implying alternation of anticline and syncline.

To identify local fold geometry, isolated bedding structural data of Domain I area (Fig.18, b) are closely analyzed. Equal area stereoplot of 23 bedding measurements in dip and dip direction format, indicates a tight upright anticline. The calculated interlimb angle is 61 °, with an axial plan dipping 81° toward 029°, and a hinge (fold axis) plunging 10° toward 117° (Fig.19, c). However the variance of 0.54 (Fig.19.c) suggests variability of data which might be due to less measurements taken within the fold closure of Domain I area (Fig.18, b). Despite this lack of structure data, the calculated ESE fold axis plunging is consistent with the map pattern

showing fold nose represented by Roan formations pinch-out and the Grand Conglomerat. It occurs to the South and East of Kaponda villages respectively (Fig.18, b).

5.3. SOIL GEOCHEMICAL EXPLORATION

5.3.1. SOIL SAMPLING

The surface expression of soil anomalies is function of the shape, width, length and depth of the causative body, as well as the topography of the landscape. The choice of soil geochemical method takes in account the mineralogical and geochemical composition of the targeted mineral body (e.g. copper sulfide and oxides minerals). It is also related to the dispersion of metal and the disposition of the target to the surface.

Copper has both hydromorphic and mechanical dispersion within high rain tropical environment of the Central African Copperbelt. In flat landscape, the overburden is highly developed and most of the regolith is in situ soil. However slop and swamp areas can contain transported soil from up-topography, therefore geochemical data should be interpreted accordingly.

In our study area any physical orientation geochemical survey was conducted. The choice of soil sampling technique when exploring Kaponda, is guided firstly by past exploration experience within the CBCB and comparison with similar exploration methods used in this metallogenic district. Firstly being part of First Quantum team of geologists who contributed to a successful exploration track recorded in the region. An example of successful use of soil geochemical survey is in the discovery of Frontier Cu deposit (Hitzman et al, 2012), about 200 Km SE of the Kaponda Prospect. Secondly most of the known Congolese Cu orebodies are close to the surface or sub-outcrop, hence they were easily picked up as positive geochemical anomalies in soil. Therefore the best soil geochemical grid design should be able to detect at least two anomaly point's locations from different traverse lines.

5.3.1.1. GRID LAYOUT

Assuming that stratiform and stratabound copper deposits of the CACB are tabular in shape, with a strike length of the ore body more than 20 time its width on average; a rectangular

grid is the best design for soil survey. A systematic soil geochemical survey of the horizon B aiming to define Cu distribution and accessorily Co, was conducted within Kaponda Prospect. A constant grid spacing of 800X100 m was utilized covering the entire Prospect (Fig.20), where traverse sampling lines were 800m spaced with sample taken every 100m. Traverse lines were oriented 40^{o} directed perpendicularly to the average strike of the rocks (129^{o} or 309^{o}) as demonstrated on rose diagram of mapping data (Fig.19).

A total of 11,023 soil samples were collected from the 800X100 m regional grid. Soil anomalies identified from this first survey, implied detailed sampling of specific areas depending on the intensity of the anomaly to test the anomaly continuity. As a result, additional 3,731 soil samples were therefore collected on grid spacing of 400 X 100 m, 200 X 100 m, 100 X 50 m and 50 X 50 (Fig.20).

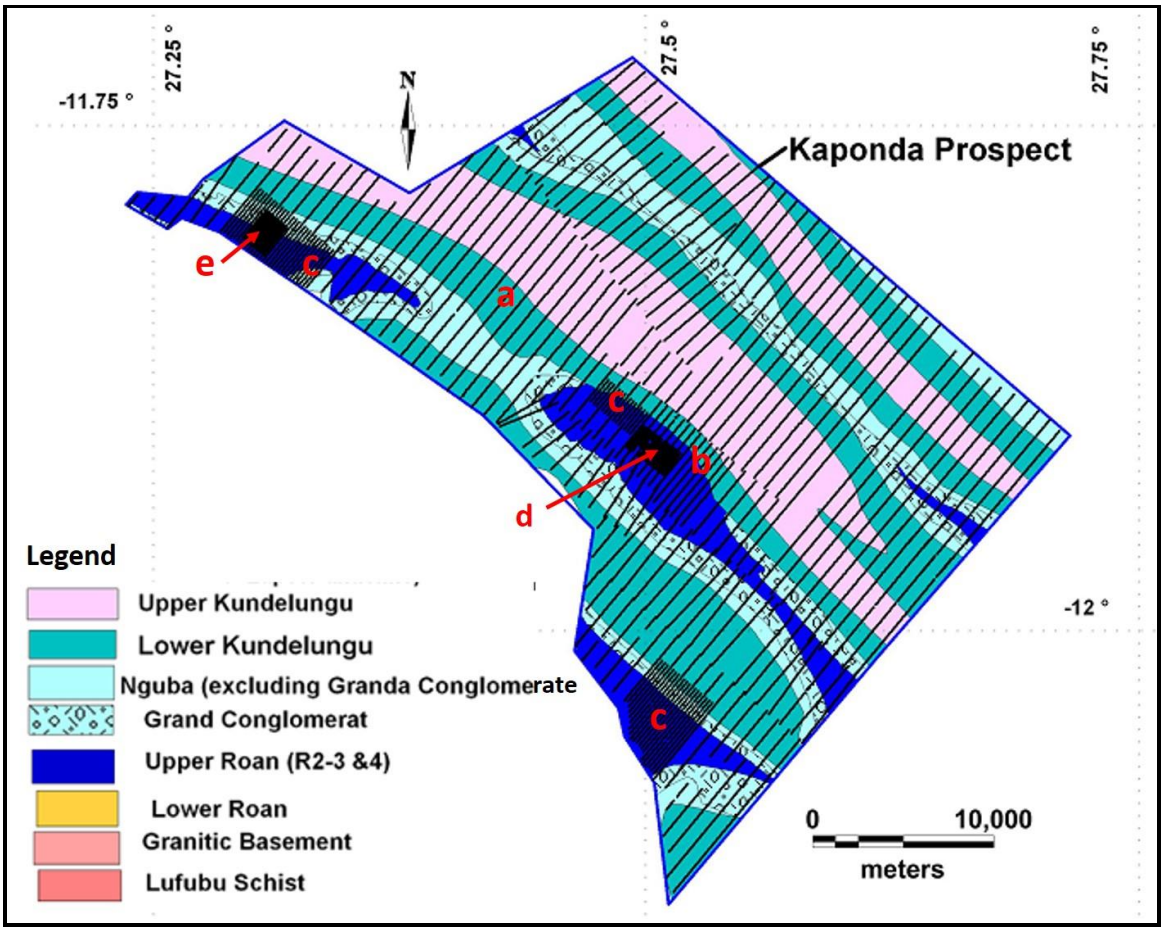

Fig.20.Collected soil samples within grids spacing of (a) 800X100m, (b) 400X100 m, (c) 200X100m, (d) 100X50 m and (e) 50X50m. Note the sampling traverse lines are perpendicular to the geology.

Soil geochemical grids were initially generated using Surpac software. Although the coordinates system of maps presented in this dissertation are in Longitude-Latitude, soil survey was planned in a more user friendly Cartesian coordinate. The UTM (Universal Transverse Mercator) system was used within a map datum of Arc1950. The UTM projection is the most recommended for geochemical survey because it creates minimal distortion of a 3-dimentional curve surface of the earth projected on 2-dimentional map. However the grid also have local coordinates which are more useful and easier to follow on the field by samplers and prospectors.

In Kaponda for instance, sampling traverse lines were labeled in numeric number with an N prefix (N=apparent Y axis of the local grid). The position of the sample within a line is labeled with E prefix (E=apparent X axis of the local grid). The base point of the grid is locally labelled N10,000 E10,000. Arithmetic sequence is used so that the next line situated at 800m in positive direction will be N10800, and the next sampling position situated 100m in the same line will be E10100 (Fig.21).

Although soil samples have planned coordinates, it is worth to pick up coordinates of the real location of a sample, after sampling. Between planned and collected sample locations, there is always a deflection of few to ten's of meters (Fig.21). This difference depend on several factors: samplers experience, the GPS accuracy and the accessibility to the place to sample.

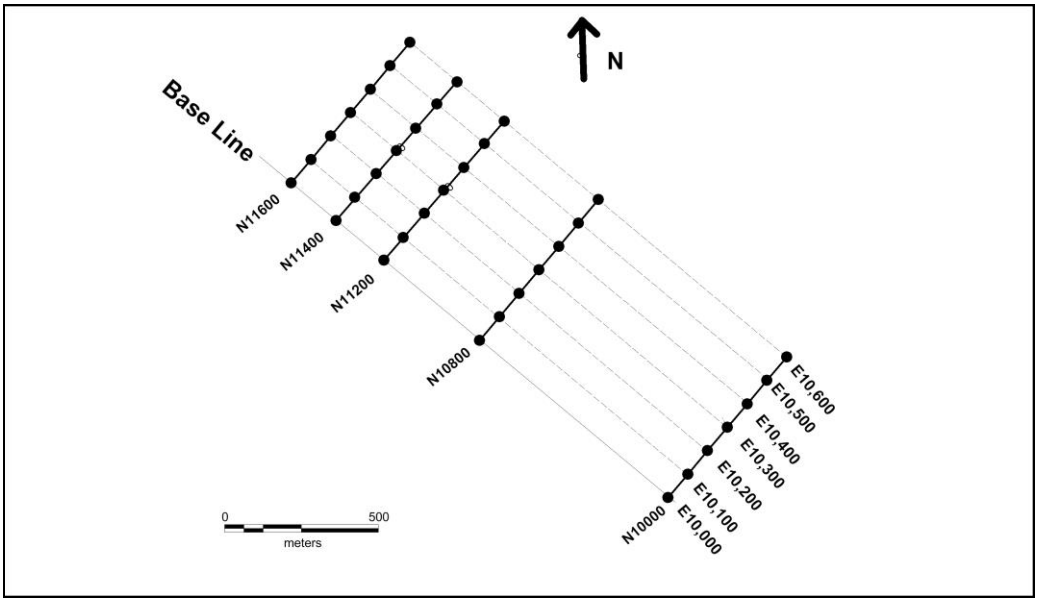

Fig.21. Illustration of local coordinate labeling used for soil survey within Kaponda Prospect. Note the direction of the grid base line (E10,000) perpendicular to sampling cross lines (N10,000; N10,800).

For example a soil sampling location can be moved if it falls in a river, swamp area full of water, road and existing tailings. After sampling, a stick of dead tree with flagging tape is pegged to materialize the grid so that any follow-up will have physical reference on the field.

Hand GPS (Global Positioning System) is used to locate grid lines and pick up coordinates of soil sample locations. In the Central African Copperbelt, the loss of GPS signal is very common both during summer when thick cloud fluctuates satellite signal strength, and also in places of thick vegetation cover such as areas in the vicinity of rivers or jungle. In case of poor or absence of GPS reception, the compass is used to indicate the direction of the traverse line and the measuring tape to indicate the distance between samples in the same line.

The GPS accuracy is also function of the type of handheld GPS devices. For detailed sampling (e.g. 100X50 m, 50X50 m or lesser), high sensible GPS device equipped with DGPS system are recommended to minimize accuracy fluctuation which can negatively impact on the real location of potential anomaly.

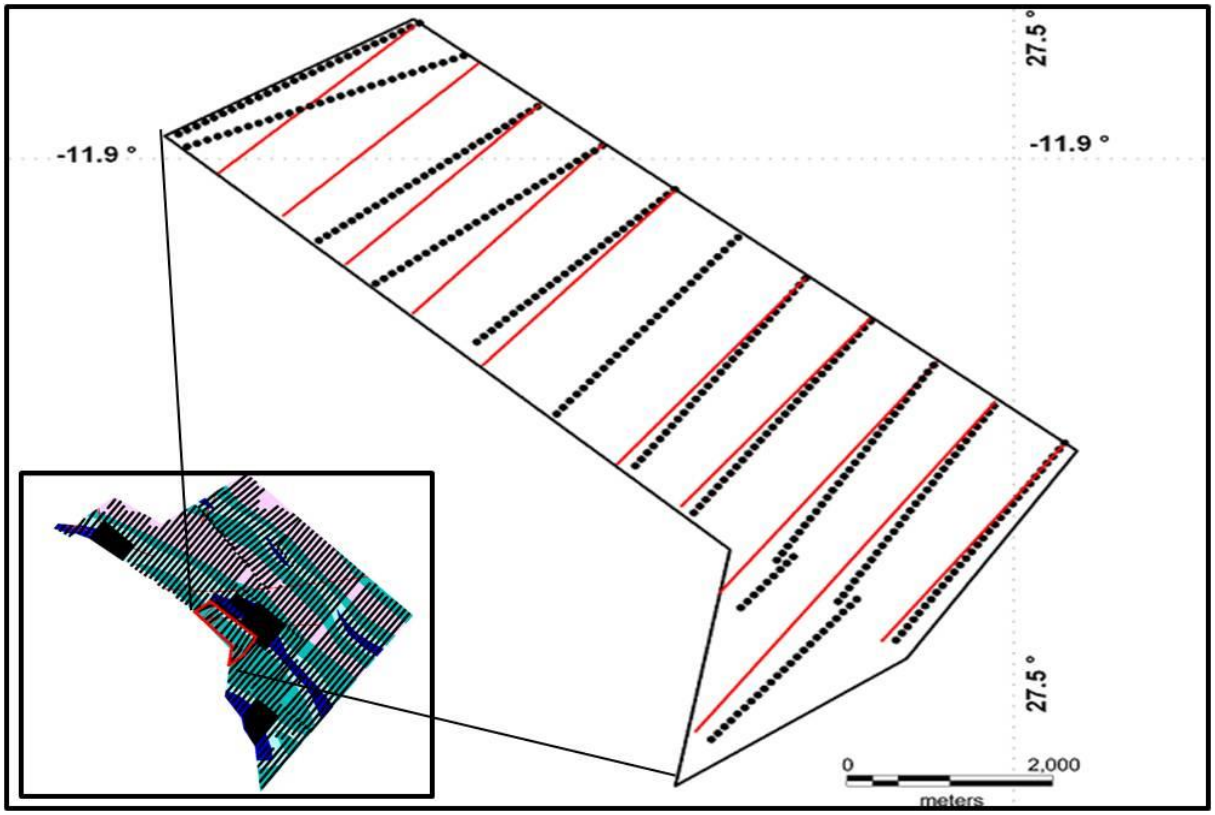

Fig.22. Portion of the soil survey (a) grid of Kaponda (b) showing offset between planned traverse sampling lines in red, and collected sample location in black dots.

5.3.1.2. SAMPLING PROCESS

The sampling process is subdivided into 4 operations: sample collection, drying, disaggregation and sieving. Firstly, geochemical samples of the study area were collected from the horizon B of soil profile at an average depth of 50 cm, expect in swamp, lateritic and rocky terrains. Since there is a thicker humic horizon A within swamp zones, soil samples were collected from up to 60 cm depth. Conversely in rocky terrain and places with hard laterite cover, samples were collected at a minimum depth of 30 cm due to difficulty of penetration.

When collected, a quantity of about 1 Kg of silt to clay size soil material was placed in a 30X45m wide plastic bag. At this stage, plastic bags are preferable than paper base bag because soil sample can have moisture. A ticket tag with sample reference number is placed inside the sample as for identification. Additional information such as GPS coordinates of the sample location, soil color and type, collected date, sampler ID was recorded and stored for future use.

Secondly collected soil samples were dried in the sun as most of the Kaponda soil samples have moisture. Wet samples are even very common during raining season. For such samples, natural drying in the sun or natural air is required. Drying over 65^{o} results in loss of volatile elements such as mercury (Koksoy et al., 1967), and high temperature hardens clay making disaggregation difficult and time consuming.

Thirdly, dried samples were gently disaggregate to get size fraction which will suite the sieving. And finally after disaggregation, soil samples were sieved on 180 micro mesh to collect the very thins material ready for analysis. This mesh size is optimum for Cu and Co analysis, assuming that these elements derived from primary sulphide minerals. Sulphides are unstable minerals, they decompose during weathering and reallocate their metal content all over the finer component of the soil. Steel screen sieve made of stainless silver was used to filter soil samples. This type of sieve is recommended to avoid both contamination from equipment and carryover contamination as it can be easily cleaned by compressed air or water, and dried before using it for the next sample.

The final soil products are two duplicate well sieved soil samples of 50 to 100 g. The first sample is stored in paper envelopes for absorption atomic analysis, and the second in a small plastic bad for XRF test. During different stages of sampling process, strict rules of quality

control are observed to avoid physical contamination resulting from mixing of different samples, cleanliness of the sieve and mislabeling. Even though the laboratory chemist has the responsibility to assure the quality of assay results, the latter is also dependent of the effectiveness of the entire sampling process.

5.3.2. ANALYTICAL METHOD AND QUALITY CONTROL

Soil samples from Kaponda Prospect were sent to Genalysis Laboratories in South Africa and Australia for atomic absorption analysis for copper and cobalt. In the field, in-house laboratory was using portable Niton XRF machine to analyze soil samples for quick results. After ten's of thousands analysis of soil samples from several locations including Kaponda area, comparison between XRF and atomic absorption results shows a very high positive correlation for Cu; and any correlation at all for lower Co values (e.g. value <1,000 ppm). However results from atomic absorption are relatively higher than XRF but within an acceptable limit. This difference can be explained by the used of strong acids such as nitric or hydrochloric acids for chemical analysis, to attack soil sample and optimize contrast for base metal element though all silicates will not be completely dissolved (Moon et al., 2009). Hence the choice of analytical method for soil samples aims at enhancing contrast of the main sought element.

To ensure the quality of results, both exploration geologists and laboratory chemists put in place control to measure the accuracy, the reproducibility or precision of the analysis, and contamination. The precision is measured by analyzing duplicate samples while the accuracy implies the analysis of reference material of known composition. The reference material are standard samples. For instance OREAS 45P is a certified reference material which can be utilized for copper and cobalt control.

Any batch with standard results outside the mean+/- 2standard deviation should be reanalyzed, while precision is monitored by calculating the average and difference between duplicates on a chart (Thompson, 1983). Contamination of sample is measured by analyzing blanks. Standards, field duplicates and blanks were used for the quality control of Kaponda samples but unfortunately these data are not available for this dissertation.

As far as the exploration geochemistry is concerned, it is worth to mention that analysis has to be precise. Unlike at evaluation stage, the accuracy is not so crucial at this stage of survey though some indication of accuracy is still needed (Moon, 2009). The interpretation of geochemical exploration data is generally based on the difference in element concentration from different locations, and the definition of threshold anomaly for further exploration follow-up.

5.3.3. DATA PROCESSING

Collecting data is the most tedious and expensive phase of geochemical survey. Once collected data were captured into Excel spread sheet following a specific coding system (Table 3) to allow an easy processing and validation of data by GIS softwares. When exploring in Kaponda Prospect, Surpac software was used for planning and interpretation of geochemical data from an Excel and Access database. As far as the dissertation is concerned, geochemical data have been reprocessed through MapInfo 12.0.1 and Discover 2013. This software package is used for statistical and spatial analysis, validation, gridding and geo-referencing, as well as creation and processing of different thematic maps. Microsoft Excel is also utilized for other statistical analysis and graph design.

The use of an Excel database is not encouraged for a larger amount of data. The inconvenience of such database are the lack of validation tools, the uncontrolled editing and writing rights. Within Exploration Corporate, ideally database software such as Sable or Datashed should be used to manage information. These softwares are very specialized in the treatment of the information with a series of validation, checking tools and operation such as the identification of mismatch and duplicate data. Thereafter only clean data has to be processed into 2D and 3G GIS softwares. As the main geochemical prospecting data are mostly numerical,

Table 3. Example of geochemical database in Excel spread sheet; where BN=brown, FD=field.

	LOCAL GRID			UNIVERSAL TRANSVERSE MERCATOR 35L		SOIL SAMPLE			ASSAY RESULTS		META DATA		
Sample ID	Line #	Local E	Local N	UTM Easting	UTM Northing	Color	Type	Depth (cm)	Cu ppm	Co ppm	Collected year	Sampler Name	Grid Name
F7354	L4	10000	2400	552173	8701514	BN	FD	50	49	17	2005	Benoit	Panda
F7355	L4	10100	2400	552097	8701447	BN	FD	50	47	15	2005	Benoit	Panda
F7356	L4	10200	2400	552022	8701381	BN	FD	50	46	13	2005	Benoit	Panda
F7357	L4	10300	2400	551946	8701314	BN	FD	50	52	14	2005	Benoit	Panda
F7358	L4	10400	2400	551870	8701248	BN	FD	50	92	15	2005	Benoit	Panda

geostatistics is the first phase at interpretation such data. It has the capability of extracting essential information from a larger numerical data set.

5.3.4. INTERPRETATION

5.3.4.1. STATISTICAL ANALYSIS

A total of 14,754 soil samples were collected from different sampling grids (Fig.20) within the Kaponda Prospect. All samples were analyzed for copper with values comprised between 0 to 8,612 ppm (Fig.23, a). However in this dissertation only 3,250 soil samples have Co assay results varying from 0 to ppm 628 ppm (Fig.23, b). The aim of statistical analysis is to understand the nature of the data distribution and thereafter to estimate the anomaly threshold.

As far as statistical analysis is concerned only samples collected on a constant grid spacing of 800X100m will be treated, however the additional soil samples collected from more reduced grid spacing will only be used in a section further down when geochemical anomalies will be spatially analyzed. The reason for this is to avoid the effect of a cluster of samples from one or few areas to influence the statistical distribution as well as the geochemical threshold of the entire Prospect.

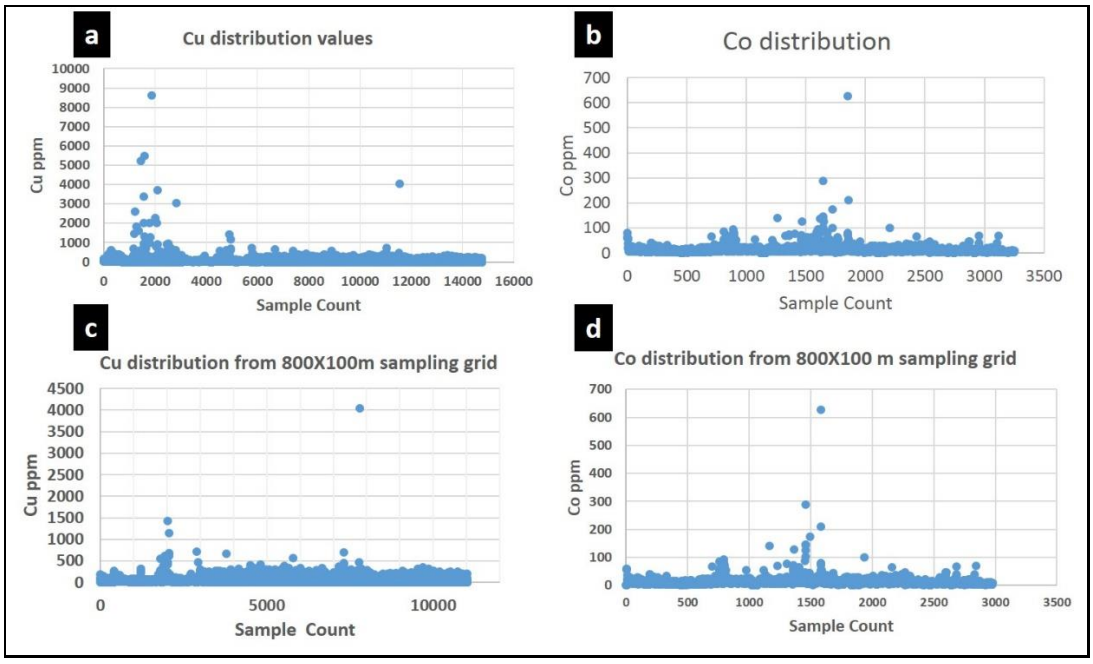

Fig.23. Scatter plots showing (a) Cu distribution for 14,754 soil samples; (b) cobalt distribution for 3,250 soil samples; (c) Cu distribution from 11,023 sample (d) Co distribution from 2,977 samples. Note that (c) and (d) group of samples were collected from 800X100m grid spacing only.

As previously mentioned, only 11,023 soil samples were collected on an 800X100m grid. All these samples have Cu assays results, while only 2,977 samples have Co values. Within these populations of samples, Cu in soil varies from 0 to 4,032.6 ppm (Fig.23.c) and Co from 0 to 628 ppm (Fig.23, d). Basic statistics for both Cu and Co are summarized in Table 4, including measures of both central tendency (mean and median) and dispersion parameters (range, standard deviation, percentile, and variance).

Isolated highest values can also bias a statistical distribution. That is why 3 highest Cu values and one for Co have been deducted from the populations to see their influence on distribution parameters. Despite retrenching 3 and 1 samples only from 11023 and 2977 respectively, dispersion parameters such as standard deviation, variance, skewness and Kurtosis have considerably been reduced (Table 4). Kurtosis measures the influence of highest values within a distribution. Therefore its values from 1093 for Cu and 609.99 for Co to 18.48 and 122 (Table 4) respectively illustrate perfectly the impact of these outlier values.

Table.4. Central tendency and dispersion statistics parameters for Cu and Co in soil samples of Kaponda.

	800X100 m grid spacing		800X100m grid excluding isolated highest value	
Statistics Parameters	**Copper**	**Cobalt**	**Copper**	**Cobalt**
Count	11023	2977	11020	2976
Range	4032.68	628	718	289
Minimum	0	0	0	0
Maximum	4032.68	628	718	289
Mean	36.58	12.6	35.99	12.41
Median	19	10	19	10
Mode	0	9	0	9
Standard deviation	68.25	17.02	54.08	12.75
Variance	4658.47	289.71	2924	162.47
Skewness	20.92	19.32	3.18	8.27
Kurtosis	1093	609.99	18.48	122
Interquartile range	49	8		
Percentile 25%	0	7		
Percentile 75%	49	15		
Percentile 95%	145.02	27		
Percentile 97.5%	186.95	36		
Percentile 98%	199.9	40		
Percentile 99%	241.02	60.24		

These kurtosis values indicate also that frequency histogram of Cu and Co will have higher sharper picks, meaning there is more variability in Cu and Co data set due to few samples with extreme difference to their respective mean.

Of course both Cu and Co histograms show asymmetric and positive skewed distributions (Fig.24). With a skewness of 20.9 for Cu and 19.3 for Co, the distributions of the two elements are highly positive skewed in reference to Bulmer (1979) rule of thumb. Also the shape of the cumulative frequency curves of both Cu (Fig.24, a) and Co (Fig.24, b) indicates that the two data sets represent populations which are closer to a lognormal distribution.

For bivariante statistical analysis, the whole data set comprising 3,250 paired Cu-Co assays results has been taken in account to calculate the correlation coefficient. The pair data show a high positive linear correlation between Cu and Co, with a coefficient correlation (R) of 0.65 (Fig.25).

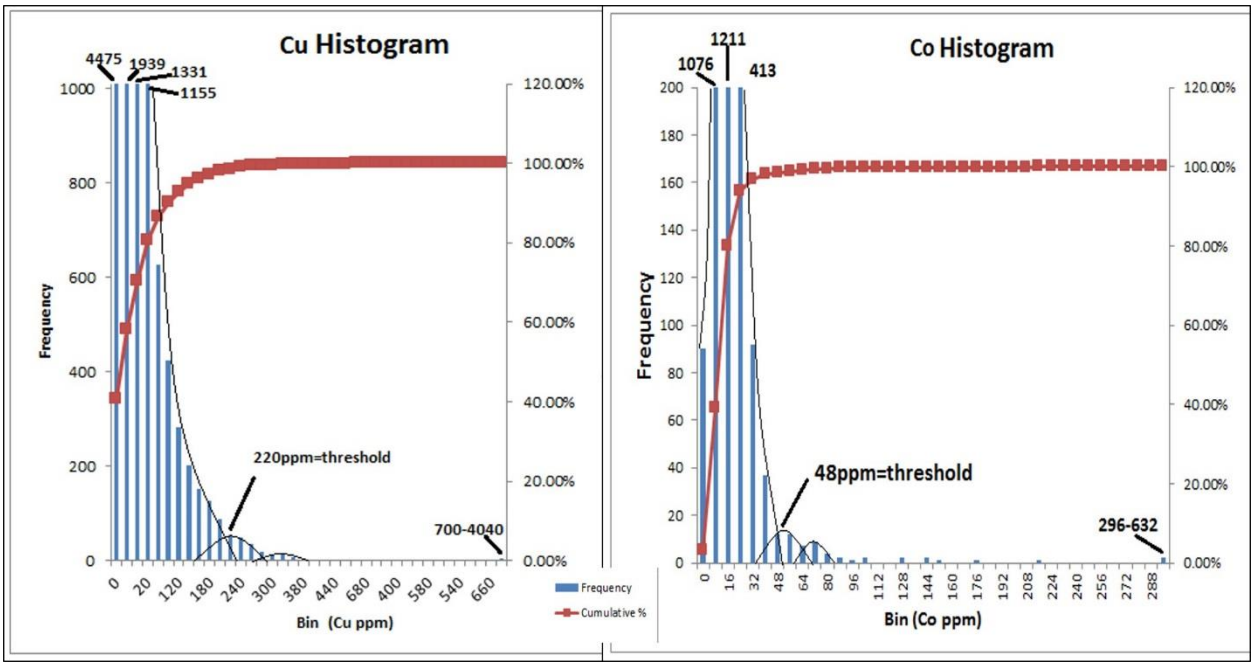

Fig.24. Frequency histograms for soil sample collected on 800X100 m grid spacing. (a) Cu histogram for 11,022 Cu samples with bin of 20ppm, and (b) Co histogram of 2,977 samples with bin of 8ppm. Note frequency curves (black lines) are interpreted multiple populations within a skewed distribution data sets.

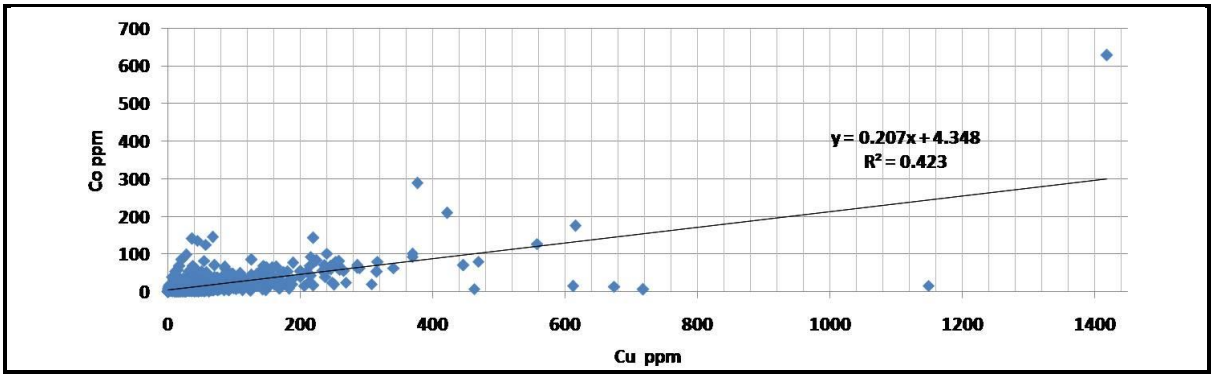

Fig.25. Scatter plot showing high positive correlation between Cu and Co for 3,250 soil samples.

This can be interpreted as copper and cobalt are originated from the same mineral phase or associated in a same paragenetic sequence. The positive correlation of the two base metals is consistent with a couple of nearby Cu-Co deposits such as Kimpe, Lupoto and Etoile Cu-Co (Fig.6) where ore is represented by both Cu-Co sulphide and oxide [e.g. carrolite Cu(Co,Ni)2S4 , heterogenite (Co,Cu)(OH)], and other Cu minerals (e.g. malachite, chrysocolla, azurite, bornite, chalcopyrite)

5.3.4.2. ANOMALY THRESHOLD DEFINITION

Several methods are used to estimate threshold for geochemical data. In these methods, a comparison between the observed geochemical data and the theoretical distribution model will be analyzed. Stanley and Sinclair (1989) propose three categories of threshold selection techniques: experiential, model-based subjective and model-based objective. In order to select the right method, it is also common for exploration geologists to compare and constrain anomaly thresholds obtained from these different methods.

The experiential methods of threshold are very subjective depending on the past experience of explorationists or literature comparison. For instance, in soil sample Cu varies generally from 2 to 100 ppm as a background grade (Levinson, 1974). For Kaponda Prospect, based on exploration experience with Fist Quantum Minerals, the threshold for Cu within this part of the CACB where the regional background is relatively high, was set at 200 ppm. In fact exploration activities of this mining company last about 10 years, covering a surface of more than 10.000 km^2 in the southeastern pedicle of the DRC, with more than 122,100 collected soil samples. It includes several green and brown field exploration projects such as the resource

development of Lonshi Cu deposit, the discovery of Frontier Cu deposit and mining of the two quoted deposits. The use of this subjective threshold definition within the Kaponda Prospect is illustrated by initial FQM drill holes which tested only soil anomalies above or equal to 200 ppm. No statistical distribution model is considered in this threshold estimation technique. The experiential method is neither reproducible among explorationists (Sinclair, 1991) nor in other different geological setting and region.

Model-based subjective techniques uses some formal statistics to estimate the threshold. It includes histogram, the "mean plus two standard deviation (+2sdev)" and the 2sdev methods. Background and anomalous samples form separate populations deriving from different causes. Each population can be possibly identified as they represent different probability density function (Langford, 1965).

After statistics the frequency histogram threshold obtained for copper is 220 ppm (Fig.24, a) and 48 ppm for Co (Fig.24, b). The histogram shows a positive skewed distribution made of multiple populations (background and anomaly populations) deriving from different geological processes. Secondly, the "mean+2sdev" method is commonly used by explorationists to threshold anomaly though it assumes that the population is normally distributed. For soil samples collected in Kaponda Prospect on 800X100m grid spacing (Table 4), the mean+2sdev threshold for Cu is 173.04 ppm and 46.64 ppm for Co. Finally, DeGeoffroy et al., 1967 considered anomalous samples above two standard deviations for a selected neighborhood data, this method thresh the anomalies in Kaponda at 136.5ppm for Cu and 34.04 ppm for Co.

At last, the two commonly used model-based objective techniques of anomaly threshold selection are the probability plot and the gap statistic approaches (Sinclair, 1974; Miesch, 1981). These methods are based on the fact that a background population in homogenous geological

Table.5. Comparison of anomaly Thresholds from several methods with their percentile.

		Experiential Method	Model-based subjective method			Model-based objective method
			2sdev	Mean+2sdev	Histogram	Log Probability plot
Cu	Threshold (ppm)	200	136.5	173.04	220	206.69
	Percentile (%)	98	94.4	96.9	98.5	98.1
Co	Threshold (ppm)	-	34.04	46.64	48	
	Percentile (%)	-	97	98.3	98.4	

setting is a probability density function resulted from processes that produces the background substrate (Sinclair, 1991). Cumulative frequency curves of Cu and Co (Fig.24) in Kaponda soil samples indicate lognormal distributions. Probability graph indicates as well lognormal distribution with the thresholds placed at 206.69 ppm for Cu (Fig.26).

The comparison of Cu results obtained from different methods show that anomaly thresholds from log probability, histogram and experiential methods are very constrained. They represent the upper 1.9%, 1.5% and 2% of the data respectively (Table 5). As a result in this dissertation 200 ppm will be used as Cu threshold. The mean+2sdev and 2sdev thresholds (173.04 and 136.5ppm Cu) correspond to respectively 96.9 and 94.3 percentiles. These thresholds are both believed to be falling into the background. This is consistent with the results from comparison of threshold methods of Reimann et al. (2005); they concluded that in geochemical exploration, values within the range of mean+2sdev were often defined as geochemical background. However Co threshold from histogram and 2sdev methods (48 and 46.64ppm) are very constrained, they represent 1.6% and 1.7% of the upper values (Table 5).

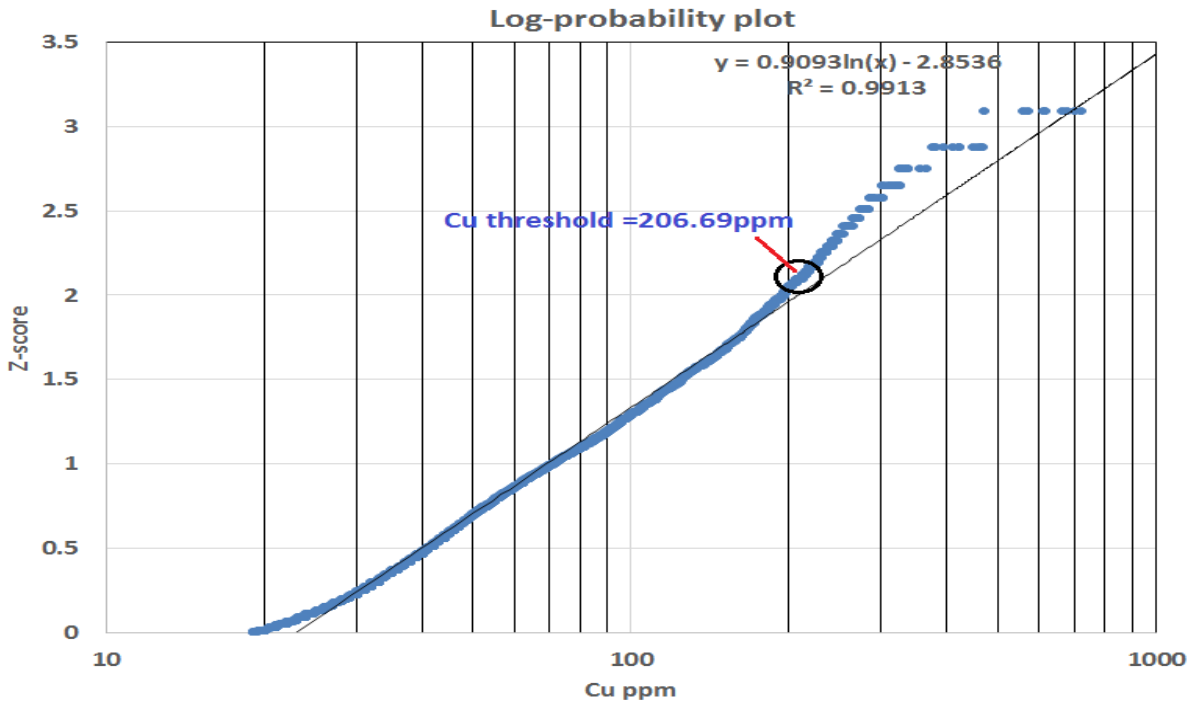

Fig.26. Log-probability graph of Cu values for a population of 11022 samples showing anomaly threshold.

5.3.4.3. SPATIAL ANALYSIS OF SOIL ANOMALIES

The positive correlation between Copper and Cobalt (Fig.25) is shown up pretty well on gridded geochemical maps (Fig.27). As previously mentioned MapInfo 12.0.1 and Discover 2013 were used to generate these gridded maps. The surface gridding method utilized here is the inverse distance weighting, using a power weighting model with the cell size of 100 and the searching distance of 1000 m.

Both high values in Cu (red) and depleted value (blue) (Fig.27, a) are positively correlated to Co map pattern (Fig.27, b). In zone 1 of the cited maps, the highest Cu values coincided to the highest Co. Zone 2 falls within swamp where cobalt red patterns occupy smaller surfaces than high copper, this may be due to the fact that Cu has a strong hydromorphic dispersion than Co.

In addition, geochemical patterns (blue to red) of the two elements indicate similarity of features oriented NW-SE on the two gridded maps. This general trend is parallel to lithostratigraphic units strike, suggesting Cu and Co values in soils are derived from stratiform or stratabound mineralization.

Conversely, another NE-SW orientation of blue pattern parallel to sampling lines, is prominent on the two gridded maps. It represents the very low to null values of both Cu and Co. These areas may either represent portions of sampling lines that have no returned assay results and the software generated a default value of zero. Or alternatively it may represent Cu and Co values which are not confident. Hence a quality control for these samples need to be checked. Unfortunately we cannot sort out this issue for now because standard data, duplicate and blank are not available in this dissertation. If the doubt persists, a re-assay or re-sampling of the specific portions is suggested for any further consideration of such data to make sure of the used of only qualitative data.

The implication of this positive correlation between Cu and Co, is the used of Co data to assess the Cu anomalies and reduce the false alarm anomaly. In other word, place with combined Cu and Co anomalies will be definitely considered true anomaly.

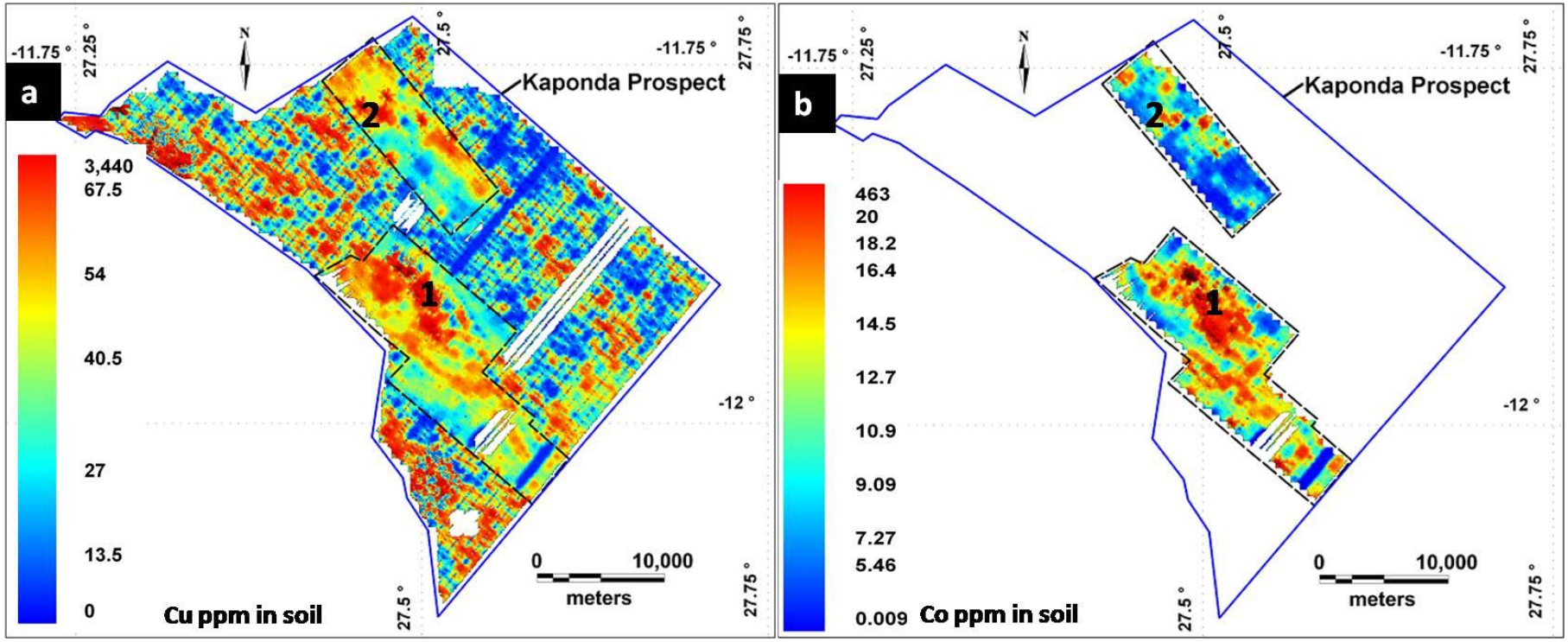

Fig.27. Gridded maps of soil geochemical data using the inverse distance weighting: (a) copper and (b) cobalt

Another important factor in the interpretation of geochemical data is the landscape type and topography. The selection of geochemical anomaly at this stage take in account the continuity of the anomaly and the landscape. As a result fifteen geochemical anomalies numbered from 1 to 15 have been highlighted (Fig.28). They have at least 2 to three consecutive anomalous grade of copper (≥200ppm) within a grid space of 800X100, or more continuous anomalous grade in a more detailed sampling grids. It is worth to also check human infrastructures such as road, railways, existing tailing dump or stoke piles of minerals because they can contribute to a fake anomaly if made of mineralized materials. Hence a caution should be taken for all anomalies closed to these infrastructures, particularly in Kaponda Prospect where railways has been used to transport Cu and Co concentrate from Kipushi to Lubumbashi, and

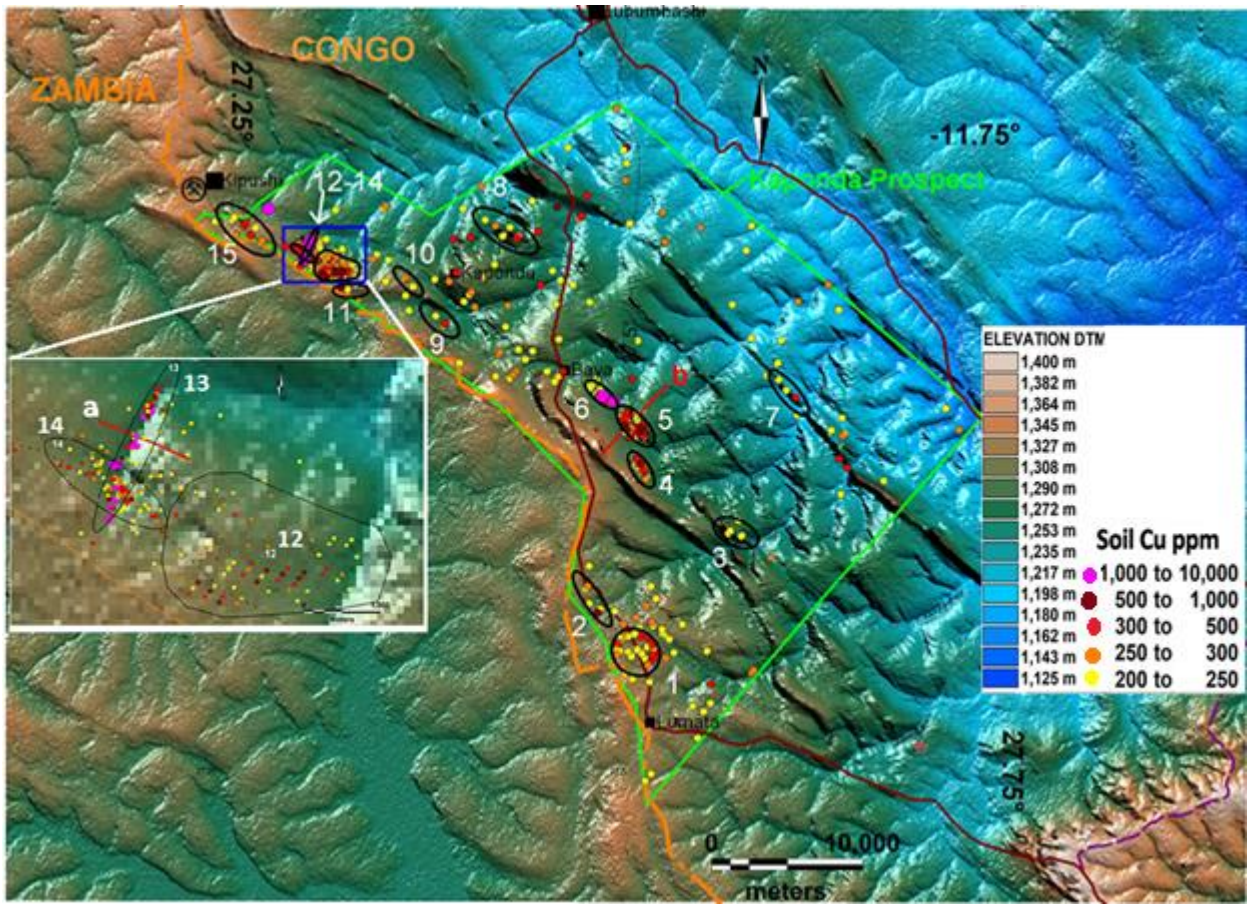

Fig.28. Soil geochemical anomalies superimposed on DTM elevation map. Note railways in black dash line and N1 road in red line.

Cu-Co ore from Lwiswishi to Kipushi concentrator plant. Also tar and gravel main roads are made up from mine waste material which can easily contaminated surrounding soil.

The topography plays a crucial role in geochemical dispersion and formation of regolith. For the Kaponda Prospect, the landscape is represented by a network of rivers with their tributary and swamps areas locally called “dambo”. These “dambo” are developed either along river or along flat surface of relatively low altitude, they can easily accumulate metal concentration from up slope. Steeper slopes favor mechanical and hydromorphic dispersion which create secondary geochemical anomalies in seepage zones; while some plane area and plateau favor in situ dispersion where anomalies seat almost on top of the causal bodies.

The easiest way to analyze the topography versus the grade in soil of an element, is to plot profiles of the two variables (Fig.29). High copper anomalies (5 & 13) displayed on Fig.28 occur respectively in a swamp area and along river (Fig.29, a), they are believed to be transported. But 7 & 8 Cu anomalies appearing on crest of relatively higher altitude, are believed to be in situ. However the geological knowledge of these areas should be always considered in order to predict an exact origin of the causative body.

The landform is generally characteristic of specific overburden which also associated to geological units. Unlike silicified dolomite of the Mines Subgroup (RSC) occupying the crest of hills, dolomite is generally not outcropping in the Kaponda Prospect. It is highly weathered into either reddish clayey soil or grey soil representing “dambo”. Within Kaponda Prospect dambo are zone of less or no vegetation, full or devoid of water. Anomalies of swamp zones such as

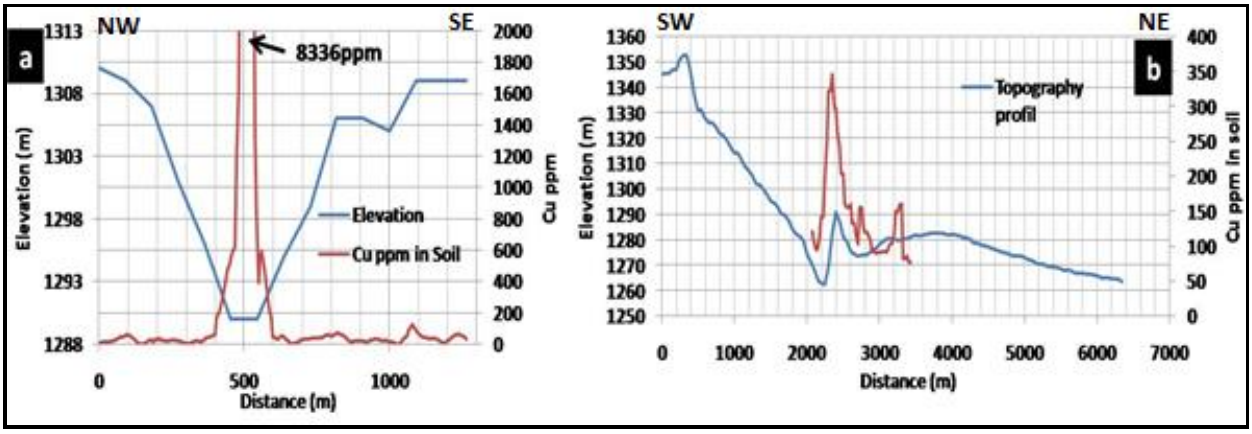

Fig.29. Analysis of profiles for Cu values in soil against topography. (a) and (b) section lines are located on map of Fig.28.

anomaly 6 might (Fig.28) either hide an in situ causative body like in Lonshi Cu deposit, or represent a locally transported anomaly (e.g. Frontier Cu deposit; Hitzman et al., 2012).

The integration of geochemical data into the geological setting is very critical at interpreting soil anomalies. As illustrated in Fig.30, the bulk of Cu anomalies occurs within the Roan Group, with only anomaly 3, 8 and 9 appearing in Grand Conglomerat, Kundelungu and Nguba formations, respectively. The distribution of Cu anomalies within Roan Group is consistent with known deposits of the Congolese Copperbelt whereas most of Cu-Co mineralization is hosted within Mines Series and accessorily in the Mwashya. However, anomalies occurring in other stratigraphic level should not be put away. The entire Katangan sequence is proven prospective to potentially host Cu mineralization at any level (Fig.4) whenever condition of such metallogenesis are met. There are few other known deposits occurs in the Nguba (e,g Kipushi, Kamoa, Lonshi) and Kundelungu (Fig.4).

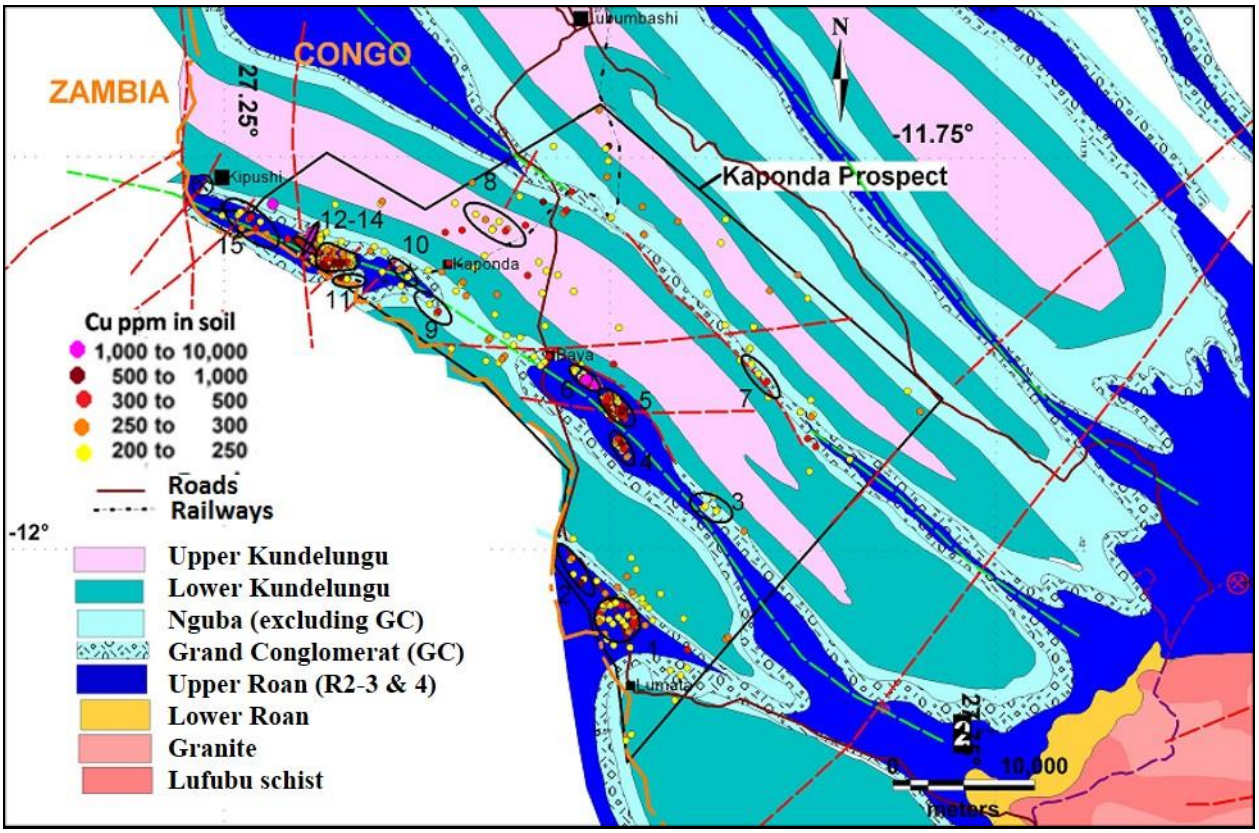

Fig.30. Soil geochemical anomalies superimposed on the regional geology (Geological map modified from Jigsaw, 2009, unpubl.). Red and green dash lines are faults and anticline axis respectively.

Finally structure such are fault intersection, fold closure and lithological thickness pinch-out should be taken into account when assessing and prioritizing soil anomalies, as they can trap mineralization. In addition, any geophysical signature associated to geochemical anomalies should be also integrated at this stage. Later in this dissertation the section of target generation will discuss the integration of all the data set prior to drilling.

5.4. AIRBORNE AND GROUND MAGNETIC SURVEY

A horizontal gradient of fixed wing airborne magnetic and radiometric surveys was conducted in 2004 by Fugro Airborne Surveys Ltd, a Netherland based geophysical company. The survey covered a number of FQM permits in the SE pedicle of the DRC, including the Kaponda Prospect. The survey was conducted on 200m line spacing. These traverse lines were oriented 023^{o}, crosscut by one tie line trending 113^{o}. Total field magnetic intensity , horizontal and longitudinal magnetic gradient measurements were made at less than 9m interval with 10 Hz frequency, at a nominal sensor altitude of 80 m terrain clearance. A Caesium Vapour 0.005nT magnetometer were used for the airborne survey, mounted in a wingtip and tail configuration. On the other hand, a Caesium Vapour 0.01nT magnetometer were taking measurement at the base station (Fugro, 2004; unpubl.).

Airborne magnetic survey did not cover the NW corner of Kaponda that is why in 2009 a ground magnetic survey was conducted in this part of the Prospect by Geophysics GPR, a Botswana-based company. The survey was run on 200 m spaces traverse lines oriented 040^{o} with a 120^{o} trending tie line. A mobile magnetometer was taking measurements every 10m while another fixe magnetometer was recording variation of the magnetic field at a base station for eventual correction of diurnal magnetic storm.

The aim of the magnetic survey was to map structure, lithostratigraphy and any other magnetic signature that could be directly or indirectly associated to mineralization. In this dissertation only image of the reduction to the pole (RTP) of the total magnetic intensity (TMI) is used. The RTP filter for low magnetic latitude utilizes an azimuthal pass in the wave number domain to minimize the directional noise caused by low geomagnetic latitude (Philipps, 1997).

The magnetic field within Kaponda Prospect is characterized by both high amplitude negative anomalies and law amplitude positive anomalies. Anomalies gradient are gentle to

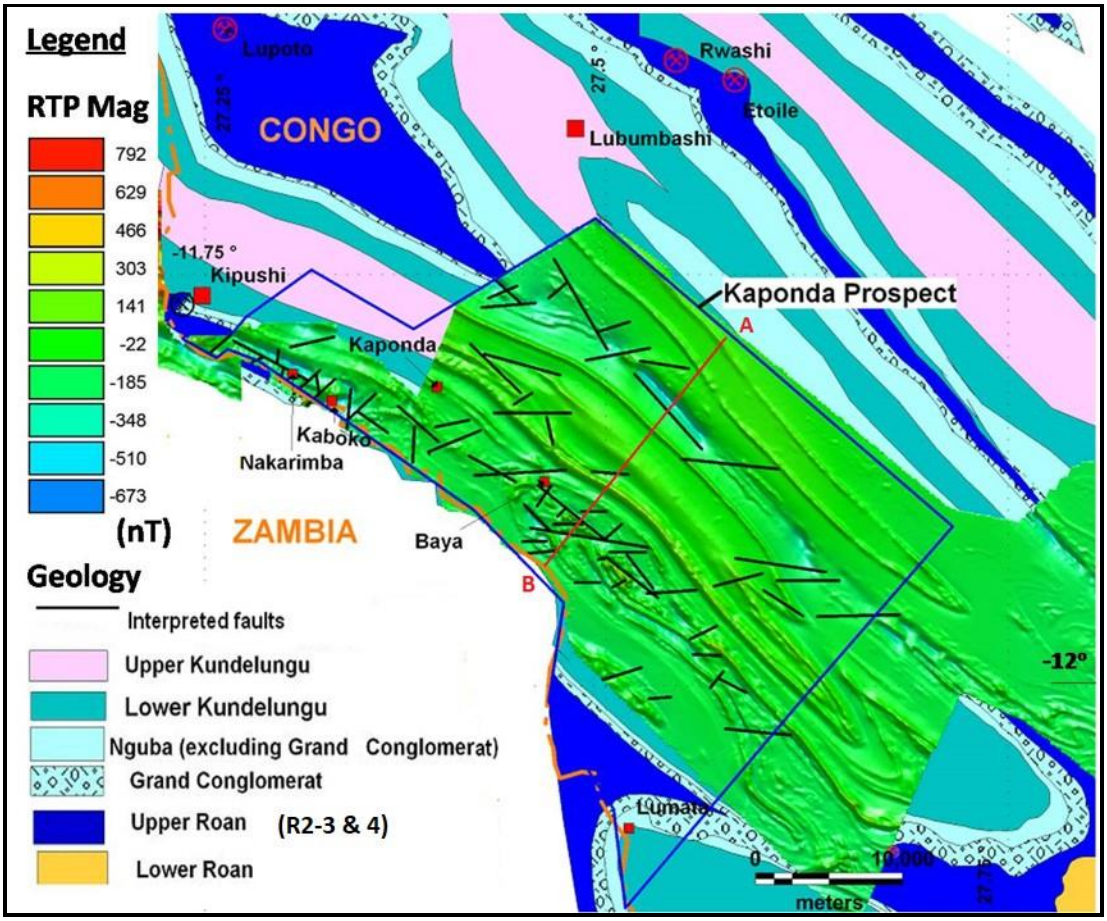

Fig.31. RTP magnetic airborne image showing lineaments associated to lithostratigraphy boundaries, fold closures and disruption interpreted as faults. The geological map in the background is modified from Jigsaw, 2009, unpubl.).

steep, generally running in NE-SW direction and mapping geological unit boundaries (Fig.31). The RTP map shows continuous NW-SE lineaments that map correctly lithostratigraphic units and its boundaries; as well as structure such as fold closure.

Despite having some magnetic minerals such pyrrhotite, the "Grand Conglomerat" is correlated to the relatively negative RTP magnetic signature (Fig.32). There is a strong positive correlation between the base of the upper Kundelungu formation represented by siliciclastic rocks which correspond to the high amplitude positive RTP anomaly with value of over 140 nT (Fig.32). The mineralogical composition associated to this high magnetic topography is to be proven as only weathered rock were analyzed when mapping. A deep negative magnetic signature (blue in color) with low is correlated to the Roan Group, probably associated to carbonate units (Fig.32), characterized by law magnetic susceptibility.

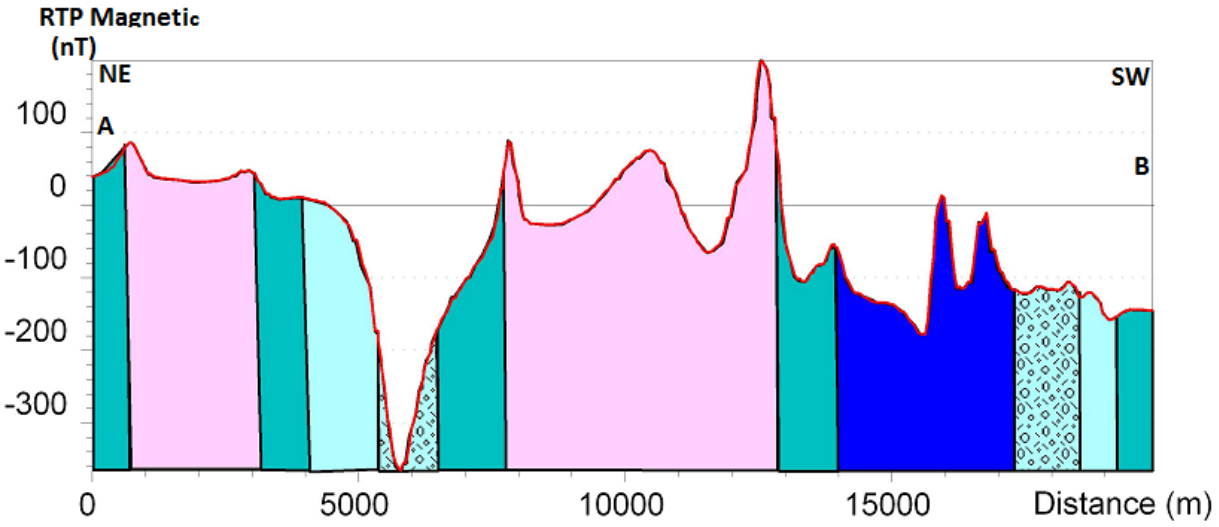

Fig.32. Profile showing the relation between RTP magnetic data with the geology. The location of the profile and geological legend are shown on Fig.31.

One of the important application of the RTP magnetic is the interpretation of faults. The disruption or steep gradient of magnetic pattern are interpreted to be associated to faults. The most prominent disrupted lineaments on RTP map occur in the vicinity of Baya. This type of feature is very typical to Mines Series blocs which are over thrusted and emplaced in any direction within RAT megabreccia. Analysis of RTP magnetic map generates about 64 inferred faults (Fig.31). MapInfo Discover software package is used to compute automatically the average strike of each interpreted faults. Thereafter GEOrient is used for stereographic projections and rose diagram plots of structure measurements.

Structural analysis using rose diagram, indicates three main orientations of faults: E-W, NE-SW and NW-SE (Fig.33). The E-W is the most representative orientation with frequency percentage over 45. Both NE-SW and EW trending faults crosscut lithological units. These set of faults are interpreted as normal deep structures or transfer faults which can serve as pathway for mineralized fluids (e.g. NE trending Kipushi fault associated to Zn-Cu-Pb deposit, Fig.6).

The third orientation though less representative, is also very important. NW-SE faults are almost parallel to fold axis and lithostratigraphy units. There believed to represent either the brittle phase of the Lufilian orogeny that folded and thrusted the Katangan rocks (Kipata et al., 2013); or intergrowth synsedimentary faults (Hitzman, 2010). NW-SE faults predate E-W and NE-SW faults.

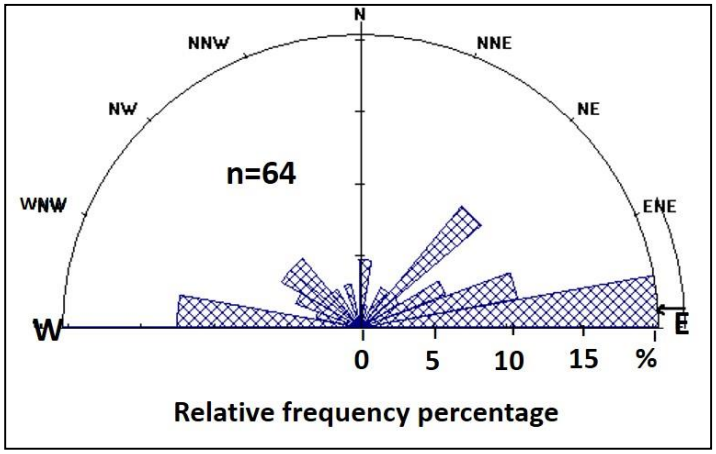

Fig.33. Rose diagram of interpreted faults from the RTP aeromagnetic map showing relative frequency of fault orientation.

5.5. AIRBORNE RADIOMETRIC SURVEY

Airborne radiometric data together with magnetic data was acquired in 2004 by Fugro Airborne Surveys. The aim of this survey was to map alteration, structure or any radiometric feature associated to the host rock or mineralization. Correlation between pattern of radiometric maps and unweathered rocks are very common (Gunn et al., 1997).

Gamma-ray spectrometric data presented in this dissertation, consist of four maps of radioactive elements: potassium (Fig.34, a), thorium (Fig.34, b), uranium (Fig. 35, a) and composite ternary images (Fig.35, b). The radiometric data are generally used to map geological features such as lithology, alteration and structure. There are similarities on features from the four images. Their pattern representing both low and high values are all NW oriented mapping different lithostratigraphy units. Accessorily disruptions in radiometric features locally indicate faults.

Of all the four maps, potassium radiometric data of zone 1 (Fig.34, a) map continuously siliciclastic rocks of the upper Kundelungu within the center of the syncline. They are oriented NW-SE and represented by high amplitude anomalies (up to 4% K). This high amount of potassium is probably associated to either feldspathic sandstone (arkose), or argillic units or

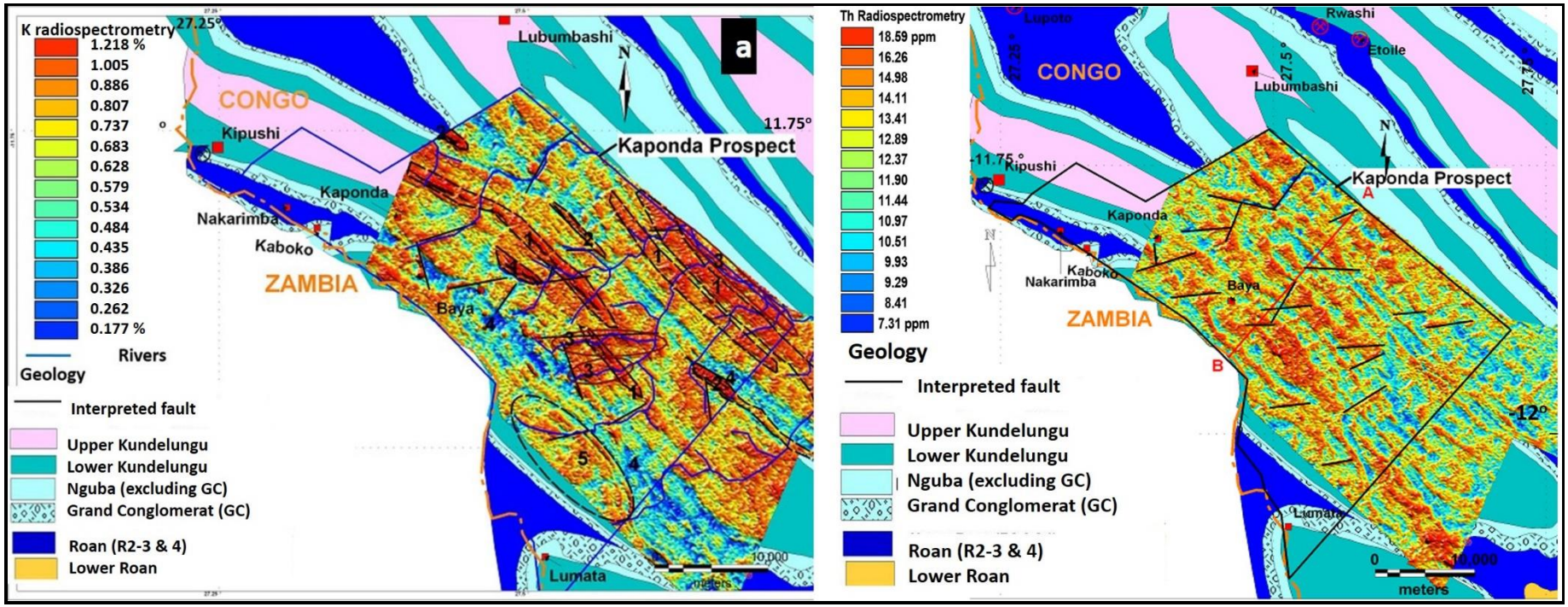

Fig.34. Airborne radiometric maps showing interpreted faults (in black lines): (a) Potassium radiometric image, note different potassic signatures numbered from 1 to 5, (b) Thorium radiometric map. Geological map is modified from Jigsaw (2009, unpubl.).

potassic alteration (e.g. k-feldspar). In the core of Lupoto anticline, discontinue NW trending potassic anomalies (zone 2) are correlated to arkosic sandstone of the upper Mwashya and the lower part of the Grand Conglomerat rich in granite and sandstone boulders and cobbles. Within Lubumbashi district, the upper Mwashya is characterized by arkosic sandstone rich in K-feldspar, occupying crests of prominent hill and underlain by the Grand Conglomerat (Cailteux et al., 2007).

Some potassic anomalies are just correlated to rivers (zone 3) expressing the higher amount of clays minerals deposited along river's ridges. E-W potassic anomalies occupied by rivers might be associated to deep lithospheric structures or important transfer faults which can possibly serve as conduit of mineralizing fluid. On the other hand, the lower potassic anomalies are mainly related to carbonate rocks of the Roan group (zone 4 of Fig.34a) and caps carbonates overlying the Grand Conglomerat.

Th and U radiometric maps does not map efficiently lithology boundaries apart from their very low amplitude anomalies associated to carbonates of the Roan Group and lower Nguba defining the central parts of Kipushi and Lupoto anticlines (Fig.34, b & Fig.35, a).

The ternary radioelement (K-Th-U) or color composite image show a strong spatial correlation with lithostratigraphic units (Fig.35, b). The Roan Group appear darker (blue) indicating the lower concentration of the three radioelement. While the Grand Conglomerat is well mapped (dark red) enclosing the Roan and bordered at its outer side by a finer blue color which potentially represents the Nguba cap carbonates. The Upper Kundelungu is lighter in color meaning a relatively higher amount of the three radioelements, though intervening reddish layers mapping geological units rich in Potassium can be seen.

Spatial analysis of grid images of K, Th and U radiometric data, using MapInfo Discover software, led to the interpretation of faults (Fig.34, a, b & Fig.35, a). The quoted software was again used to compute the average fault orientation in a range 0-180^{o}. Three data sets of fault orientations comprising 17, 19 and 16 strike values derived from K, Th and U maps respectively, has been analyzed using GEOrient. Rose diagram plots of the three data sets identified four fault directions: E-W, ENE-WNW or NE-SW and NW-SE (Fig.36). These fault trends are consistent with the orientations obtained from RTP magnetic map. The E-W and ENE-WNE are interpreted

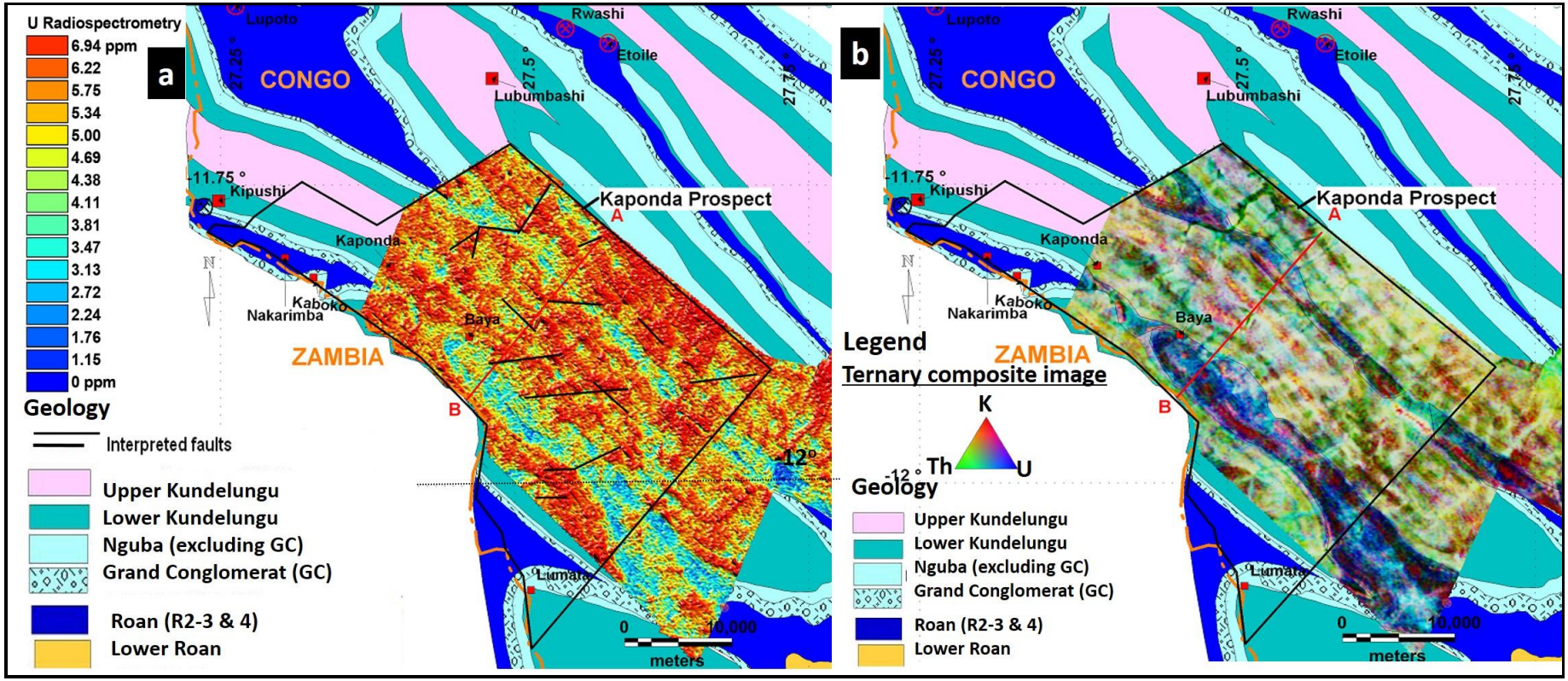

Fig.35. (a) Uranium radiometric image showing interpreted faults (in black lines), (b) Ternary radioelement composite (K, Th, U) image mapping lithostratigraphy. Geological map is modified from Jigsaw (2009, unpubl.

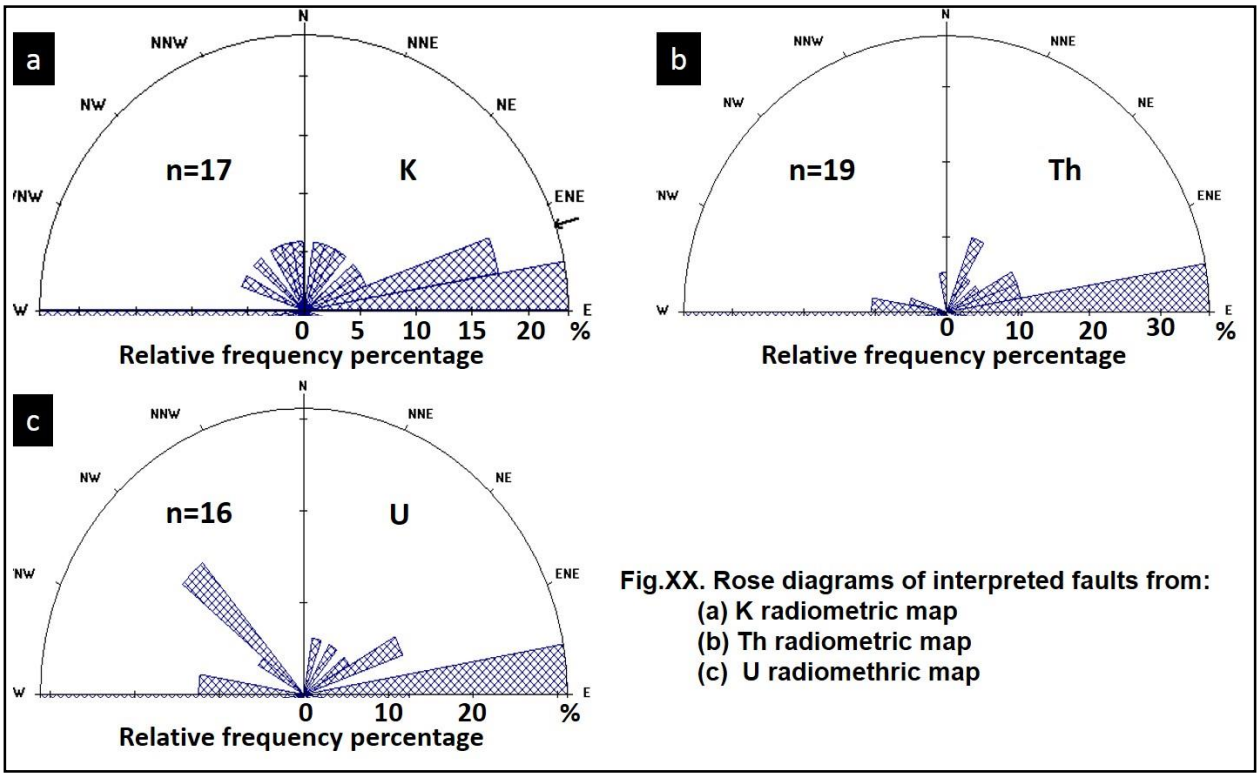

Fig.36. Rose diagrams of interpretation faults from (a) K radiometric map, (b) Th radiometric map and (c) U radiometric map.

from the 3 radioelement maps (K, Th, U). They has a higher frequency of appearance, about 50% of faults fall in this group. They represent together with NE trend faults, normal transfer faults. Finally the NW-SE orientation is mainly identified on U radiospectrometric map (Fig.36, c) and in RTP magnetic map as well. These faults are almost parallel to the folds axis, they are locally parallel to lithological units and can be interpreted as either synsedimentary intergrowth fault or strike slip-fault associated to the brittle regime of the Lufilian orogeny (Kipata et al., 2013)

5.6. INDUCED POLARISATION SURVEY

In 2007 the induced polarization (IP) survey was conducted in Nakarimba area as a follow-up to strong geochemical soil anomaly (up to above 8,000 ppm Cu) occurring along a river NE oriented. The aim of the survey was to locate sulphide mineralization associated to this high geochemical anomaly even though previous drilling was unsuccessful. Geophysics GPR was contracted to run the survey. NW oriented 21 lines of 1km each were surveyed with 100m

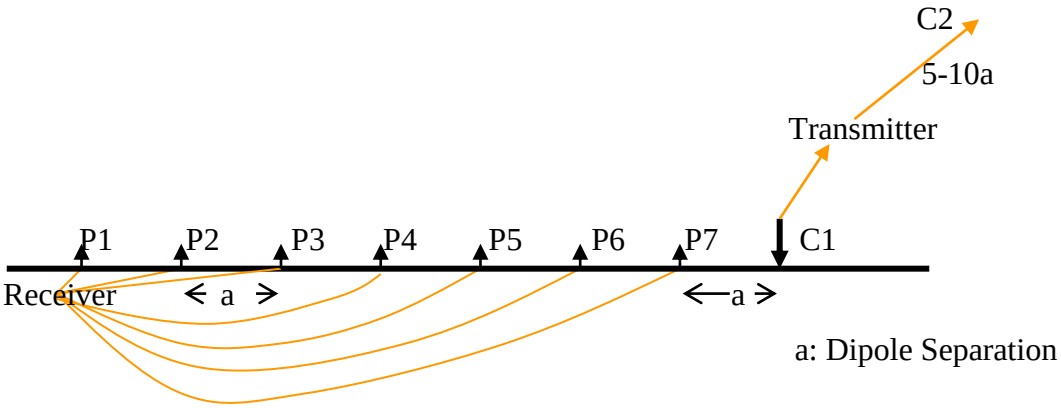

Fig 37. IP pole-dipole array set-up used for IP survey of Fig.38 in Nakarimba area (Geophysics GPR, 2008, unpubl.).

space between lines. The field instrumentation and set up of the IP survey is described in Fig.37. It consist of pole-dipole array with a 50m dipole size. A Phoenix IPT time domain current transmitter and an IPR-12 Digital Receiver were used with steel pegs current electrodes for current input into the ground. Potential electrodes made of porous pots with copper sulfate electrolyte were measuring ground chargeability and resistivity at the same time. Apparent resistivity and chargeability, self-potential and chargeability standard deviation were taken for every dipole position. To ensure high quality measurements, readings were taken ten time on each station. Reading were take up to n=6, with increment of n corresponding to the increase penetration depth.

A NW-SE strong chargeability (over 40 mV/V) anomaly associated to low resistivity, occurs in the center of the surveyed area (IP 5 and IP6, Fig.38). While two other well defined high chargeability anomalies with the same trend, occur respectively in the Southwest of the first anomaly and they are also associated to low resistivity (IP).

The strong chargeability anomalies (IP5 & 6) map carbonaceous shale (graphitic shale) and the lower part of the Grand Conglomerat which has a carbonaceous matrix (Fig.38). The back shale has on average 1 to 3% disseminated pyrite (Fig.8), while the Grand Conglomerat contains locally pyrrhotite and pyrite. IP3 & 4 map as well back shale as intercepted in drill holes (Fig.38). The IP pseudo section (Fig.39) indicate a double dipping high chargeability

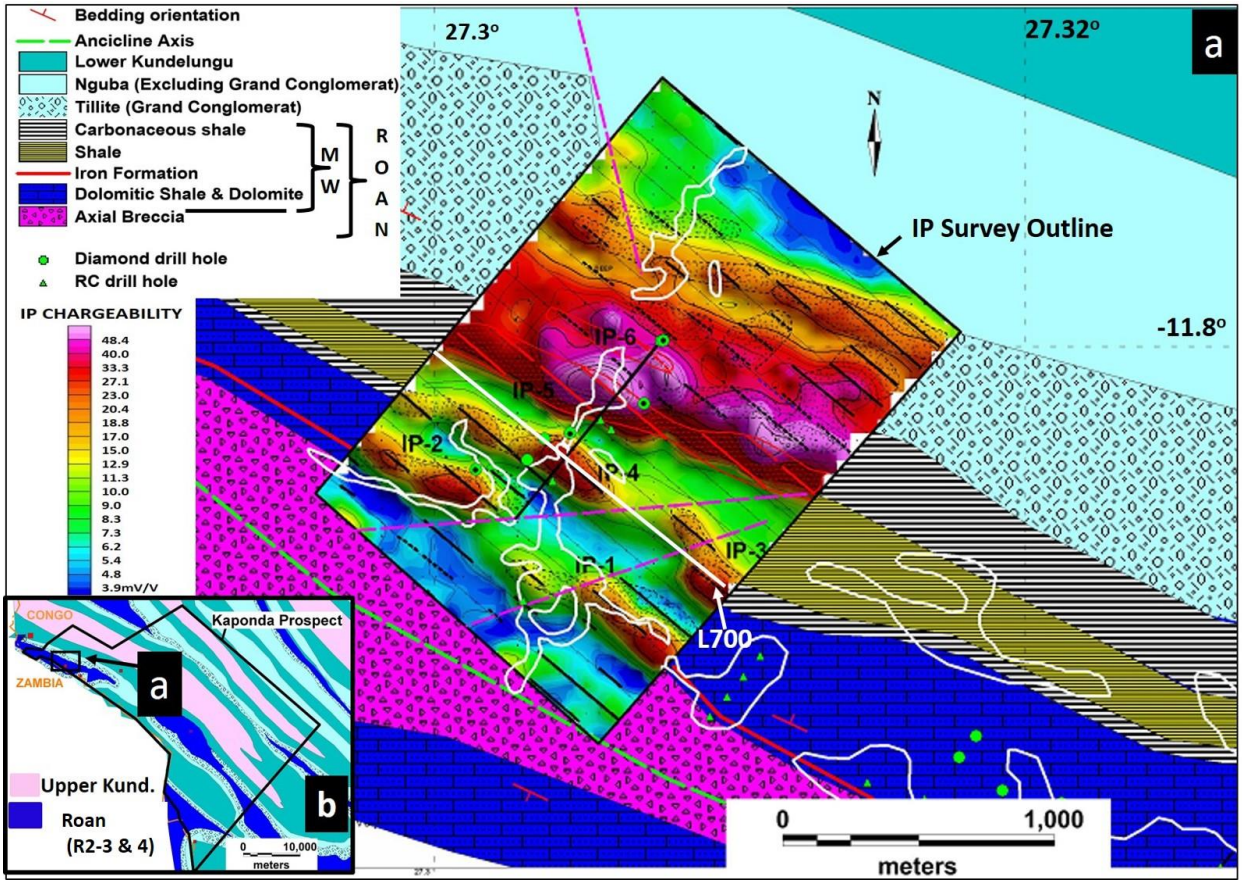

Fig.38. (a) IP pole-dipole chargeability map (modified from Geophysics GPR, 2008, unpubl.). NW oriented surveyed traverse (black) lines are perpendicular to NNE oriented geochemical anomalies (white contour lines). The geophysical map is superimposed on local detailed geological map, interpreted from drill holes (green dots and triangles) and mapping data. Note the highest chargeability mapping the carbonaceous shale. Purple dashed lines are interpreted faults White line L700 is section of pseudo-section of Fig.39. (b) Geological map (modified from Jigsaw, 2009, unpubl.) showing location of (a).

associated to double plunging low resistivity. The apparent dips of anomalies on pseudo section reflect measurements geometry rather than the geometry of causative body. In fact causative bodies in section L700 correspond to black shale which is known to be stratiform and dipping to the NW.

There is a strong correlation between the axial breccia and the low chargeability in the SW of the survey area. Other very law chargeability are associated to Nguba carbonate in the Northeast and the dolomitic shale and dolomite in the southern survey area. However high chargeability anomalies (IP 1 & 2) occur within the same dolomitic shale-dolomite succession. They might be associated to Iron Formation that outcrop in the SW of the anomaly or associated

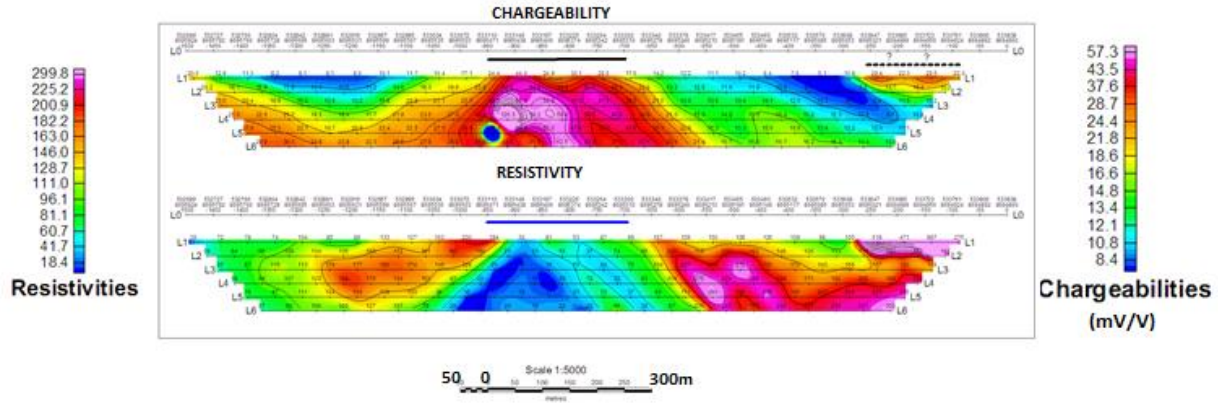

Fig.39. IP pole-dipole pseudo-section L700 showing chargeability and resistivity anomalies along depth (Geophysics GPR, 2008, unpubl.). Location of the section line is on map of Fig.38.

to sulphide bodies as mineralization has been already intercepted within dolomitic shale at the same lithostratigraphy level (Fig.10, f and Fig.11). Therefore these anomalies represent drilling target to test.

Prominent break in high chargeability anomalies (between IP3 and IP4, and IP1 and IP2) are interpreted as faults (Fig.38). These faults crosscut geological units and are associated to very low chargeability that may be regarded as transfer faults. Geophysics GPR (2008, unpubl.) interpreted these breaks and low chargeability as a result of silicification alteration and faulting.

5.7. REVERSE CIRCULATION DRILLING

The reverse circulation (RC) drilling is used as first drilling method to test soil geochemical anomalies. The choice of RC is motivated by its lower cost and its relative high speed in terms of drilled meters per time unit. RC drilling is very critical to execute in wet tropical environment like in CACB where wet sample are very common due to the higher level of ground water table. To minimize sample contamination, the use of compressed air and driven percussion hummer drill bits are preferred to rotary tricone bits. In such conditions, RC drill rig with both high capacity compressor booster, a cyclone to prevent fine particles from blowing away, and skilled drillers are needed to collect a very representative dry rock chip sample devoid of contamination.

A total of 76 RC drill holes were drilled within Kaponda Prospect for an average depth of 100 meters per hole (Fig.40). Boart Longyear, a Canadian based drilling company, was

contracted between 2005 and 2006 to execute RC drilling. Since formations in Kaponda are NW-SE oriented with gently to steeply dip, drill holes are in general oriented -60 ^{o} toward 40^{o} or 220^{o}. Vertical holes are drilled in places where dip and dip direction of geological units were unknown, especially in area without outcrops, and also due to the fact any significant mapping was done before drilling.

Of the fifteen geochemical targets identified in this dissertation, six of them (1, 4, 5, 6, 12 and 13) were already recognized during exploration period and tested with RC, prior to any further diamond drilling (Fig.40 &41). The first RC drill holes were placed directly on geochemical anomalies where causative bodies were believed to be lying. Drilling results show that some of the soil anomalies are in situ or closer to their causative body (e.g. anomalies 5 and 12). Other located along river or swamp zone (anomalies 6 and 13) are probably transported (Fig, 28 & 29, a.).

A successful RC drilling test of soil geochemical anomaly is illustrated in the new interpreted geological section of Fig.42. Drill holes intersects near surface copper mineralization which is well expressed in surface soil geochemistry data. It is worth to mention the dispersion of copper in oxidized and weathered rocks; it enhances surficial geochemical anomaly and make the later wider than the underneath reef (Fig.42). Interpretation of drilling data shows an upright tight anticline (Fig.42), consistent with fold geometry identified after structural analysis of mapping data (Fig.18, b & 19, c). The core of fold is occupied by an axial breccia overlain by dolomitic rocks of lower Mwashya. Stratabound copper mineralization of chalcopyrite and malachite in fresh and oxidized facies respectively, is hosted within dolomite and dolomitic shale

When causative body of the soil anomaly is intersected with RC, the need of increasing the geological knowledge arises. Therefore diamond drilling substitutes RC as rock chips samples do not provide neither structure measurements (e.g. bedding, foliation, fault, fold axial plane) nor geotechnical data for a later evaluation stage.

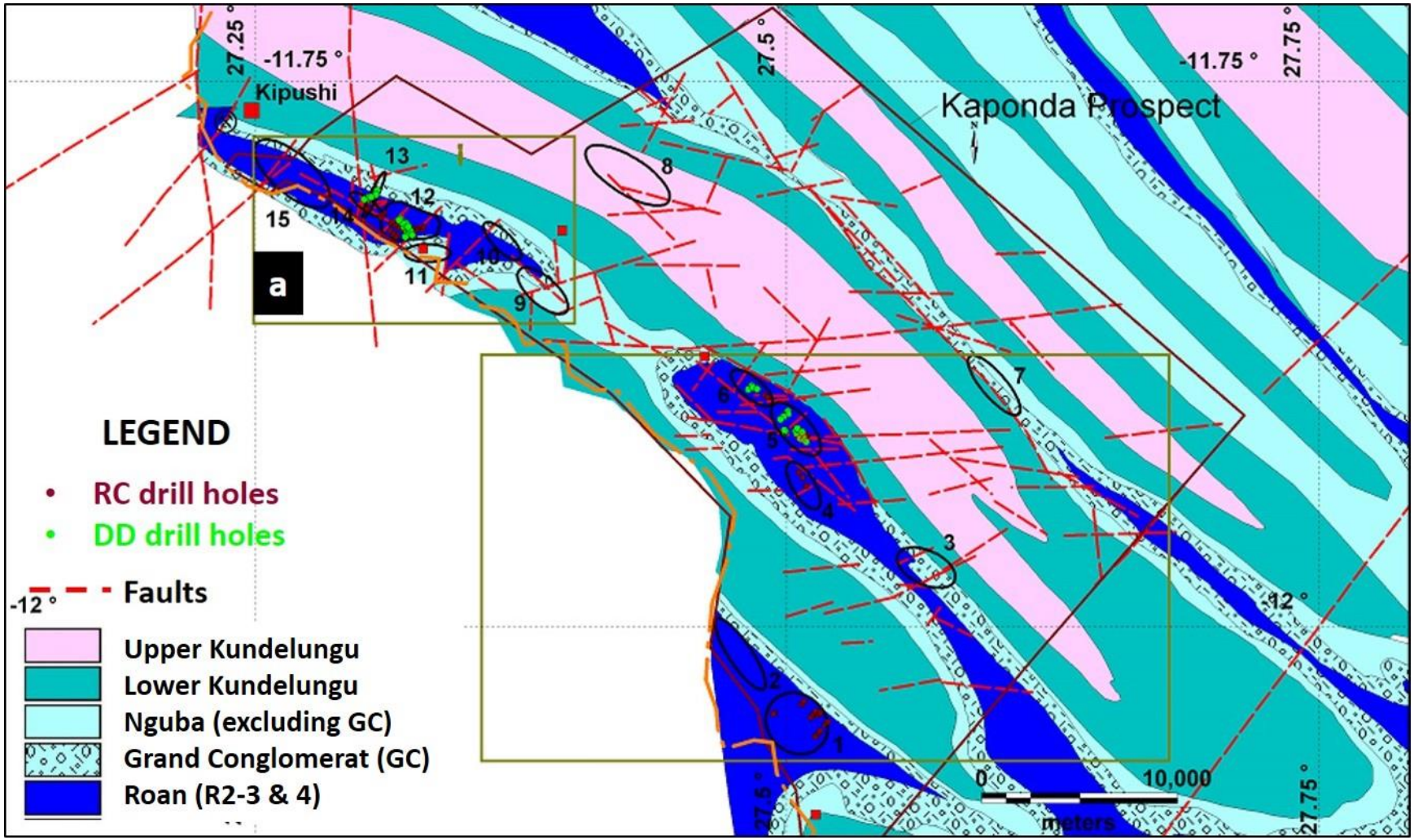

Fig.40. Targets (black elliptic polylines) generated from soil geochemical data; interpreted structures from geophysics (red dash lines) and geology of Kaponda Prospect modified from Jigsaw (2009, unpubl.).

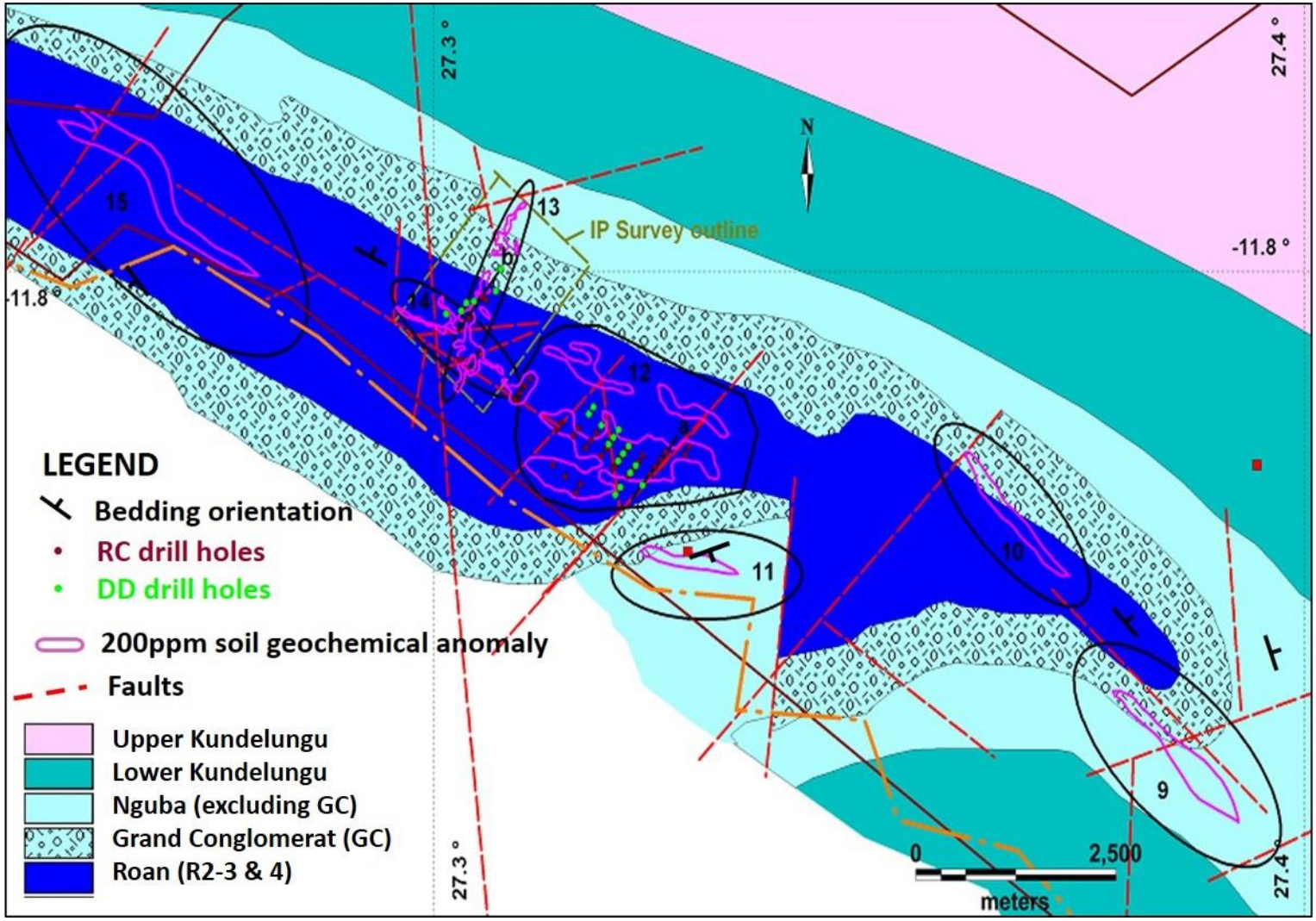

Fig.41. Geological mapping showing Targets generated (black polylines) from soil geochemical anomalies, IP survey, with structure deriving from ground magnetic survey and geological mapping modified from Jigsaw (2009, unpubl.). Note lines “a” & “b” correspond to locations of geological sections of Fig.42 & 43, respectively.

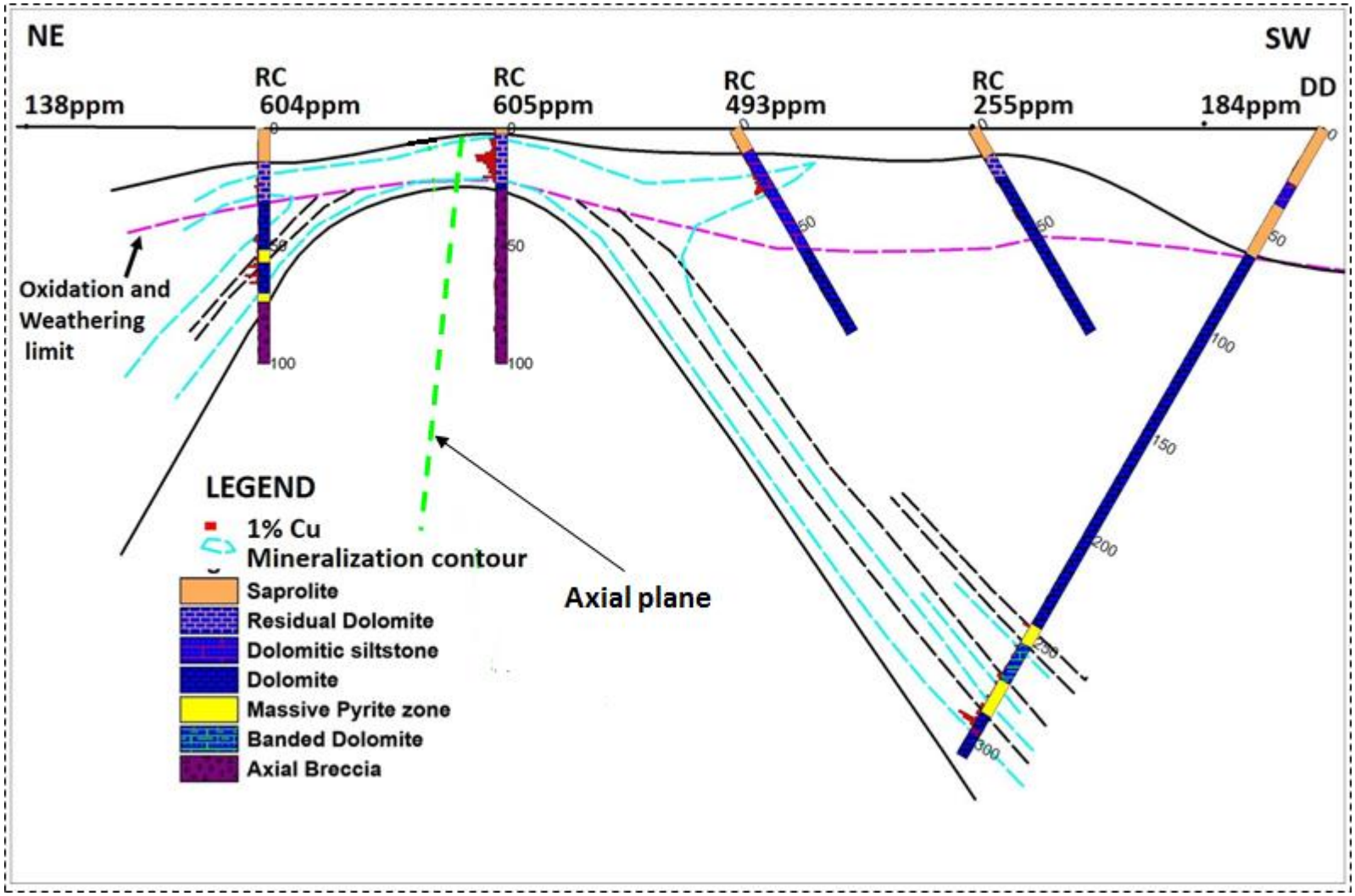

Fig.42. Interpreted geological section with 4 RC drillholes and one diamond hole (DD) showing anticlinal structure and the relation between the surface geochemical anomalies (in ppm) with copper mineralization. Section location is shown as line “a” in Fig.41.

5.8. DIAMOND DRILLING

A total of 50 diamond holes were drilled at an average depth of 250 m, during the period between 2005 and 2008. The majority of holes were drilled by Kluane International and Ox Drilling, a Canadian and Zambian based drilling companies respectively. Boart Longyear also drilled a 600 m deep hole. Among the fifteen geochemical anomalies identified in this dissertation, four of them (5, 6, 12 and 13) were already diamond drilled (Fig.40 & 41) after being tested with RC. Although geological mapping was carried after diamond drilling campaign, initial exploration techniques applied in these specific areas, including airborne radiometric, ground and airborne magnetics, soil geochemistry and IP survey, increase the geological knowledge of each target.

Within anomalies 5 and 12, diamond drilling was used to (1) well constrain mineralization initially intersected in RC, and (2) increase the geological knowledge and understanding of the geometry of areas (Fig.42). Even though RC drilling did not intersect significant Cu mineralization in 6 and 13 geochemical anomaly areas, diamond drilling was used to better understand the geology and structure, and subsequently chase up causative bodies of these geochemical anomalies. Despite being along river and swamp, geochemical anomalies 6 and 13 are the highest within the Kaponda Prospect. Cu value of 1,419 ppm and 628 ppm Co occur in soil Anomaly 6; whereas highest Cu values of the study area occurs in Anomaly 13 with a maximum value of 8,612 ppm (Fig.28 & 30).

The soil anomaly 13 is NE oriented, following a river's valley and crosscutting lithological units (Fig.38 & 41). During exploration time, the anomaly was believed to be parallel to a possible NE trending structure such as Kipushi fault which is associated to Zn-Cu-Pb deposit of the same name (Fig.6), a more or less MVT deposit type (Kampunzu et al., 2009). Therefore initial RC holes were drilled with an azimuth toward the SW and NW, both perpendicular to geological units and geochemical anomaly respectively, did not intersect significant mineralization. Moreover diamond drill holes were also planned and drilled both perpendicular to soil anomaly and lithological units. No significant mineralization was either intersected.

The combination of different genetic models for the sought mineralization within Kaponda, led to a complex drilling pattern where a cluster of drill holes in area 13 (Fig.41 & 38) are neither aligned into straight line section nor parallel to each other. They are oriented in several directions. This kind of drilling pattern (Fig.38) does not allow an easy geological interpretation of section. For stratiform and stratabound copper mineralization a rectangular drilling pattern provide a good statistical coverage when estimating fairly the mineral resource.

An example of an interpreted section is illustrated in Fig.43. The section is generated by MapInfo Discover software, by integrating four SW oriented holes which are not located in a common straight line. For instance the first hole to the SW side of the section is located 250m away from the section line where is projected (Fig.38).

The geological section shows steep dipping NE limb of Kipushi anticline. On top of the sequence, it is represented by the tillite ("Grand Conglomerat") underlain by carbonaceous shale, shale, dolomitic shale and dolomite of the Mwashya respectively (Fig.43). Drilling data confirm that some of the IP chargeability anomalies (IP3, IP4, IP5 and IP6) identified later within this area, are associated barren to pyritic graphitic shale and carbonaceous diamictite (Fig.38 & 8).

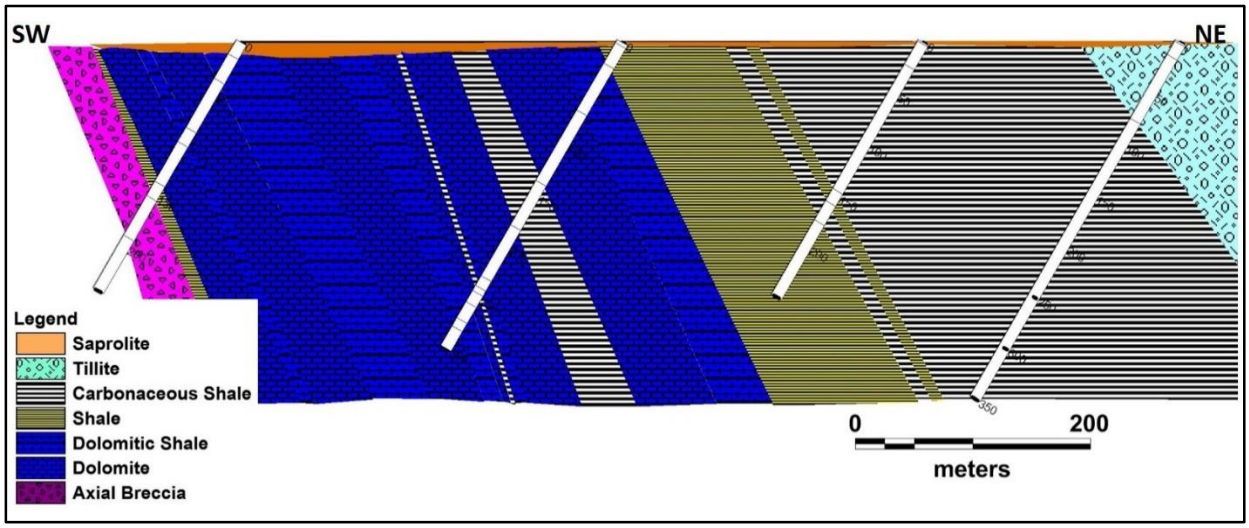

Fig.43. Interpreted geological section of diamond drillholes intersecting barren lithological units. Note that the section line is located on Fig.38 & 41 where a very highest geochemical anomaly occurred.

5.9. TARGET GENERATION

Traditionally generating targets is an exploration step taken before any drilling. The reason why in this dissertation the target generation is presented after drilling sections, is simply because this section reevaluates and integrates all the existing exploration data including soil geochemistry, geophysics and remote sensing, geological mapping, diamond and RC drillings for two mains purposes: (1) to generate and evaluate the prospectivity of news targets and (2) to reassess existing targets and sites which was already drilled in the past.

Among the exploration methods used in Kaponda Prospect, only IP and soil geochemical surveys target directly copper mineralization, even though IP covered only less than 1% of the whole Prospect. Since soil geochemical survey covered the whole Prospect and based on the role that it has played in the discovery history of Cu deposits within the CACB (Broughton and Rogers, 2010; Hitzman et al., 2012; Fleischer, 1984), soil data will be used as a first choice criteria for the target generation. Therefore the fifteen geochemical anomalies identified after reprocessing geochemical data (Fig.28 & 40) will form our fifteen targets. It is worth to mention that only five targets out of fifteen were identified and tested with drilling during FQM exploration period between 2004 and 2010, before the company withdrew from DRC the same year.

The Targeting matrix model presented in this dissertation (Table 6) is a modified version from FQM Exploration (2012). The model was developed by the company with a huge contribution of some external consultant geologists. However this targeting model was never used when exploring permits which includes the Kaponda Prospect. The matrix used in this dissertation aims at identifying, evaluating and prioritizing and monitoring of different targets. Based on these variables further exploration works will be advised, or historical targets might be right-off.

The target generation depends on geological model and style of sought mineralization. Copper mineralization in the Central African Copperbelt is generally stratabound or stratiform, hosted in sediments. Several authors favored the multistage origin for Cu mineralization in this province of the world (selley et al., 2005, El Desouky et al., 2008 & 2010; Hitzman et al., 2012), with contribution from early diagenetic, diagenetic to post orogenic. Three main conditions have to be fulfilled to account for genesis of copper deposits within this world class metallogenic

Table 6. Targeting matrix (modified from FQM Exploration, 2012, unpubl.) showing ranking and prioritization of fifteen generated Targets (Targets are located on map of Fig.40 & 41). Note the three group of targeting criteria with fifteen attributes, with exploration techniques. H=high, M=medium and L=Low priority, unk=unknown, numbers underscore are inferred not fact.

	CRITERIA		Targets														
			1	2	3	4	5	6	7	8	9	10	11	12	13	14	15
	Source of Metal (Copper and sulfur)	EXPLORATION TECHNIQUES															
1	Evaporite and existing pyrite (source for sulfur)	Geological mapping	(1)	unk	0	unk	1	(1)	0	0	unk	0	0	1	1	1	unk
2	Basement rocks	Geological mapping, Magnetic, Radiometry	0	0	0	0	0	0	0	0	0	0	0	0	0	0	0
3	Red bed	Mapping,	(1)	unk	unk	unk	1	(1)	unk	unk	0	0	0	0	0	0	0
4	rift setting basin -oxidized acidic brine from deep so	Mapping, magnetic	1	1	1	1	1	1	1	1	1	1	1	1	1	1	1
	Fluid Migration (Pathway)	EXPLORATION TECHNIQUES															
5	Transfer faults	geological mapping, geophysics and remote sensing	unk	unk	1	1	1	1	0	0	1	1	1	1	1	1	1
6	Wide spread alteration (hematite, talc, albite, potassium, silicification)	radiometric, geological mapping, multielement soil geochemistry	1	unk	unk	unk	1	1	unk	1	0	unk	unk	1	0	unk	unk
	Trap	EXPLORATION TECHNIQUES															
7	Chemical signature of trap (Cu anomaly)	Soil geochemical survey	1	1	1	1	1	1	1	1	1	1	1	1	1	1	1
8	Geophysical signature of trap (high charbility and low resistivity body)	IP	unk	unk	unk	unk	unk	unk	unk	unk	unk	unk	unk	1	1	1	unk
9	Favorable reduced lithostratigraphy host rock (carbonaceous shale, carbonate)	geological mapping, EM and IP	1	1	1	1	1	1	1	unk	1	1	1	1	1	1	(1)
10	Preferred host - porous siliciclastic sealed by carbonate or very fine grained pellitic rock	geological mapping , geochemical multi	0	0	1	0	0	0	1	(1)	1	0	1	0	0	0	0
11	Transfer and synsedimentary basin intergrowth faults intersection (e.g. graben)	geological mapping , geophysics and remote sensing	unk	unk	0	1	1	0	0	0	1	0	0	1	0	1	1
12	Redox front (contact between reduced and oxidized formations)	Geological mapping, multielement soil geochemistry	unk	unk	unk	unk	1	unk	unk	unk	0	unk	unk	1	1	1	unk
13	Fold closure	mapping, geophysics, remote sensing	1	0	0	0	1	0	0	0	1	1	0	1	0	0	0
14	Lithostratigraphy pinch-out	mapping, geophysics	0	0	1	0	1	0	0	0	0	0	1	1	0	0	0
15	Displacement	mapping, geophysics	unk	unk	1	unk	1	0	0	0	0	1	1	0	0	0	0
		Total score	7	3	7	5	12	7	4	4	6	6	7	11	7	8	4
		Rank %	70.0%	42.0%	63.6%	55.5%	85.7%	53.8%	36.3%	36.4%	46.2%	50.0%	58.3%	73.3%	46.6%	57.1%	40.0%
		Priority	M	L	M	M	H	M	L	L	L	M	M	H	L	M	L

province. They are (1) the source of metals and sulfur, (2) the fluid conduit and (3) mineralization trap (Roberts et al., 2013).

Targeting criteria presented in this dissertation takes in account the three quoted factors for genesis of Cu mineralization. Table 6 represents the targeting matrix used to reassess the prospectivity within Kaponda. It also ontains criteria and exploration techniques used for each site. Although there are impressive amount of Cu deposits with reserves totaling more than 200 Mt contained Cu (Hitzman et al, 2012), the source of metal within the Katangan basin is still not clear to account for such amount of metal. In the Congolese Copperbelt, RAT rocks underlying the Mines Subgroup are considered as red beds and potential source for copper. Copper deriving from basement rocks has been also considered among different potential sources of Cu in the Katangan basin. However no basement rocks has been identified within the study area, the nearest outcrops of Granitic basement occur at about 25 km SE of Kaponda Prospect within the Luina dome (Fig.6). Evaporite occurring in Mines Subgroup and pyritic horizons for instance, are considered as source of sulfur.

The main possible fluid pathways are normal transfer faults and wide spread alteration halos (Table 6). Normal faults interpreted from geophysical data and identified from geological map are potential conduit of mineralizing fluids in Kaponda. These faults crosscut the lithostratigraphy, they are E-W and SW-NE oriented (Fig.40). The wide spread alteration was not particularly observed though pervasive hematitic alteration is laterally distributed within the RAT breccia of the thrusted and folded belt in general. Within Kaponda, RAT rocks occur in the SE of Baya. Airborne potassic radiometry reveals some relative higher anomalies corresponding to Kundelungu Group within synclines (Fig.34, a). These potassic patterns are likely to be associated to siltstone mapped east of Baya instead of K-feldspar alteration halos.

Finally the last group of criteria to account for the genesis of Cu deposit is the trap of mineralization. Traditionally Cu mineralization within the CACB was believed to be stratigraphic controlled, restricted to silisiclastic units such as the ore shale in the lower Roan in the Zambian Copperbelt and carbonate of Mines Series in the DRC. These lithostratigraphic units are associated to organic matter, making them favorable reduced environment at trapping oxidized fluid containing copper. However with discovery of Cu deposits throughout the entire

Katangan stratigraphy (Fig.4), the prospectivity of the all Katanga sequence has increased. The similarity between the different host rocks is the fact that they are reduced horizons.

The very obvious reduced horizon of Kaponda are the black shale of Mwashya, the Grand Conglomerat, Mines Subgroup carbonates and dolomitic shale of the Nguba. Other potential host rock are considered such as porous siliciclastic rocks (e.g. arkosic sandstone) sealed by carbonates or very fine pelitic rocks.

Furthermore, rheological trap for mineralization are represented by fold closure, orthogonal faults intersection and lithology pinch-out (Target 3, Fig.40), sediment embayment or graben setting, and strain gradient. The fold nose are prominent within domal structures of Kipushi anticline in Domain I area and Baya (Fig.18, a & b). The intersection between NE-SW or E-W transfer faults with NW-SE intergrowth faults are potential zone at trapping and redistributing mineralization. Strain gradient such as alternation between ductile and brittle domains may be critical for metallogenesis.

To summarize, Table 6 provides ranking description of Targets generated within Kaponda Prospect. It has three group of criteria containing a total of fifteen attribute for fifteen Targets. The integration of data and interpretation of remote sensing, geological mapping, geochemical and geophysical surveys, and drilling measure the prospectivity of Targets by totaling their attribute score. A ranking percentage is calculated based on only known data. For instance Target 1 has a total score of 7 out of 10 with a rank percentage of 70% (Table 6). The percentage is instead calculated on a ratio of 7/10 and not 7/15, simply because five other attributes are unknown. However the prioritization of Targets is relative but fair, it is a function of both total score from criteria attributes and rank percentage. Depending on conditions fixed in this dissertation and stated below, the priority can be qualified as law, medium or high.

As far as this dissertation is concerned, a high priority target has a total score ≥ 9 and a rank % ≥ 60. A medium priority target scores in total values ≥ 5 and < 9 with a rank percentage ≥ 50. Finally all targets scoring below 5 and of less than 50% in rank are of low priority.

As a result, Targets 5 and 12 scoring 12/14 and 11/15 respectively, are high priority Targets (Table 6). They correspond to the most advanced stage of exploration (brownfield) where mineralization has been already identified through previous drilling (Fig.40, 41 & 42). The result of the target matrix and drilling results suggest that exploration strategies applied to

these two targets were efficient. However in order to get economic Cu resources, additional drilling is needed to define mineralization extension.

Targets 1, 3, 4, 6, 10, 11, and 14 are all of them medium priority (table 6). This group includes Targets which have been already tested with couple of drill holes (e.g. Target 1, 4 & 6; Fig.40) even though mineralization is not well constrained. Other interesting untested sites of the same priority order, are Targets 3, 10, 11 & 14 (Fig.40 & 41). Some of them such as Targets 3, 11 & 10 require detailed soil sampling to prove the continuity of geochemical anomaly. While a direct drill to test both IP chargeability anomalies and soil geochemical anomalies is required for Target 14 (Fig.38 & 41).

The low priority Targets are namely 2, 7, 8, 9, 13 and 15 (Table 6). This category comprised Targets (e.g. 2, 7, 8, and 9) which need follow-up of both detailed soil sampling and geological mapping, to increase the geological knowledge before considering any further work. Considering the fact that Target 15 is in the vicinity of Kipushi Zn-Cu-Pb mine (Fig.40), a physical field visit is required to check if soil anomaly within this area is not associated to floating materials deriving from ore mining.

On the other hand, it is worth to mention that Target 13 has a particularity of having known values for all fifteen attribute criteria. However it is ranked as low priority with a score of 7/15. This means more exploration works have been done on this target without encouraging results. Exploration activities include ground magnetic, IP survey, soil survey and geological mapping, reverse circulation and diamond drilling (Fig.41). Although Target 13 has the highest Cu anomaly of the study area (Fig.28 & 29, a), drilling did not intersect any significant Cu mineralization (Fig.43). The NNE trending geochemical anomaly is now believed to be transported from upslope. It might derive from moderate NW trending soil anomaly located in Target 14 (Fig.38 & 41). The strong IP chargeability and low resistivity anomaly which crosscut Target 13, map lithological units corresponding to pyritic carbonaceous shale and Grand Conglomerat (Fig.38 & 39) devoid of significant Cu mineralization. As demonstrated, Target 13 is based on transported soil anomaly occurring along river, it was drilled and thought to be associated to NE structure such as Kipushi fault. The result of the present target ranking classified Target 13 as law and dead. Therefore this target should be write off and neglected.

To sum up, targets of low to medium priority can move to an upper rank when additional exploration works encountered positive results in terms of mineralization. Conversely a target can be ranked downward when follow-up works do not intersect encouraging results. The entries of targeting matrix will be variable depending on the ongoing exploration results. Hence this targeting model for sediment-hosted copper mineralization is a dynamic tool that utilizes Cartesian approach to evaluate geological information in order to monitor the prospectivity of properties. It helps (1) to reevaluate the prospectivity of projects, (2) to plan the next exploration activities, and (2) to decide when a property has to be written off

Chapter 6 DISCUSSION

The exploration for sediment-hosted Cu mineralization within the CACB can be successful conducted by integrating information from different sources such as remote sensing, geology, geological mapping, soil geochemistry, geophysics and drilling. The targeting criteria for stratiform and stratabound Cu mineralization take in account all available information derived from these different exploration techniques.

In the Central African Copperbelt the application of Remote Sensing in mineral exploration is rather focalized on structure analysis (lineaments, lithostratigraphy boundaries and faults interpretation) than lithology and alteration identification. This may be explained by the presence of thick vegetation cover and the limited outcrops in the region. Remote sensing has been successful used in the region to locate Mines Series hosting the bulk of the Congolese Cu mineralization style as they occur on high topography devoid of vegetation. Although transfer faults within Kaponda Prospect are not well constrained on Landsat and google earth images due to their coarse spectral resolution, the two satellite images show clearly lineaments corresponding to lithostratigraphy boundaries and domal folds. The domal anticlines with a core of Roan formations are classic structure associated to Cu mineralization within the Congolese Copperbelt (e.g. Lupoto and Kasonta Cu-Co deposit; Fig.6 & 16).

Interestingly fact geological map and structure measurement from mapping indicate a local lithostratigraphy of Roan Group represented by breccia, dolostones, iron formation, limonitic shale and carbonaceous shale. Roan formations occupy domal anticlines in both

Nakarimba and Baya (Fig.6). Reduced horizons within Roan Group, together with the Grand Conglomerat identifying on mapping are potential host rocks that can trap Cu mineralization.

Spatial analysis of structure measurements is a targeting tool at defining the geometry of brittle and ductile domains within prospective zone such as Nakarimba (Fig.18, a & b) where the anticline axial plane is calculated to be dipping 81^{o} toward 029^{o}, and its hinge plunging 10^{o} toward 117^{o} (Fig.19). As Cu mineralization of this area was already identified through drilling of Target 12 (Fig.41 & 42), if mineralization is proved to be structurally controlled or associated to the folding, the implication for exploration will be looking for deep mineralization extension toward the ESE fold plunging direction.

Some of the mapped lithostratigraphic units have distinct magnetic or radiometric signatures which can be used as aid to geological mapping in places without outcrops. A dark blue-red pattern of ternary radiometric image is characteristic of "Grand Conglomerat" tillite, implying that the latter is relatively rich in K, slightly in U and poor in Th (Fig.35, b). The Grand Conglomerat is also associated to both high positive and negative RTP magnetic signals (Fig.31 & 32). The high negative magnetism is believed to be associated to remnant pyrrhotite. Another high amplitude K radiometry anomaly is positively correlated to pink siltstone of the Upper Kundelungu with potential pervasive argillic or potassic alteration. Target 8 is associated to high potassic radiometry anomaly (Table 6). The wide spread pervasive alteration are indication of hydrothermal fluid passage probably distal or proximal to mineralization.

There is a positive correlation of structure interpreted from magnetic and radiometric maps. Three major fault direction have been identified: E-W, NE-SW and NW-SE trends (Fig.40). These directions are also consistent with initial fault trends observed on regional geological map (Fig.6). The E and NE trends are the most frequent, they are interpreted as normal transfer faults capable of serving as mineralizing fluid pathway. For instance the NE trend Kipushi fault is associated to Zn-Cu-Pb deposit of the same name (Fig.6). Kipata et al. (2013) describe the NE trending normal faults as resulting from the late orogenic extension of the Lufilian belt which have locally remobilized mineralization (e.g. Shituru Cu-Co deposit in Likasi district).

Finally the NW-SW directed fault are parallel to fold axis. They are believed to be either associated to the brittle phase of thrusting and folding event of the Lufilian orogeny, or they

correspond to synsedimentary intergrowth faults. The thickening of “Grand Conglomerat” within the NE and SW limbs of Lupoto and Kipushi anticlines respectively (Fig.6), is interpreted as a result of the presence of NW directed intergrowth faults. The interaction of sedimentary intergrowth faults and orthogonal transfer faults can form structure such as graben capable of trapping Cu mineralization.

Of all exploration techniques used in the study area, only IP and soil geochemical surveys target directly Cu mineralization. High chargeability associated to low resistivity IP anomalies identified in Nakarimba (Fig.38), are generally interesting targets which could be associated to disseminated sulphide bodies. However in Nakarimba surrounding, a strong chargeability coupled with low resistivity responses map non-mineralized or pyritic reduced rocks namely graphitic shale of Mwashya and the “Grand Conglomerat” (Fig.38, 39 & 43).

Although IP pole-dipole pseudo-section can provide an apparent dip of the conductive body (Fig.39), it is worth to mention that this dip can be sometime misleading in many cases. It is generally reflect the geometry of measurement at depth rather than the geometry of the causative body. The classic example is the so-called “pant’s leg” anomaly apparently caused by body dipping both ways from the surface. This is due to a small near surface source which is close to one specific dipole position (Milsom, 2009). Nowadays the use of several inversion modelling techniques are much better than pseudo-section in term of both shape and geometry of the causative body.

Despite generating direct Cu Target, IP survey is relatively expensive, slow to execute and require a large field crew and consequently restricted to small area. However soil geochemical survey is cost-effective and covers the whole surface of Kaponda Prospect, reason why this exploration technique is our first choice criteria to select area of interest for follow-up. Based on the exploration case study of the Kaponda Prospect, the reassessment of its data and the past experience in this district, soil geochemical survey remains one of the most critical method for the search of Cu mineralization in the CACB. This is consistent with the deposit discovery history in the region where soil geochemical surveys played a key role (Fleischer, 1984; Broughton and Rogers, 2010; Hitzman et al., 2012).

Traditionally statistical methods has been widely applied to interpret and define anomaly threshold. These methods have to be used cautiously due to the fact that geochemical data have

variable characteristics depending on uncommon processes such as weathering, element dispersion and ore forming process, which concentrate particular element. A range of statistical techniques are used to explore the nature of geochemical data. The frequency histogram and cumulative-frequency plots show that Kaponda soil geochemical data distribution for Cu and Co are positive skewed with a long tail toward higher values and approximate a lognormal distribution. Generally this kind of distribution represents more than one population in the data set. Other different techniques have been tested to threshold the anomaly of these populations.

Despite being widely used by Explorationists, the mean + 2 standard deviation (sdev) method at defining threshold, is only best applied to a normal distribution where the upper 2.5% extreme values are anomalous. In exploration geochemistry Reiman et al. (2005) demonstrated that values within the range of "mean+2sdev" fall often within "geochemical background". This is a case for Kaponda data where the "mean+2sdev" threshold for Cu (173.04ppm) fall within background values representing the upper 3.9% of the data. The 2sdev threshold of 136.5ppm for Cu corresponding to 94.4 percentile, is naturally within background as well. However probability plots, histogram and experimental thresholds are very well constrained respectively at 200 ppm, 220 ppm and 206.69 ppm for Cu. Surprisingly the mean+2sdev and histogram threshold for Co are very well constrained, and subsequently are best fit for Co anomaly definition. To summarize, the probability graph and frequency histogram combined with spatial representation and the practical experience of the region are the best practice to define geochemical threshold anomaly at Kaponda Prospect.

The interpretation of landscape geochemistry of the study area helps to discriminate false and true geochemical anomalies, transported and in situ soil anomalies. The integration of remote sensing and geological mapping data, geophysical and previous drilling to soil geochemistry results led to generation of 15 Targets of different ranks in term of mineral prospectivity. The high priority targets (5 and 12; Table 6 and Fig.40) are already the most advanced exploration stage (brown field) with more RC and diamonds drilled holes. Although Cu mineralization has been already identified in the two sites, the control of mineralization has to be determined in order to target mineralization which can lead to economic resource.

The medium and law priority targets do not necessarily mean of less importance. This might be due to less information available on these sites; in other word additional explorations

works such as infill sampling, geological mapping, and interpretation of high definition remote sensing have to be carried out prior to any drilling. Although Targets 6 and 13 have the highest Cu and Co anomalies, initial drilling of these two sites did not intersect significant Cu-Co mineralization. Therefore mechanical and hydromorphic dispersion of metals must be considered as these high anomalies occur around rivers and swamps. The source of the anomalies should lies up slope. Also drilling results prove that Target 13 is dead and has to be neglected (Fig.41 & 43). The IP chargeability response within Target 13 correspond to barren graphitic shale and carbonaceous diamictite (Fig.38). The source of its strong soil geochemical anomalies lies up slope, probably deriving from Target 14 which has moderate soil anomaly (Fig.41).

The reinterpretation of existing data (e.g. soil geochemistry, geophysics and drilling) and integration of recent available information such as IP and geological mapping conducted after drilling, should guide the next drilling effort aiming to delineate Cu mineralization and locate causative bodies of soil anomalies.

Chapter 7 CONCLUSION

The Kaponda Prospect is highly prospective for sediment-hosted copper mineralization. Exploration activities encountered in this area shows encouraging geological, geochemical, geophysical and drilling results. The reinterpretation and integration of all data sets has enhanced the prospectivity of the Prospect. Identified area of interest comprises untested green field targets to brown field projects where follow-up drilling might add significant economic value to the property if extension of Cu mineralization is defined. In order to achieve the ultimate goal of successfully complete and potentially determine economic resources, the following further works are recommended:

(1) A review of high definition remote sensing image such as Quickbird, Aster, Ikonos or Spot, aiming to determine major structures which can be associated to mineralization. Target 1 and 2 which are not covered by any airborne geophysics, are a big concern in term of structure definition. Defining faults associated to mineralization will guide further drilling in these particular zones.

(2) Additional geological mapping is required to cover specific places where previous mapping did not reach (e.g. Targets 3 and 7). The campaign will both identified rocks

strain, the geometry and deformation regime (brittle or ductile), and locates transfer faults and their intersection with potential host rocks.

(3) For high priority Targets 5 and 12 which are already at brown field stage, a re-logging of existing drillholes will help at identifying the control of mineralization by identifying alteration and major structure associated to mineralization. This will guide further drilling to define extensions of mineralization and develop economic mineral resource.

(4) The second order priority targets are divided in two groups:

- Targets 1, 4 & 6 which have been already drilled even though mineralization is not yet well constrained. A reevaluation and reinterpretation of all existing data including drillhole re-logging, should be carried out before any further drilling. Particularly drilling was unsuccessful in Target 6 despite its strong soil anomaly. The source of the anomaly has to be found; it should lie up slope as the anomaly occur in swamp area. If necessary, multielement analysis of soil samples from this region will help to constrain the true geochemical anomaly and identify transported soil anomalies.
- For the second group of medium priority targets: soil anomaly and IP chargeability response of Target 14 need to be directly tested with drilling, while Targets 3, 10 & 11 require detailed soil sampling (e.g. 200X100m grid spacing) to prove the continuity of anomaly. If the continuity is proven, test drilling should be warranted.

(5) Low priority Targets 2, 7, 8 and 9 necessitate detailed soil sampling to define the continuity of anomalies. In addition a geological mapping should be carried out in the surrounding of Target 7 where fact map does not exist. Field inspection of Target 15 is mandatory in order to check if its soil anomaly is not associated to floats material deriving from the mining of Kipushi Zn-Cu-Pb ore deposit occurring in less than 4 km.

(6) Finally Target 13 ranked as low priority has to be neglected, it appears to be barren through drilling as demonstrated above in the target generation and discussion sections. Its soil anomaly is transported and the IP response corresponds to barren to carbonaceous and pyritic units.

To sum up, any follow-up works within Kaponda Prospect will aim at increasing the geological knowledge of the area of interest. Thereafter the nature of results will always dictates weather or not additional exploration works are required.

REFERENCES

Annels, A. (1974). Some aspects of the stratiform ore deposits of the Zambian Copperbelt and their genetic significance. ." *Annales de la Société Géologique de Belgique*; Gisements Stratiformes Et Provinces Cuprifères*. Centenaire Société Géologique Belgique, Liège*, 235-254.

Annels, A. (1979). The genetic relevance of recent studies at Mufulira mine. *Zambia: Annales De La Société Géologique De Belgique, 102*, 431-449.

Annels, A. (1989). Ore genesis in the Zambian Copperbelt, with particular reference to the northern sector of the Chambeshi basin. *Geological Association of Canada, Special Paper, 36*, 427-452.

Armstrong, R., Master, S., & Robb, L. (2005). Geochronology of the Nchanga granite, and constraints on the maximum age of the Katanga Supergroup, Zambian Copperbelt. *Journal of African Earth Sciences, 42*(1), 32-40.

Bartholomé, P. (1974). Gisements stratiformes et provinces cuprifères*. Société géologique de Belgique*, Liège.

Bartholomé, P., Evrard, P., Katekesha, F., Ngongo, M., & Lopez-Ruiz, J. (1973). Diagenetic ore-forming processes at Kamoto, Katanga, Republic of the Congo. *Ores in sediments* (pp. 21-41) Springer.

Batumike, M., Cailteux, J., & Kampunzu, A. (2007). Lithostratigraphy, basin development, base metal deposits, and regional correlations of the Neoproterozoic Nguba and Kundelungu rock successions, Central African Copperbelt. *Gondwana Research, 11*(3), 432-447.

Batumike, M., Kampunzu, A., & Cailteux, J. (2006). Petrology and geochemistry of the Neoproterozoic Nguba and Kundelungu Groups, Katangan Supergroup, southeast Congo: Implications for provenance, paleoweathering and geotectonic setting. *Journal of African Earth Sciences, 44*(1), 97-115.

Belliere, J., (1969). Polymétamorphisme et superposition de tectoniques dans le massif calcareux de Kikosa (Katanga, Congo). *Annales de la Société Géologique de Belgique* 92, pp. 78-88.

Belperio, A., Flint, R., & Freeman, H. (2007). Prominent hill: A hematite-dominated, iron oxide copper-gold system. *Economic Geology, 102*(8), 1499-1510.

Bernau, R. (2007). The Geology and Geochemistry of the Lumwana Basement Hosted Copper-Cobalt (Uranium) Deposits, NW Zambia; *Unpubl. Ph.D. thesis, University of Southampton, School of Ocean and Earth Sciences, 187p.*

Binda, P. L. (1975). Detrital bornite grains in the late Precambrian B greywacke of Mufulira, Zambia. *Mineralium Deposita, 10*(2), 101-107.

Binda, P. L. (1994). Stratigraphy of Zambian Copperbelt orebodies. *Journal of African Earth Sciences, 19*(4), 251-264.

Binda, P., & Van Eden, J. (1972). Sedimentological evidence on the origin of the Precambrian great conglomerate (Kundelungu tillite), Zambia. *Palaeogeography, Palaeoclimatology, Palaeoecology, 12*(3), 151-168.

Broughton, D., Hitzman, M., & Stephens, A. (2002). Exploration history and geology of the Kansanshi cu (-au) deposit, Zambia. *Special Publication-Society of Economic Geologists, 9*, 141-154.

Broughton, D., & Rogers, T. (2010). Discovery of the Kamoa copper deposit, Central African Copperbelt, DRC. *Society of Economic Geologists, Special Publication, 15*, 287-297.

Buffard, R., & Muhagaze, L. (1981). Sur les modalités de dépôts des filons hématifères du Mwashya supérieur (précambrien supérieur) de la région de Lubumbashi, Shaba, Zaïre. *Annales De La Société Géologique De Belgique, 104*, 193-203.

Bulmer, M. G. (1979). Principles of statistics. *Courier Dover Publications*.

Buttgenbach, H. (1906). La cassitérite du Katanga. liége, soc. géol. *Bull,*

Cahen, L. (Ed.). (1954). *Géologie du Congo belge* (Vaillant Carmene Ed.). Liège:

Cahen, L. (1978). *Les mixitites anté-cambriennes de l'est du Zaïre: Mise au point intérimaires.* (Annuel No. p33-64). Tervuren, Belgique: Musé royal de l'Afrique centrale.

Cailteux, J., (1992, unplub.). Gisement de Kipushi: Pré-estimation partielle E 301/1/M de la tranche 1300 et 1500. *Gécamines Geological Department (Likasi, DRC), unpublished report (R.A. 964).*

Cailteux, J. (1994). Lithostratigraphy of the Neoproterozoic Shaba-type (Zaire) Roan Supergroup and metallogenesis of associated stratiform mineralization. *Journal of African Earth Sciences, 19*(4), 279-301.

Cailteux, J. (2003). Proterozoic sediment-hosted base metal deposits of western Gondwana (IGCP 450) 3rd conference and field workshop. *Lubumbashi, DR Congo, Abstract, 2003*, 223.

Cailteux, J., Binda, P., Katekesha, W., Kampunzu, A., Intiomale, M., Kapenda, D., et al. (1994). Lithostratigraphical correlation of the Neoproterozoic Roan Supergroup from

Shaba (Zaire) and Zambia, in the Central African copper-cobalt metallogenic province. *Journal of African Earth Sciences, 19*(4), 265-278.

Cailteux, J., & Kampunzu, A.B. (1995). The Katangan tectonic breccias in the Shaba province (Zaïre) and their genetic significance. Musée Royal de l'Afrique Centrale, Tervuren (Belgium). Annales des Sciences Géologiques101, 63–76.

Cailteux, J., Kampunzu, A., & Batumike, M. (2005a). Lithostratigraphic position and petrographic characteristics of RAT ("Roches argilo-talqueuses") subgroup, Neoproterozoic Katangan belt (Congo). *Journal of African Earth Sciences, 42*(1), 82-94.

Cailteux, J., Kampunzu, A., Lerouge, C., Kaputo, A., & Milesi, J. (2005b). Genesis of sediment-hosted stratiform copper–cobalt deposits, Central African Copperbelt. *Journal of African Earth Sciences, 42*(1), 134-158.

Cailteux, J., Kampunzu, A., & Lerouge, C. (2007). The Neoproterozoic Mwashya–Kansuki sedimentary rock succession in the Central African Copperbelt, its Cu–Co mineralization, and regional correlations. *Gondwana Research, 11*(3), 414-431.

Closs, L., & Nichol, I. (1989). Design and planning of geochemical programs. *Proceedings of Exploration '87*, 569-583.

Cluzel, D. (1986). Contribution à l'étude du métamorphisme des gisements cupro-cobaltifères stratiformes du Sud-Shaba, Zaïre. Le district minier de Luishia, *Journal of African Earth Sciences* 5, 6, pp. 557-574.

Cosi, M., De Bonis, A., Gosso, G., Hunziker, J., Martinotti, G., Moratto, S., et al. (1992). Late Proterozoic thrust tectonics, high-pressure metamorphism and uranium mineralization in the domes area, lufilian arc, northwestern Zambia. *Precambrian Research, 58*(1), 215-240.

Corner, B. (2012, unpubl.). Applied geophysics for geologists. *MSc. Course in Exploration Geology, at Rhodes University*, Grahamstown.

Coward, M., & Daly, M. (1984). Crustal lineaments and shear zones in Africa: Their relationship to plate movements. *Precambrian Research, 24*(1), 27-45.

Daly, M. (1986). Crustal shear zones and thrust belts: Their geometry and continuity in Central Africa. *Royal Society of London Philosophical Transactions Series A*, *317*, 111-127.

Daly, M., Chakraborty, S., Kasolo, P., Musiwa, M., Mumba, P., Naidu, B., et al. (1984). The lufilian arc and irumide belt of Zambia: Results of a geotraverse across their intersection. *Journal of African Earth Sciences (1983), 2*(4), 311-318.

Darnley, A. (1960). Petrology of some rhodesian Copperbelt orebodies and associated rocks. *Trans Inst Min Metall, 69*, 137-173.

De Magnée, I., & François, A. (1988). The origin of the Kipushi (Cu, Zn, Pb) deposit in direct relation with a Proterozoic salt diapir. Copperbelt of Central Africa, Shaba, republic of Zaïre. *Base metal sulfide deposits in sedimentary and volcanic environments* (pp. 74-93) Springer.

DeGeoffroy, J., Wu, S., & Heins, R. (1967). Geochemical coverage by spring sampling method in the southwest wisconsin zinc area. *Economic Geology, 62*(5), 679-697.

Demesmaeker, G., François, A. & Oosterbosch, R (1963). La tectonique des gisements cuprifères stratiformes du Katanga. *In J.Lombard and P.Nicolini (Eds), Gisements Stratiformes de cuivre en Afrique*, 47-115.

Dewaele, S., Muchez, P., Vets, J., Fernandez-Alonzo, M., & Tack, L. (2006). Multiphase origin of the Cu–Co ore deposits in the western part of the lufilian fold-and-thrust belt, Katanga (Democratic Republic of Congo). *Journal of African Earth Sciences, 46*(5), 455-469.

Drysdall, A.R., Johnson, R.L., Moore, T.A., & Thieme, J.G., 1972. Outline of the geology of Zambia*. Geologie en Mijnbouw*, 53, 265-276.

Dumont, P. & Cahen, L. 1977. Les complexes conglomératiques de la bordure sud-orientale de la Chaine Kibarienne et leurs relations avec les couches Katangiennes de l'Arc Lufilienne, *Rapport Annuelle 1977. Musée royal de l'Afrique centrale*, Département de Géologie et Minéralogie, Tervuren, Belgique, 111–135.

El Desouky, H. A., Muchez, P., Boyce, A. J., Schneider, J., Cailteux, J. L., Dewaele, S., et al. (2010). Genesis of sediment-hosted stratiform copper–cobalt mineralization at Luiswishi and Kamoto, Katanga Copperbelt (Democratic Republic of Congo). *Mineralium Deposita, 45*(8), 735-763.

El Desouky, H. A., Muchez, P., Dewaele, S., Boutwood, A., & Tyler, R. (2008). Postorogenic origin of the stratiform Cu mineralization at Lukufwe, lufilian foreland, Democratic Republic of Congo. *Economic Geology, 103*(3), 555-582.

Fleischer, V. (1984). Discovery, geology and genesis of copper—cobalt mineralization at Chambeshi southeast Prospect, Zambia. *Precambrian Research, 25*(1), 119-133.

Fleischer, V., Garlick, W., & Haldane, R. (1976). Geology of the Zambian Copperbelt. *Handbook of Stratabound and Stratiform Ore Deposits, 6*, 223-352.

Fletcher, W. K. (1986a). Exploration geochemistry: Design and interpretation of soil surveys *The Economic Geology Publishing Company*.

Fletcher, W. K. (1986b). Analysis of soil samples. *Reviews in Economic Geology, (USA).*

Ford, K., Keating, P., & Thomas, M. (2006). *Overview of Geophysical Signatures Associated with Canadian Ore Deposits,*

FQM Exploration (2012, unpubl.). Exploration targeting matrix model. *Internal report.*

François, A., 1973, L'extrémité occidentale de l'Arc cuprifère Shabien. Étude Géologique: *Bureaux d'Études Géologiques, Gécamines-Exploitation*, Likasi, Zaïre, p. 65.

François, A. (1974). Stratigraphie, tectonique et minéralisations dans l'arc cuprifère du Shaba (république du zaïre). In: Bartholomé P (ed) gisements stratiformes et provinces cuprifères. *La Société Géologique De Belgique, Liège, Pp 79–101,*

François, A. (1987). Synthèse géologique sur l'arc cuprifère du Shaba (Rép. du zaïre). *Bulletin De La Société Belge De Géologie*, 15-65.

François, A. (1995). Problèmes relatifs au katanguien du Shaba. *Annales-Musée Royal De l'Afrique Centrale. Serie in 8vo Sciences Géologiques,* pp. 1-20.

Fugro (2004). Fixed wing borne Magnetic and radiometric survey over the Project Area situated in the Katanga Province of the Democratic Republic of Congo and Zambia. *FQM Exploration internal report, 177p, unpubl.*

Garlick, W.G., 1961. The syngenetic Theory. *In: Mendelsohn, F. (Ed.).* The Geology of the Northern Rhodesian Copperbelt. Macdonald: London, p.146-165.

Garlick, W., & Fleischer, V. (1972). Sedimentary environment of zambian copper deposition. *Geologie En Mijnbouw, 51*(3), 277-298.

Geophysics GPR (2008). Kipushi East copper cobalt project, Induced polarization, ground geophysical report. *FQM internal report, 6p, unpubl.*

Gunn, P., Minty, B., & Milligan, P. (1997). The airborne gamma-ray spectrometric response over arid australian terranes. *Exploration, 97.* pp. 733-740.

Hanson, R. E., Wardlaw, M. S., Wilson, T. J., & Mwale, G. (1993). U-Pb zircon ages from the hook granite massif and mwembeshi dislocation: Constraints on pan-African deformation, plutonism, and transcurrent shearing in central Zambia. *Precambrian Research, 63*(3), 189-209.

Hanson, R. E., Wilson, T. J., & Munyanyiwa, H. (1994). Geologic evolution of the Neoproterozoic Zambezi orogenic belt in Zambia. *Journal of African Earth Sciences, 18*(2), 135-150.

Hitzman, M. (2010). Alteration associated with sulphide mineralization at the Lupoto and Kasonta copper deposits, southern Congolese Copperbelt, Democratic Republic of Congo. *AMIRA report, 31p.*

Hitzman, M. W., & Large, D. (1986). A review and classification of the irish carbonate-hosted base metal deposits. *Geology and Genesis of Mineral Deposits in Ireland: Dublin, Irish Association for Economic Geology*, 217-238.

Hitzman, M., Kirkham, R., Broughton, D., Thorson, J., & Selley, D. (2005). The sediment-hosted stratiform copper ore system. *Economic Geology*, *100* (Anniversary Volume), 609-642.

Hitzman, M. W., Selley, D., & Bull, S. (2010). Formation of sedimentary rock-hosted stratiform copper deposits through earth history. *Economic Geology, 105*(3), 627-639.

Hitzman, M., Broughton, D., Selley, D., Woodhead, J., Wood, D., & Bull, S. (2012). The Central African Copperbelt: Diverse stratigraphic, structural, and temporal settings the world's largest sedimentary copper district: Society of economic geologists. *Society of Economic Geologists, Special Publication, 16*, 487-514.

Hoffmann, K., Condon, D., Bowring, S., & Crowley, J. (2004). U-Pb zircon date from the Neoproterozoic Ghaub formation, Namibia: Constraints on marinoan glaciation. *Geology, 32*(9), 817-820.

Hunt, G. R., & Ashley, R. P. (1979). Spectra of altered rocks in the visible and near infrared. *Economic Geology*, *74*(7), 1613-1629.

Hunt, G. R., & Salisbury, J. W. (1970). Visible and near-infrared spectra of minerals and rocks: I. silicate materials. *Modern Geology, 1, p. 283-300,*

Hunt, G.R., and Salisbury, J.W. (1971a). Visible and near-infrared spectra of minerals and rocks: II. Carbonates. *Modern Geology, v. 2, p. 23-30,*

Hunt, G.R., and Salisbury, J.W. (1971b). Visible and near-infrared spectra of minerals and rocks: III. Oxides and hydroxides. *Modern Geology, v. 2, p. 195-205,*

Intiomale, M. (1982). Le gisement Zn-Pb-Cu de Kipushi (Shaba, Zaïre). Etude géologique et métallogénique. *Unpublished Ph.D.Thesis, Louvain-La-Neuve, Belgium, Université Catholique De Louvain,*

Intiomale, M. M., & Oosterbosch, R. (1974). Géologie et géochimie du gisement de Kipushi, Zaïre. *Annales de la Société Géologique de Belgique*, Gisements stratiformes et provinces cuprifères-Centenaire de la Société Géologique de Belgique, pp.123-164.

Izawa, E., Urashima, Y., Ibaraki, K., Suzuki, R., Yokoyama, T., Kawasaki, K., et al. (1990). The Hishikari gold deposit: High-grade epithermal veins in quaternary volcanics of southern Kyushu, Japan. *Journal of Geochemical Exploration, 36*(1), 1-56.

Jackson, M., Warin, O., Woad, G., & Hudec, M. (2003). Neoproterozoic allochthonous salt tectonics during the lufilian orogeny in the Katangan Copperbelt, Central Africa. *Geological Society of America Bulletin, 115*(3), 314-330.

Jigsaw (2009). Prospect summary and evaluation: Kipushi East fact sheet, and interpreted regional geological map. *FQM internal report, unpubl*.

John, T., Schhenk, V., Mezger, K., & Tembo, F., (2004). Timing and PT evolution of white schist metamorphism in the Lufilian Arc-Zambezi Belt Orogen (Zambia); implications for the assembly of the Gondwana. *Journal of Geology*, 112, 71-90.

Johnson, B., Montante-Martinez, A., Canela-Barboza, M., & Danielson, T. (2000). Geology of the san nicolás deposit, Zacatecas, Mexico. *VMS Deposits of Latin America: Geological Association of Canada, Mineral Deposits Division Special Publication, 2*, 71-85.

Kabengele, M., R. T. Lubala, and B. Cabanis (1987). Le magmatisme du plateau des Marungu, secteur de Pepa-Lubumba, nord-est du Shaba, Zaïre—Caractéristiques pétrologiques et géochimiques—Signification géodynamique dans l'évolution de la chaîne Ubendienne. *Colloquium on african geology. 14*.

Kampunzu, A., & Cailteux, J. (1999). Tectonic evolution of the Lufilian arc (Central Africa Copperbelt) during Neoproterozoic pan-African orogenesis. *Gondwana Research, 2*(3), 401-421.

Kampunzu, A., Cailteux, J., Batumike, J., & Loris, N. (2003). Syn-orogenic sedimentation in the Katangan belt: Myth or reality? Multi-proxy constraints. *Proterozoic Sediment-Hosted Base Metals Deposits of Western Gondwana (IGCP 450), 3rd Conference, Abst. Vol. Lubumbashi, Congo,* pp. 98-102.

Kampunzu, A., Cailteux, J., Kamona, A., Intiomale, M., & Melcher, F. (2009). Sediment-hosted Zn–Pb–Cu deposits in the Central African Copperbelt. *Ore Geology Reviews, 35*(3), 263-297.

Kampunzu, A., Kanika, M., Kapenda, D., & Tshimanga, K. (1993). Geochemistry and geotectonic setting of late Proterozoic Katangan basic rocks from Kibambale in central Shaba (Zaire). *Geologische Rundschau, 82*(4), 619-630.

Kampunzu, A., Tembo, F., Matheis, G., Kapenda, D., & Huntsman-Mapila, P. (2000). Geochemistry and tectonic setting of mafic igneous units in the Neoproterozoic Katangan basin, Central Africa: Implications for Rodinia break-up. *Gondwana Research, 3*(2), 125-153.

Kampunzu, A. B., Cailteux, J. L. H., Moine, B., & Loris, H. N. B. T. (2005). Geochemical characterization, provenance, source and depositional environment of 'Roches argilo-talqueuses' (RAT) and mines subgroups sedimentary rocks in the Neoproterozoic Katangan belt (Congo): Lithostratigraphic implications. *Journal of African Earth Sciences, 42*(1–5), 119-133.

Katekesha, W. M. (1975). Condition de formation du gisement cupro-cobaltifere da Kamoto principal (Shaba-Zaïre). (Ph.D. Dissertation, Université de Liège). , 237p.

Key, R., Liyungu, A., Njamu, F., Somwe, V., Banda, J., Mosley, P., et al. (2001). The western arm of the lufilian arc in NW Zambia and its potential for copper mineralization. *Journal of African Earth Sciences, 33* (3), 503-528.

Killeen, P. (1997). Nuclear techniques for ore grade estimation. *Proceedings of Exploration, 97.* pp. 677-684.

Kipata, M. L., Delvaux, D., Sebagenzi, M. N., Cailteux, J., & Sintubin, M. (2013). Brittle tectonic and stress field evolution in the pan-African lufilian arc and its foreland (Katanga, DRC): From orogenic compression to extensional collapse, transpressional inversion and transition to rifting. *Geologica Belgica*, 001-017.

Koksoy,M. (1967). Dispersion of mercury and other ore elements from mineral deposits in Turkey.

Langford, F. F. (1965). A method to evaluate the probability of success of a geochemical survey. *Economic Geology, 60*(2), 360-372.

Leca, X. (1990). Discovery of concealed massive-sulphide bodies at Neves-Corvo, southern Portugal-a case history. *Institution of Mining and Metallurgy Transactions. Section B. Applied Earth Science*, *99*.

Lefebvre, J. (1973). Présence d'une sédimentation pyroclastique dans le Mwashya inférieur du Shaba méridional (ex-Katanga). *Annales de la Société Géologiques De Belgique, 96*, 197-247.

Lefebvre, J. (1974). Minéralisations cupro-cobaltifères associées aux horizons pyroclastiques situés dans le faisceau supérieur de la série de Roan, a Shituru, Shaba, zaïre. *Gisement Stratiformes et Provinces Cuprifères: Liège, La Société Géologique De Belgique,* 103-122.

Lefebvre, J. (1975). Les roches ignées dans le Katangien du Shaba (zaïre). Le district du cuivre. *Annales De La Société Géologique De Belgique, 98*, 47-73.

Lefebvre, J. (1976). Phénomènes post-diagénétiques dans l'écaille Nord-Est du gisement de Kabolela, Shaba, Zaïre. *Bulletin Société Belge Géologie, 85, 7-29.*

Lefebvre, J. (1978). Le groupe de Mwashya, mégacyclthème terminal du Roan (Shaba, Zaïre sudoriental). I—Approche lithostratigraphique et étude de l'environnement sédimentaire. *Ann Soc Geol Belg, 101*, 209-225.

Legault, J., Gordon, R., Reddig, M., & Slama, E. (2002). Geophysical survey interpretation report regarding the Quantec titan-24 distributed array system tensor magnetotelluric and DCIP resistivity surveys over the kidd creek mine project. *Kidd Twp., Near Timmins, ON, on Behalf of Ontario Ministry of Northern Development and Mines and Falconbridge Ltd (OMET Project 13-2001a), Toronto: Quantec Geoscience Inc., Internal Company Report, 99p, QG-215,*

Lemmon, T., Boutwood, A., & Turner, B., (2003). The Dikulushi copper–silver deposit, Katanga, DRC. *In: Cailteux, J. (Ed.),* Proterozoic Sediment-Hosted Base Metal Deposits of Western Gondwana*. Abstracts of the IGCP 450 Conference and Field Workshop*, July 14–24, 2003, Lubumbashi, Democratic Republic of Congo, pp. 147–149.

Lepersonne, J. & Musee royale de l'Afrique centrale (1974). *Carte géologique du Zaïre 1: 2,000,000.* Musée royale de l'Afrique Centrale, Institut géographique militaire de Belgique.

Levinson, A.A. (1974). Introduction to exploration geochemistry. Textbook.

Lillesand, T. M., Kiefer, R. W., & Chipman, J. W. (2004). Remote sensing and image interpretation*. No. Ed. 5. John Wiley & Sons Ltd*.

Loris, N., Charlet, J., Pechman, E., Clare, C., Chabu, M., & Quinif, Y. (1997). Caractéristiques minéralogiques, cristallographiques, physico-chimiques et âges des minéralisations uranifères de Luiswishi (Shaba, Zaïre). *Colloque International Cornet, Gisements Stratiformes de Cuivre et Minéralisations Associées, Mons (1994). Académie Royale Des Sciences d'Outre-Mer,* pp. 285-306.

Loughlin, W. (1979). The geology of the Luma river area. Rep. Geol. Surv. Zambia, N0.87.

Marjoribanks, R. W. (2010*). Geological methods in mineral exploration and mining. Springer.*

Master, S., Rainaud, C., Armstrong, R., Phillips, D., & Robb, L. (2005). Provenance ages of the Neoproterozoic Katanga Supergroup (Central African Copperbelt), with implications for basin evolution. *Journal of African Earth Sciences, 42*(1), 41-60.

Master, S., & Wendorff, M. (2011). Neoproterozoic glaciogenic diamictites of the Katanga Supergroup, central Africa. *Geological Society, London, Memoirs, 36*(1), 173-184.

McMonnies, B. & Gerrie, V. (2007). Ground geophysics and borehole logging—A decade of improvements. In *Exploration in the New Millennium: Proceedings of the Fifth Decennial International Conference on Mineral Exploration,* pp. 39-49.

McQueen, K. (2008). Identifying geochemical anomalies. *A Guide for Mineral Exploration through the Regolith of the Central Gawler Craton, South Australia,* 1-7.

Mendelsohn, F. (1961). *The geology of the northern Rhodesia Copperbelt,* Macdonald.

Mendelsohn, F. (1989). Central/southern African Ore Shale deposits: *Geological Association of Canada*, Special Paper 36, p. 453–470.

Miesch, A. (1981). Estimation of the geochemical threshold and its statistical significance. *Journal of Geochemical Exploration, 16*(1), 49-76.

Milsom, J. (2009). Geophysical methods*; in Moon, C., Whateley, M., & Evans, A. M. (Ed.),* introduction to mineral exploration (2nd Ed.), *blackwell publishing*, *p.127-153*.

Moon, C. (2009). Exploration Geochemistry. *In Moon, C., Whateley, M., & Evans, A. M. (Ed.),* introduction to mineral exploration (2nd Ed.), *blackwell publishing*, *p.155-178.*

Moon, C., Whateley, M., & Evans, A. M. (2009). Introduction to mineral exploration (2nd Ed.) *Blackwell Publishing*, *481p.*

Okitaudji, R. L. (2001). Modèle de formation des gisements de cuivre-cobalt du Shaba en République Démocratique du Congo. *Académie et société lorraines des sciences, Villers-lès-Nancy (FRA.).*

Outhwaite, M., Wood, D., and Beeson, J., (2010, unpubl.), Geological traversing and interpretation of the Trident Project, Republic of Zambia: unpubl. *report from Jigsaw Geoscience to First Quantum Minerals Ltd.*, Dec. 15, 2011, 150p.

Phillips, J. D. (1997). *Potential-field geophysical software for the PC, version 2.2* US Department of the Interior, US Geological Survey.

Porada, H. (1989). Pan-African rifting and orogenesis in southern to equatorial Africa and eastern Brazil. *Precambrian Research, 44*(2), 103-136.

Porada, H., and Berhost, V., 1998, Thrust tectonics in the Domes region and Copperbelt of Zambia: Outline and outlook: Frieberger Forschungshefte, Hefte C., v. 475, p. 145–162.

Porada, H., & Berhorst, V. (2000). Towards a new understanding of the Neoproterozoic-early Paleozoic lufilian and northern Zambezi belts in Zambia and the Democratic Republic of Congo. *Journal of African Earth Sciences, 30*(3), 727-771.

Rainaud, C., Master, S., Armstrong, R.A., Phillips, D. & Robb, L.J., 2005. Monazite U-Pb dating and ^{40}Ar-^{39}Ar thermochronology of metamorphic events in the Central African Copperbelt during the Pan African Lufilian Orogeny. *Journal of African Earth Sciences, 42, 183-199.*

Ramsay, C. R., & Ridgway, J. (1977). Metamorphic patterns in Zambia and their bearing on problems of Zambian tectonic history. *Precambrian Research*, *4*(4), 321-337.

Reeve, J., Cross, K., Smith, R., & Oreskes, N. (1990). Olympic dam copper-uranium-gold-silver deposit. *Geology of the Mineral Deposits of Australia and Papua New Guinea, 2*, 1009-1035.

Reimann, C., Filzmoser, P., & Garrett, R. G. (2005). Background and threshold: critical comparison of methods of determination. *Science of the Total Environment*, *346*(1), 1-16.

Roberts, S., Hitzman, M., Munchez, P., Walsh, J., Wilkilson, J., Wood, D., & Broughton, D. (2013, unpubl.). Base metals in basin; *Short Course on African Metallogeny*, Kitwe, Zambia.

Rutter, H. & Esdale.D.J. (1985). The geophysics of the Olympic Dam discovery. Bull. Aust. Soc. Explor. Geophys. 16:273-276

Schmandt, D., Broughton, D., Hitzman, M. W., Plink-Bjorklund, P., Edwards, D., & Humphrey, J. (2013). The Kamoa copper deposit, democratic republic of Congo: Stratigraphy, diagenetic and hydrothermal alteration, and mineralization. *Economic Geology, 108*(6), 1301-1324.

Schneider, J., Melcher, F., & Brauns, M. (2007). Concordant ages for the giant Kipushi base metal deposit (DR congo) from direct Rb–Sr and Re–Os dating of sulfides. *Mineralium Deposita, 42*(7), 791-797.

Schneiderhöhn, H., 1931. Mineralische Bodenschätze im südlichen Afrika. *NEM-Verlag*, Berlin, 111 p.

Schuh, W. (2008). Tenke-Fungurume—a new world-class sediment-hosted copper cobalt district in the DR Congo [abs.]: Society of Mining Engineers, Salt Lake City, 2008, Conference Abstracts, p. 38.

Schuh, W. Leveille, R., Fay, I. and North, R., 2012, Geology of the Tenke- Fungurume sediment-hosted strata-bound copper-cobalt district, Democratic Republic of Congo: *Society of Economic Geologists*, Special Publication 16, p. 269–301.

Selley, D. (2012). Overviews of the sediment-hosted Cu system and ores of the Central African Copperbelt. *Red metal conference, London*.

Selley, D., Broughton, D., Scott, R., Hitzman, M., Bull, S., Large, R., Mc- Goldrick, P., Croaker, M., Pollington, N. and Barra, F. (2005). A new look at the geology of the Zambian Copperbelt. *Economic Geology 100th Anniversary Volume, p. 965–1000,*

Sinclair, A. (1974). Selection of threshold values in geochemical data using probability graphs. *Journal of Geochemical Exploration, 3*(2), 129-149.

Sinclair, A. (1991). A fundamental approach to threshold estimation in exploration geochemistry: Probability plots revisited. *Journal of Geochemical Exploration, 41*(1), 1-22.

Stanley, C. R., & Sinclair, A. J. (1989). Comparison of probability plots and the gap statistic in the selection of thresholds for exploration geochemistry data. *Journal of Geochemical Exploration, 32*(1), 355-357.

Studt, F. E. 1908. Carte géologique du Katanga (1/500.000e) et notice explicative. *Annales du Musée de Congo belge*, sér. 2, 1, 5–16.

Studt, F. E. 1913. The geology of Katanga and Northern Rhodesia: an outline of the geology of South Central Africa. *Transactions of the Geological Society of South Africa*, 16, 44–106.

Studt, F. E., Cornet, J. & Buttgenbach, H. 1908. Carte géologique du Katanga et notes descriptives. *Annales Musée du Congo, Bruxelles*, Géologie, Géophysique, Minéralogie & Paléontologie, série 2, Katanga, 1, 94.

Sweeney, M., Binda, P., & Vaughan, D. (1991). Genesis of the ores of the Zambian Copperbelt. *Ore Geology Reviews, 6*(1), 51-76.

Tassel, A., 2003. Dikulushi-setting a new benchmark. *African Mining*, 8: 24-35.

Telford, W. M., Geldart, L. P. & Sheriff, R. E. (1990). Applied geophysics.

Thomas, M., Walker, J., Keating, P., Shives, R., Kiss, F., & Goodfellow, W. (2000). Geophysical atlas of massive sulphide signatures. *Bathurst Mining Camp, New Brunswick, CD-ROM Version: Geological Survey of Canada Open File D, 3887*

Thompson, M. (1983). Control procedures in geochemical analysis*. In* Howarth, R.J (Ed*).* Statistics and data analysis in geochemical prospecting. Handbook of exploration geochemistry*. Elsevier scientific publishing company.*

Thomson, I. (1986). Get it right. *In Fletcher, W. K.* (*Ed*). Exploration geochemistry: Design and interpretation of soil surveys. *The Economic Geology Publishing Company*.

Unrug, R. (1987). Geodynamic evolution of the Lufilian arc and the Kundelungu aulacogen Angola, Zambia and Zaïre. In *Colloquium on African geology. 14* (pp. 117-120).

Unrug, R. (1988). Mineralization controls and source of metals in the Lufilian fold belt, Shaba (Zaïre), Zambia, and Angola. *Economic Geology, 83*(6), 1247-1258.

Unrug, R. (1997). Rodinia to Gondwana: The geodynamic map of Gondwana supercontinent assembly. *GSA Today, 7*(1), 1-6.

Vanden Brande, P. 1936. Etudes géologiques dans la feuille Lukafu. Comité Spécial du Katanga, *Annales des Services des Mines,* 6, 51–69

Walters, S., Skrzeczynski, B., Whiting, T., Bunting, F., & Arnold, G. (2002). Discovery and geology of the Cannington Ag-Pb-Zn deposit, Mount Isa eastern succession, Australia: Development and application of an exploration model for broken hill-type deposits. *Special Publication-Society of Economic Geologists, 9*, 95-118.

Wendorff, M. (2000). Genetic aspects of the Katangan megabreccias: Neoproterozoic of Central Africa. *Journal of African Earth Sciences, 30*(3), 703-715.

Wendorff, M. (2003). Stratigraphy of the Fungurume group-evolving foreland basin succession in the lufilian fold-thrust belt, Neoproterozoic-lower Paleozoic, Democratic Republic of Congo. *South African Journal of Geology, 106*(1), 17-34.

Wendorff, M. (2005). Evolution of Neoproterozoic–Lower Paleozoic lufilian arc, Central Africa: A new model based on syntectonic conglomerates. *Journal of the Geological Society, 162*(1), 5-8.

Whateley, M. (2009). Remote sensing. *In Moon* C., *Whateley, M., & Evans, A. M. (Ed*), Introduction to mineral exploration (2nd Ed.); *Blackwell Publishing*; p.104-126.

Wilson, T., Hanson, R., & Wardlaw, M. (1993). Late Proterozoic evolution of the Zambezi belt, Zambia: Implications for regional pan-African tectonics and shear displacements in Gondwana. *Gondwana, 8*, 69-82.